AD-A017 373

PRACTICAL SENSITIVITY LIMITS OF PRODUCTION NONDESTRUCTIVE TESTING METHODS IN ALUMINUM AND STEEL

Howard L. Southworth, et al

Boeing Commercial Airplane Company

Prepared for:

Air Force Materials Laboratory

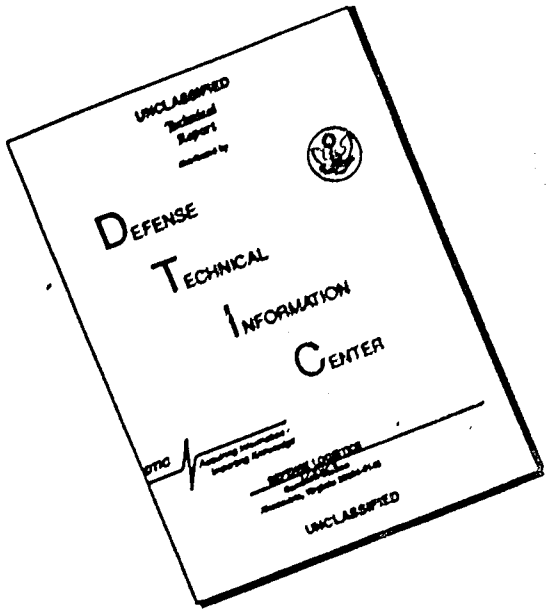
January 1975

DISTRIBUTED BY:

NTIS

National Technical Information Service
U. S. DEPARTMENT OF COMMERCE

DISCLAIMER NOTICE



THIS DOCUMENT IS BEST QUALITY AVAILABLE. THE COPY FURNISHED TO DTIC CONTAINED A SIGNIFICANT NUMBER OF PAGES WHICH DO NOT REPRODUCE LEGIBLY.

325121

AFML-TR-74-241

AD A016 126

PRACTICAL SENSITIVITY LIMITS OF PRODUCTION NONDESTRUCTIVE TESTING METHODS IN ALUMINUM AND STEEL

BOEING COMMERCIAL AIRPLANE COMPANY

DDC
RECEIVED
NOV 19 1975
C

MARCH 1975

Approved for public release; distribution unlimited

AIR FORCE MATERIALS LABORATORY
AIR FORCE SYSTEMS COMMAND
WRIGHT-PATTERSON AIR FORCE BASE, OHIO

Reproduced by
NATIONAL TECHNICAL
INFORMATION SERVICE
US Department of Commerce
Springfield, VA. 22151

UNCLASSIFIED

SECURITY CLASSIFICATION OF THIS PAGE *(When Data Entered)*

REPORT DOCUMENTATION PAGE

READ INSTRUCTIONS BEFORE COMPLETING FORM

1 REPORT NUMBER
AFML-TR-74-241

2 GOVT ACCESSION NO.

3 RECIPIENT'S CATALOG NUMBER

4 TITLE *(and Subtitle)*
PRACTICAL SENSITIVITY LIMITS OF PRODUCTION NONDESTRUCTIVE TESTING METHODS IN ALUMINUM AND STEEL

5 TYPE OF REPORT & PERIOD COVERED
FINAL REPORT
15 March 1973 - 15 September 74

6 PERFORMING ORG. REPORT NUMBER
D6-41978

7 AUTHOR(s)
Howard L. Southworth, Norman W. Steele, Peter P. Torelli

8 CONTRACT OR GRANT NUMBER(s)
F33615-72-C-2202

9 PERFORMING ORGANIZATION NAME AND ADDRESS
Boeing Commercial Airplane Company
Seattle, Washington 98124

10 PROGRAM ELEMENT, PROJECT, TASK AREA & WORK UNIT NUMBERS
7351

11 CONTROLLING OFFICE NAME AND ADDRESS
AFML/LLP
Metals and Ceramics Division
Wright-Patterson Air Force Base, Ohio 45433

12 REPORT DATE
January 1975

13 NUMBER OF PAGES
12

14 MONITORING AGENCY NAME & ADDRESS *(if different from Controlling Office)*

15 SECURITY CLASS. *(of this report)*
UNCLASSIFIED

15a DECLASSIFICATION/DOWNGRADING SCHEDULE

16 DISTRIBUTION STATEMENT *(of this Report)*
Approved for public release, distribution unlimited.

17 DISTRIBUTION STATEMENT *(of the abstract entered in Block 20, if different from Report)*

18 SUPPLEMENTARY NOTES

19 KEY WORDS *(Continue on reverse side if necessary and identify by block number)*

Nondestructive testing	Radiography
Artificial flaws	Magnetic particle inspection
Statistical evaluation	Eddy-current inspection
Penetrant inspection	Ultrasonic inspection

20 ABSTRACT *(Continue on reverse side if necessary and identify by block number)*

This report describes the work accomplished under an 18-month program conducted to evaluate the sensitivity capabilities of current state-of-the-art nondestructive inspection methods. The methods include magnetic particle, penetrant, eddy-current, ultrasonic, and radiographic. These capabilities were demonstrated in response to varied surface flaws and were statistically defined in terms of probability and confidence of detection. This was accomplished with differing specimen configurations in two representative aircraft structural alloys and for both laboratory and production inspections.

DD FORM 1 JAN 73 1473 EDITION OF 1 NOV 65 IS OBSOLETE

UNCLASSIFIED

SECURITY CLASSIFICATION OF THIS PAGE *(When Data Entered)*

Block 20 (Continued)

Two innovative approaches to the development and fabrication of controlled, reproducible surface discontinuities in the inspection test specimens were reported. The primary approach was to place electrodischarge machined (EDM) slots in grooved specimen blanks and to subsequently compress these blanks to close the slots by permanent, plastic deformation. The blanks were then machined to configurations of varying degrees of complexity. The second approach utilized the combined effects of controlled introduction of hydrogen into the specimen surface and the presence of residual or applied stresses. The development of these methods and the fabrication of the numerous and varied specimens are described in sufficient detail to allow duplication.

Repeated inspections of all specimens were performed both in the laboratory and in production areas to provide a statistically meaningful data base for each of the nondestructive methods. A broad variety of equipment, technique differences, and skills, within the confines of accepted practice and specification controls, was included to accurately represent industry practice. Selected specimen discontinuities were further investigated, including destructive examinations, to characterize and confirm the flaw geometries.

Using the test results in a statistical analysis, the sensitivity capabilities of the five methods were determined in terms of 0.90 probability of detection with 95% confidence for a given flaw size. Comparative capabilities such as between laboratory and production inspections, methods, and flaw types are shown for differences of significance.

The test data and statistical analysis results are detailed in this report.

PREFACE

This is a final technical report and covers work performed under AFML contract F33615-72-C-2202, project no. 7351, for the period 15 March 1973 through 15 September 1974. This contract was accomplished under the technical direction of Mr. F.D. Mullins, Nondestructive Evaluation Branch (AFML/LLP), Metals and Ceramics Division, Air Force Materials Laboratory, Wright-Patterson AFB, Ohio.

The contract work was performed by the Boeing Commercial Airplane Company, Renton, Washington. Mr. M.L. Phelps was the Program Manager and H.L. Southworth was the Technical Leader. Messrs. P.P. Torelli, W.J. Harris, W.B. Keene, M.L. Squires, N.W. Steele, S. Takashima and R.K. Woodbury directly supported the program. Many additional personnel in engineering support shops, laboratories, and production inspection facilities actively contributed to the program, and their assistance is gratefully acknowledged.

This report has been assigned Boeing document D6-41978 as the performing organization report number for internal use.

The nondestructive testing equipment and materials identified in this program were selected from a large range of products commonly available in industry. The data reported were not generated for a comparison between materials and equipment; therefore, results relative to commercial products should not be used, in whole or in part, for advertising or promotional purposes, nor should any government or industry endorsement be inferred.

CONTENTS

Section		Page
I	INTRODUCTION	1
II	PROGRAM OBJECTIVES AND APPROACH	3
III	SPECIMEN DEVELOPMENT	5
	Introduction	5
	Materials Selection	5
	Flaw Types	6
	Compressed Notch Flaw - Steel	6
	Compressed Notch Flaws - Aluminum	9
	Hydrogen Embrittlement Cracks	11
	Grinding Cracks	15
IV	SPECIMEN FABRICATION	17
	Introduction	17
	Final Fabrication Procedures	17
	Compressed Notches - Steel	17
	Compressed Notches - Aluminum	20
	Grinding and Hydrogen Embrittlement Cracks	20
	Contaminated Flaw Specimens	23
	Final Specimen Configurations	25
	Flaw Characterizations	25
	Fabrication Summary	37
V	NONDESTRUCTIVE INSPECTIONS	47
	Introduction	47
	Inspection Facilities and Equipment	47
	Personnel	48
	Inspection Lots	48
	Routing of Inspection Lots	48
	Specimen Cleaning and Preservation	49
	Reference Standards	49
	Magnetic Particle Inspection	51
	Penetrant Inspection	51
	Ultrasonic Inspection	53
	Eddy-Current Inspection	55
	Radiographic Inspection	58
VI	INSPECTION RESULTS AND EVALUATION	61
	Introduction	61
	Statistical Evaluation	61
	Summary of Results	65
	Externally Flawed Steel Specimens	65

CONTENTS (Continued)

Section		Page
	Magnetic Particle Inspection	65
	Penetrant Inspection	65
	Eddy-Current Inspection	77
	Ultrasonic Inspection	77
	Radiographic Inspection	77
	Externally Flawed Aluminum Specimens	77
	Penetrant Inspection	77
	Eddy-Current Inspection	97
	Ultrasonic Inspection	97
	Radiographic Inspection	97
	Internally Flawed Hollow Steel Specimens	97
	Grinding and Embrittlement Crack Specimens	130
	Threaded Steel Specimens	132
	Effects of Specimen Configuration and Flaw Types on Detectability	152
	Intentionally Oxidized Flaws	168
	Specimen Degradation	168
	Nonrelevant Callouts	171
VII	CONCLUSIONS	175
VIII	RECOMMENDATIONS	177
IX	REFERENCES	179

FIGURES

No.		Page
1	Steps in Fabricating a Compressed-Notch NDI Specimen	7
2	Externally Notched, Cylindrical Specimen Before and After Axial Compression	8
3	Two Specimen Blanks Before and After Compression	10
4	Three Sections of BAC 1520-1168 Extrusion With Pairs of Grooves in Three Locations Before Compression	12
5	EDM Notch in Aluminum Blank	13
6	Electrolytic Charging at a Local Area of a Flat Bar Specimen Under Sustained Bending Stress	14
7	Compression of Externally Notched Steel Specimen in 1,200,000-lb Test Machine	18
8	Drawing of Grooved Blank for Externally Flawed Specimens	19
9	Drawing of Grooved Blank for Internal Surface Flawed Specimens	19
10	Load-Strain Diagrams of Compression of Solid Steel Specimen Blanks	21
11	Load Strain Diagrams of Compression of Hollow Steel Specimen Blanks	22
12	Cross Section of BAC 1520-1168 With Typical Groove Locations	23
13	Load-Strain Diagrams of Compression of Extruded Aluminum Specimen Blanks	24
14	Straight Cylinder Specimen and Blank	26
15	Filleted Cylinder Specimen and Blank	27
16	Threaded Cylinder Specimen and Blank	28
17	Straight Hollow Cylinder Specimen and Blank	29
18	Internal Filleted Hollow Cylinder Specimen and Blank	30
19	Sketch of Internal Fillet Hollow Specimen	31
20	Extruded Aluminum Specimen and Blank	32
21	Hydrogen and Grinding Crack Specimen	33
22	Typical Liquid RTV Rubber Replica of an EDM Notch in an External Groove Specimen Blank (8X)	34
23	Fluorescent Magnetic Particle Flaw Indications (2.5X)	35
24	Two Typical Fluorescent Penetrant Indications of Compressed Notch Flaws in an Aluminum Specimen (2X)	36
25	Two Fractures Exposing Compressed Notch Flaws in a Hollow Specimen and in a Solid Steel Specimen (7X)	36
26	Metallographic Sections Through Compressed Notch Flaws in Steel Specimens (75X)	38
27	Fractures Exposing Two Hydrogen Embrittlement Crack Surfaces, Surface Lengths[l] and Depths[d] of Flaws Are Delineated (7X)	38
28	Metallographic Characterization of Typical Cracks in Ground Steel Surfaces (75X)	39
29	Two Representative Compressed Notch Flaws in Extruded Aluminum Specimens (7X)	39

CONTENTS (Concluded)

No.		Page
30	Metallographic Sections Through Two Compressed Notch Flaws in Aluminum (the Wide Root of the One Flaw is Indicative of Nonuniform Compression Associated With Buckling) (75X)	40
31	Laboratory Ultrasonic Cleaning Equipment	50
32	Laboratory Magnetization of Test Specimen for Magnetic Particle Inspection	52
33	Laboratory Ultrasonic Inspection of Solid Steel Specimen	54
34	Laboratory Eddy Current Inspection of Solid Steel Specimens	56
35	Expansion Holder for Eddy Current Probe	57
36	Radiographic Setup for Solid Cylinder Specimens	59
37	Radiographic Setup for Hollow Cylinder Specimens	59
38	Effect of Number of Inspections and Misses on 95% Confidence Limit Probabilities	64
39	Magnetic Particle Results on Externally Flawed Steel Specimens	71
40	Penetrant Results on Externally Flawed Steel Specimens	76
41	Eddy Current Results on Externally Flawed Steel Specimens	82
42	Ultrasonic Results on Externally Flawed Steel Specimens	87
43	Radiographic Results on Externally Flawed Steel Specimens	92
44	Penetrant Results on Flawed Aluminum Specimens	96
45	Eddy Current Results on Flawed Aluminum Specimens	101
46	Ultrasonic Results on Flawed Aluminum Specimens	105
47	Radiographic Results on Flawed Aluminum Specimens	109
48	Magnetic Particle Results on Internally Flawed Hollow Steel Specimens	113
49	Penetrant Results on Internally Flawed Hollow Steel Specimens	117
50	Eddy Current Results on Internally Flawed Hollow Steel Specimens	121
51	Ultrasonic Results on Internally Flawed Hollow Steel Specimens	125
52	Radiographic Results on Internally Flawed Hollow Steel Specimens	129
53	Fluorescent Indications of Multiple Grinding Cracks: Specimen Number and Dimensions of Cracked Area are Given (2X)	131
54	Magnetic Particle Results on Grinding and Embrittlement Cracked Steel Specimens	136
55	Ultrasonic Results on Grinding and Embrittlement Cracked Steel Specimens	140
56	Eddy Current Results on Grinding and Embrittlement Cracked Steel Specimens	144
57	Abusive Grinding to Develop Cracks Interferes with Eddy Current Inspection	145
58	Effects of Flaw Type on Detectability (Combined Laboratory and Production Data)	165
59	Effects of Specimen Configuration on Detectability by Magnetic Particle Inspection	166
60	Effects of Specimen Configuration on Detectability by Ultrasonics and Radiography (Combined Laboratory and Production Date)	167

TABLES

No.		Page
1	Specimen and Flaw Summary	4.
2	Externally Flawed Steel Specimens	42
3	Aluminum Cruciform Specimens	43
4	Internally Flawed Hollow Steel Specimens	44
5	Flat Bar Steel Specimens	45
6	Threaded Steel Specimens	46
7	Summary of Results	66
8	Results of Magnetic Particle Inspections on Externally Flawed Steel Specimens	67
9	Statistical Analysis of Magnetic Particle Inspection Results on Externally Flawed Steel Specimens	70
10	Results of Penetrant Inspections on Externally Flawed Steel Specimens	72
11	Statistical Analysis of Penetrant Inspections Results on Externally Flawed Steel Specimens	75
12	Results of Eddy Current Inspections on Externally Flawed Steel Specimens	78
13	Statistical Analysis of Eddy Current Inspection Results on Externally Flawed Steel Specimens	81
14	Results of Ultrasonic Inspections on Externally Flawed Steel Specimens	83
15	Statistical Analysis of Ultrasonic Inspection Results on Externally Flawed Steel Specimens	86
16	Results of Radiographic Inspections on Externally Flawed Steel Specimens	88
17	Statistical Analysis of Radiographic Inspection Results on Externally Flawed Steel Specimens	91
18	Results of Penetrant Inspections on Flawed Aluminum Specimens	93
19	Statistical Analysis of Penetrant Inspection Results on Flawed Aluminum Specimens	95
20	Results of Eddy Current Inspections on Flawed Aluminum Specimens	98
21	Statistical Analysis of Eddy Current Inspection Results on Flawed Aluminum Specimens	100
22	Results of Ultrasonic Inspections on Flawed Aluminum Specimens	102
23	Statistical Analysis of Ultrasonic Inspection Results on Flawed Aluminum Specimens	104
24	Results of Radiographic Inspections on Flawed Aluminum Specimens	106
25	Statistical Analysis of Radiographic Inspection Results on Flawed Aluminum Specimens	108
26	Results of Magnetic Particle Inspections on Internally Flawed Hollow Steel Specimens	110
27	Statistical Analysis of Magnetic Particle Inspection Results on Internally Flawed Hollow Steel Specimens	112
28	Results of Penetrant Inspections on Internally Flawed Hollow Steel Specimens	114

TABLES (Continued)

No.		Page
29	Statistical Analysis of Penetrant Inspection Results on Internally Flawed Hollow Steel Specimens	116
30	Results of Eddy Current Inspections on Internally Flawed Hollow Steel Specimens	118
31	Statistical Analysis of Eddy Current Inspection Results on Internally Flawed Hollow Steel Specimens	120
32	Results of Ultrasonic Inspections on Internally Flawed Hollow Steel Specimens	122
33	Statistical Analysis of Ultrasonic Inspection Results on Internally Flawed Hollow Steel Specimens	124
34	Results of Radiographic Inspections on Internally Flawed Hollow Steel Specimens	126
35	Statistical Analysis of Radiographic Inspection Results on Internally Flawed Hollow Steel Specimens	128
36	Results of Magnetic Particle Inspections on Grinding and Embrittlement Cracked Steel Specimens	133
37	Statistical Analysis of Magnetic Particle Inspection Results on Grinding and Embrittlement Cracked Specimens	135
38	Results of Ultrasonic Inspections on Grinding and Embrittlement Cracked Steel Specimens	137
39	Statistical Analysis of Ultrasonic Inspection Results on Grinding and Embrittlement Cracked Steel Specimens	139
40	Eddy Current Inspections on Grinding and Embrittlement Cracked Steel Specimens	141
41	Statistical Analysis of Eddy Current Inspection Results on Grinding and Embrittlement Cracked Steel Specimens	143
42	Results of Penetrant Inspections on Grinding and Embrittlement Cracked Steel Specimens	146
43	Statistical Analysis of Penetrant Inspection Results on Grinding and Embrittlement Cracked Steel Specimens	148
44	Results of Radiographic Inspections on Grinding and Embrittlement Cracked Steel Specimens	149
45	Statistical Analysis of Radiographic Inspection Results on Grinding and Embrittlement Cracked Steel Specimens	151
46	Results of Magnetic Particle Inspections on Flawed Threaded Steel Specimens	153
47	Statistical Analysis of Magnetic Particle Inspection Results (1) on Flawed Threaded Steel Specimens	155
48	Results of Penetrant Inspections on Flawed Threaded Steel Specimens	156
49	Statistical Analysis of Penetrant Inspection Results on Flawed Threaded Steel Specimens	158
50	Results of Ultrasonic Inspections on Flawed Threaded Steel Specimens	159

TABLES (Concluded)

No.		Page
51	Statistical Analysis of Ultrasonic Inspection Results on Flawed Threaded Steel Specimens	161
52	Results of Radiographic Inspections on Flawed Threaded Steel Specimens	162
53	Statistical Analysis of Radiographic Inspection Results on Flawed Threaded Steel Specimens	164
54	Intentionally Oxidized Flaws Comparative Results on External Flaw Steel Specimens	169
55	Intentionally Oxidized Flaws Comparative Results on Aluminum Specimens	170
56	Effects of Repeated Inspections on Penetrant Results	172
57	Summary of Nonrelevant Callouts	173

SECTION I
INTRODUCTION

Recent advances in structure analysis techniques based on linear elastic fracture mechanics are now permitting mathematical prediction of performance of many flawed structures prior to their use. These analytical procedures are also proving useful in developing proof testing requirements that will assure the absence of discontinuities leading to early failure in some structures. However, most structures are not amenable to proofload testing and the cost of testing may be prohibitive. Further, a proof load may cause initiation or incrementally extend subcritical flaws that will reduce the ultimate life capability of a totally flawless structure. Better results would be obtained if totally nondestructive evaluations could provide the desired assurance of freedom from harmful discontinuities. In this imperfect world, the best attainable assurance will be less than perfect and must be qualified in terms of probability and confidence.

Accurate knowledge of the sensitivity capabilities of the major nondestructive test methods is very sparse. Many studies have been conducted to evaluate inspection equipment, develop specialized inspection techniques, design and fabricate reference standards, derive material acceptance criteria, and detect the first cracks developing in structural tests or during service. However, none of this work yielded statistically useful data partly because of failure to document program results and shortcomings in the scope and design of the experimental programs. Many programs have determined minimum flaw size detectability in a laboratory environment but practical limits in production situations have been misleading. In other cases, the practical limits and acceptance standards that evolved were closely influenced by what level of quality could be reasonably provided by the current commercial practice. With no accurate means of analyzing the effects of material imperfections, safety factors were established to accommodate the lesser flaws inherent in the material. Therefore unnecessary rejections or excessive weight penalties arising from conservative design factors have resulted.

Because of the growing applications of fracture mechanics concepts in structural designs, the need became pressing for information on size, geometry, and location of flaws within the fabricated product, and particularly for accurate definition of the minimum flaw sensitivities of the various nondestructive testing methods employed to gain this information. If such information is obtained in a manner statistically acceptable for design reliability purposes, the potential benefit in performance predictions and efficiency of designs is great. This program was begun with these benefits in mind and with the goal of providing baseline information.

SECTION II
PROGRAM OBJECTIVES AND APPROACH

The overall objective of this program was to develop statistically sound data defining the sensitivity capabilities of state-of-the-art nondestructive tests in response to surface flaws in aircraft structural alloys. Specifically, the objectives were:

- Determine the size of the minimum surface flaw that can be nondestructively detected with a 0.90 probability and 95% confidence.
- As defined above, assess the detection capabilities of current state-of-the-art radiographic, eddy-current, ultrasonic, penetrant, and magnetic particle inspection techniques.
- Determine these capabilities on 2024 aluminum and 4340M steel alloys.
- Ascertain the variability in detection limits as a function of this type of surface flaw.
- Evaluate the detection capabilities of laboratory and standard production inspections used on aerospace structures.

The program provided for and emphasized development of artificially flawed specimens to represent defective production parts. The specimen designs were to incorporate several geometric complexities such as compound curved surfaces, hollow and solid sections, and abrupt changes in section size. The flaw locations were also to be chosen to present varied degrees of accessibility and inspection difficulties. Flaws were created on external surfaces, at changes of sections, on internal surfaces of hollow parts, and on both flat and curved surfaces. Then, to provide for assessing the variability of detection capabilities as a function of flaw type, more than one kind of flaw was to be created.

As natural flaws can exhibit extreme variability in their attributes, it was decided to confine the study to those production flaw geometries best analyzed by linear elastic fracture mechanics methods. Accordingly, the test specimens would contain narrow-width, sharply terminated surface flaws of greater surface length than depth and perpendicularly oriented to the inspection surface.

To create flaws of controlled size and orientation and to locate these flaws precisely in varied specimen geometries, the following fabrication methods were to be used. Flaws of controlled size and orientation would be achieved by compression of a notch machined into a specimen blank as described in section III, Specimen Development. Following compression, the specimen would then be machined to provide final flaw locations as required in radii, flat surfaces, internal surfaces, etc.

The minimum size flaw that could be detected would then be determined for each of the nondestructive testing methods on the fabricated test specimens containing flaws near the

Preceding page blank

threshold of detectability and larger. Repeated specimen inspections were to be made to acquire a statistically significant number of observations both in the laboratory and production environments.

SECTION III
SPECIMEN DEVELOPMENT

INTRODUCTION

An enduring problem in all investigations of NDT sensitivity capabilities has been the acquisition of suitable flawed test articles, which truly represent the various discontinuities encountered in production hardware. Most recently, the refinement of structural analysis techniques based on linear elastic fracture mechanics has accented the need for reliably defined NDT flaw detection capability. This information is not attainable in a reasonably economical or timely manner because natural flaws are not encountered often enough to provide sufficient test material. The bulk of such testing must ultimately come from carefully developed and closely controlled artificially created discontinuities. There were also significant problems in the field of fracture mechanics, and their studies are now based on very carefully created artificial flaws.

The investigation to define NDT capabilities in terms of reliable flaw detection (as opposed to the minimum detectable flaw size) by a particular system imposed additional requirements on the test articles. Test specimens must present configuration variations relating to actual structural designs. The threshold sensitivity limits of an NDT system can usually be demonstrated and reproduced in a laboratory on artificial specimens of simple shape. However, when natural flaws are sought in complex configurations of functional designs in production or field service environments, such sensitivity is not attained. The NDT system capability potential has not necessarily changed with the application environment; however, to a large degree the complexities may interfere with the most efficient application of the method and thus pose interpretation problems. These and other aspects relating to expedient operation decisions, repetitious error-free performance, and fatigue involve human factors not normally causing deficient performance in the laboratory.

MATERIALS SELECTION

The materials selected for this program are commonly used in aerospace structures. A low alloy steel rolled bar, 4340 vanadium modified and vacuum are remelted, was selected because of its universally established role in critically stressed aircraft mechanisms, landing gears, and structures. In most of these applications this alloy was used at the ultra high-strength levels, and accordingly, the test specimens were heat treated to 270 000- to 300 000-psi ultimate tensile strength. These high-strength applications of this alloy also require the most critical inspections by NDT to facilitate fracture mechanics applications to design.

A Boeing standard extruded shape of 2024 aluminum alloy was selected as representative of the 2000 alloy series, which has had widespread usage in aircraft for many years. In this instance, the selection of an extruded form was influenced by the frequent use of extruded sections of aluminum in primary structure. This alloy also was to be used in its higher strength conditions.

These materials provide two distinct ferrous and nonferrous alloy chemistries with widely differing physical and mechanical properties to reveal any differences in sensitivity that might be caused by differences in these properties. Using these alloys in their higher strength conditions also provides maximum resistance to wear and damage during many repeated inspections and associated handlings.

FLAW TYPES

There are many types of naturally occurring flaws with extremely varied characteristics. However, the kinds of flaws most significant in fracture mechanics analyses are much fewer and are generally characterized as a planar discontinuity, sharply terminated, and oriented normal to the predominant tensile stress. In most designs this orientation will be transverse to the long axis of the part and perpendicular to the surface. For most NDT procedures and type of discontinuity, this position is most favorable for detection. Therefore, the types of flaws fabricated in this program include these characteristics in order to provide the most useful information to both design and quality control personnel.

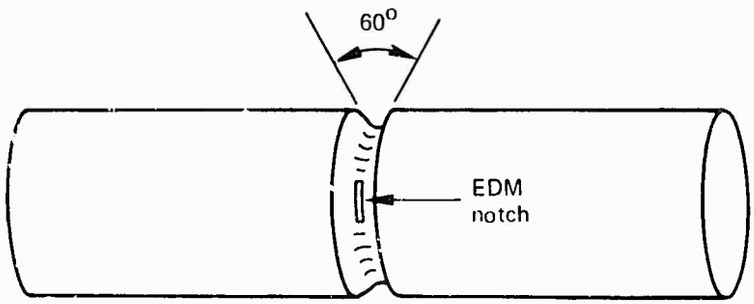
COMPRESSED NOTCH FLAW -STEEL

The majority of specimens fabricated in this program incorporate compressed notch flaws. The concept of compressing blocks of material containing saw-cuts or other notches to create artificial flaws is not new, but in order to avoid overall deformation during closure of the notch, this approach was improved by machining a groove placed at the desired flaw location before notching. This method proved to be very satisfactory as one of the least expensive and most reproducible means of obtaining surface discontinuities in test specimens of varied configurations.

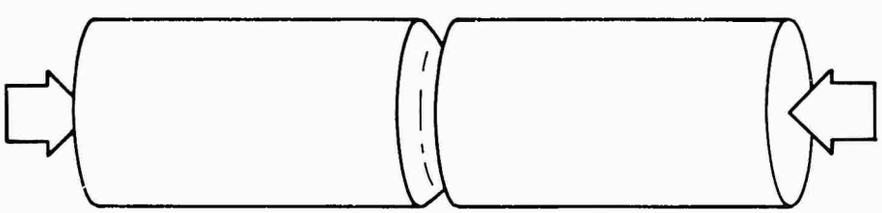
This method involved machining a specimen blank to provide a relatively deep groove in which to place an EDM notch of the desired size and shape. The groove served to reduce the cross-section area and concentrated the plastic deformation during compressive loading of the blank. Following compression, the deformed blank was machined to the desired final specimen configuration. This procedure is illustrated schematically in figure 1. This method can be used to obtain multiple flaws and multiple flaw locations. It also lends itself to many different finished specimen configurations.

Initial trail steel specimen blanks were made using the grooved solid cylindrical configuration. Variations in groove shapes, radii, and depths as well as differences in EDM notch widths, depths, and shapes were investigated. Figure 2 illustrates a specimen blank containing three different grooves, each with EDM notches, before and after axial compression. When finish machined, this early trial specimen contained six artificial flaws in six different locations.

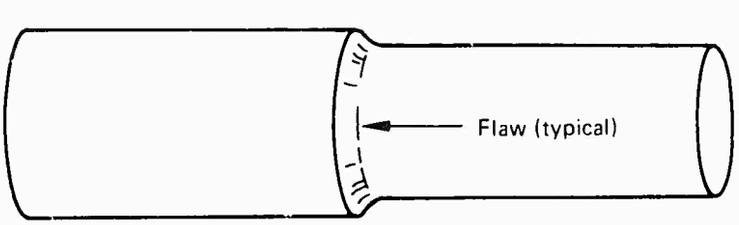
The fabrication of flawed specimens by plastically compressing notches was relatively straightforward, but attention to some details was required to avoid excessive or uncontrolled deformation. The net area at the root of the groove was not reduced sufficiently in the initial trial specimen blanks. Because of work hardening and lateral expansion in the reduced section under compression yielding, the load required to close the EDM notches increased until stresses exceeded the compressive yield strength in the larger diameter



Grooved and Notched Specimen Blank

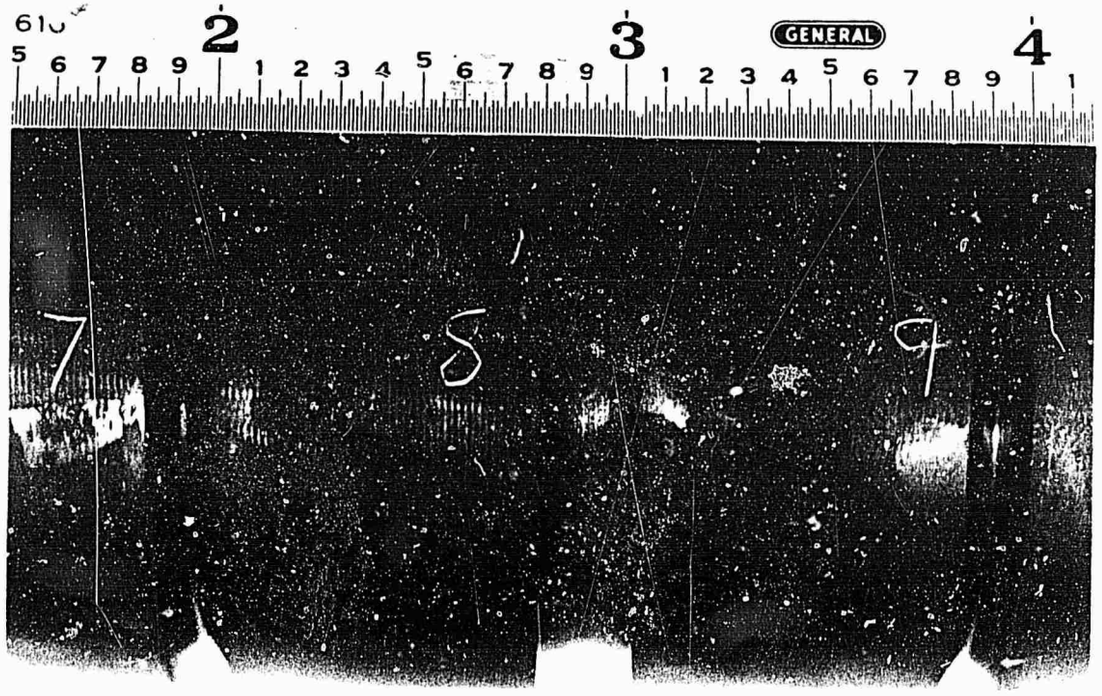


Axial Compression to Close Notch

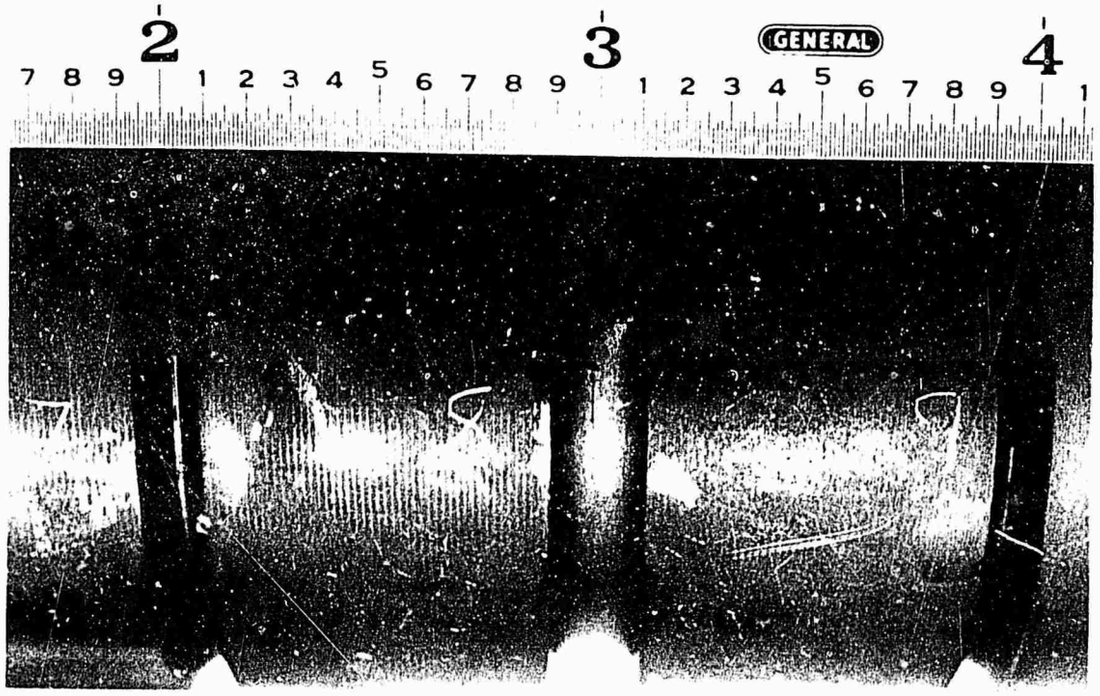


Finish-Machined NDT Specimen

Figure 1.—Steps in Fabricating a Compressed-Notch NDT Specimen



a. Before Compression



b. After Compression

Figure 2.–Externally Notched, Cylindrical Specimen Before and After Axial Compression

portions of the blank. With gross yielding, lateral instability developed and extensive buckling occurred. After buckling occurred, the root of the groove was no longer concentric with the original axis, and final machining to remove the groove tended to significantly change the compressed flaw dimensions or completely remove the smaller flaws. Also, the platens of the test machine or shop press used for compression had to be in proper alignment and closely parallel to inhibit buckling. The effects of lateral expansion and buckling tendencies encountered with a particular specimen blank design and the available machine for compression had to be compensated in the dimensioning of the blank and the depth of the EDM notch, especially when control of small final flaw sizes was desired. Experience in this program proved it was best to start with a slightly oversize notch and adjust the final machining to attain the desired flaw size. With a notch length-to-depth ratio of 2, removal of 0.010 in. from the surface diminished the surface flaw length by 0.020 in.

Several changes in design of the cylindrical blanks evolved in order to reduce buckling and the amount of overall compression required to close the EDM notches. The ratio of the reduced area to the gross cross-sectional area was decreased from 0.76 to the order of 0.6. The original groove was changed from a simple 0.125-in. radius to a 60° configuration with a 0.020 in. radius root. This deeper, sharper groove reduced the total overall strain required for notch closure by further concentrating the plastic compression within the region of the sharper groove. Reducing the thickness of the EDM electrode also reduced the compression strain required. However, when the electrode thickness was less than 0.006 in. maintaining notch shape became a problem and the costs of machining thin notches to depths greater than about 0.20 in. became excessive.

Reduction of the area ratios to 0.6 was achieved by increasing the larger diameter thus improving lateral stability of the specimens by presenting a less slender column. Further improvement included positioning the plane of the groove closer to the ends of the blank and controlling flatness and parallelism of the table and crosshead of the compression machine as well as the ends of the specimen blanks. See figure 3.

Following closure of the EDM notches by compression loading, the specimen blanks were rough machined to the final configuration and heat treated to a level of 270-300 ksi ultimate tensile strength. Marquenching heat treatment was employed to minimize the possibility of quench cracks developing from the flaws. This procedure proved quite successful, and no flawed specimen cracked during the final heat treatment. Cracking during heat treatment was one serious source of concern at the beginning of the program because of the built-in stress concentrations.

Following heat treatment, the test specimens were finished by grinding. This operation also can be a source of extraneous, unwanted cracking unless carefully performed. Again, no accidental cracks were encountered.

COMPRESSED NOTCH FLAWS--ALUMINUM

Only one specimen configuration was fabricated in the aluminum alloy. The basic design is the section of the Boeing standard extrusion designated BAC 1520-1168. Because of anticipated difficulty in machining the strain concentrating groove transverse to the specimen

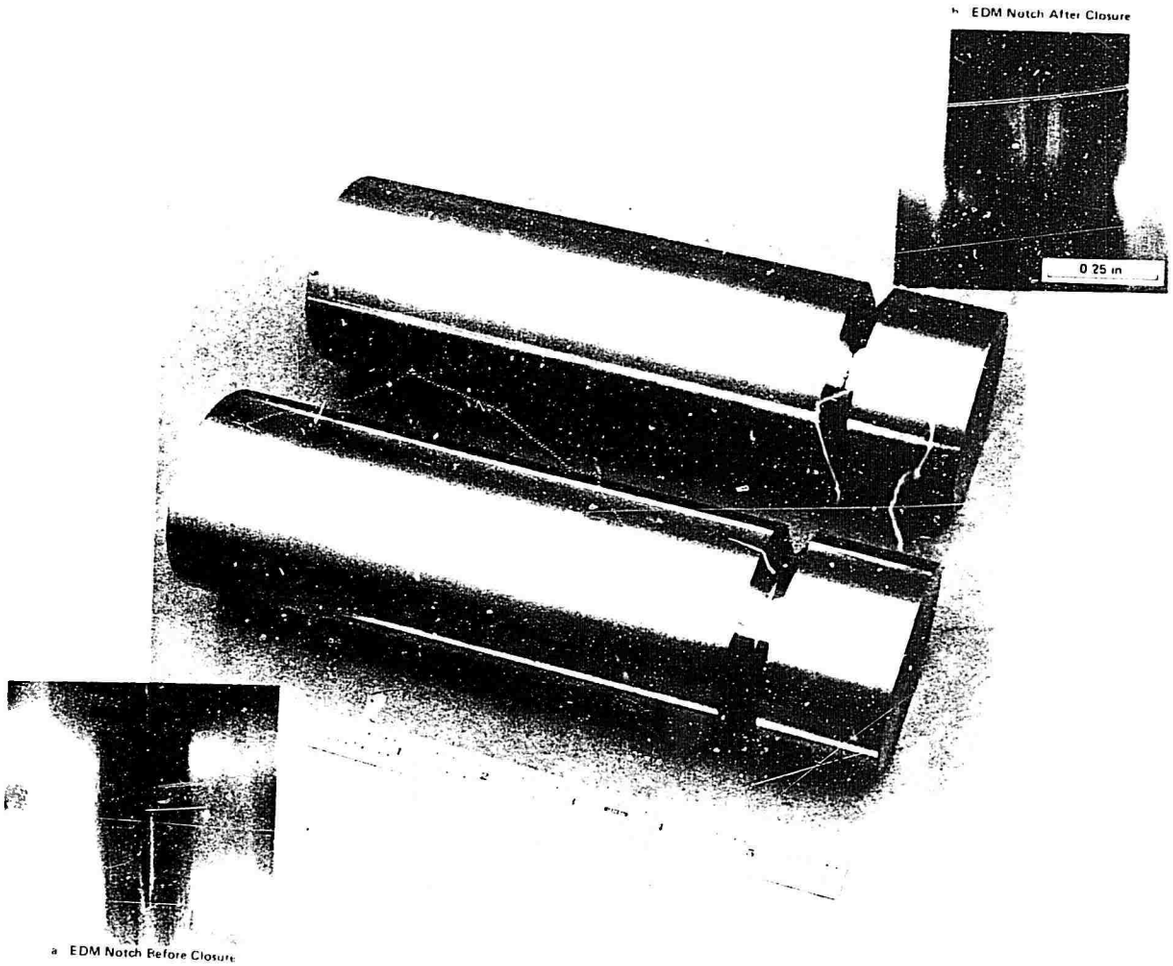


Figure 3.—Two Specimen Blanks Before and After Compression

axis and round the periphery of the section, longitudinal flaws were developed along the lengths of the legs and web of this specimen design. The longitudinally grooved blanks prepared for compression are shown in figure 4 and closure of an EDM notch is illustrated in figure 5.

Several difficulties were encountered in the initial trial specimens. Pronounced buckling of the relatively slender sections developed during compression. When alignment of the blanks in the test machine was more favorable, failures occurred at 45° to the axis of compression by catastrophic shear through the grooved region of the web. These problems were alleviated by annealing the material prior to compression and providing restraining fixtures. The compressed blanks were subsequently re-solution treated and age hardened.

HYDROGEN EMBRITTLEMENT CRACKS

Although the cracks developed with the aid of hydrogen were created deliberately, this type of flaw can be termed natural. The necessary conditions of simultaneous presence of tensile stress and hydrogen were created, and cracks appeared more or less spontaneously by the mechanism known as hydrogen embrittlement.

The role of hydrogen in promoting cracks in ground steel surfaces is well known. The hydrogen may be present either in the original material or introduced by chemical or electrochemical means such as pickling and electroplating. The initial attempt to create this type of cracked specimen was to expose freshly ground surfaces to an acid solution. Various levels of residual stress were induced in the blanks by control of the grinding procedures. The acid applied was a 4% solution of H_2SO_4 containing phosphorous pentasulphide as a "poison." (Poisons act to greatly increase the quantity of hydrogen that passes into the steel.) The initial attempts were unsuccessful; however, a procedure was eventually developed by which cracks could be readily produced with good control of size. This procedure involved electrolytic charging of hydrogen into a ground, high-strength specimen while it was under a steady bending stress. Cracks of the order of 0.10 in. long were created in about 15 minutes in this manner.

Cracks of desired length were obtained by controlling the hydrogen-charged area. This was accomplished by painting the specimen surface with stop-off lacquer leaving a "window" with a length equal to the crack length desired. Crack depth was controlled by varying the stress and current density applied to the specimen. Shallow cracks, 0.010 to 0.020 in. deep, were made by charging hydrogen into the surface while it was stressed to approximately 85 000 psi. At this stress level, the shallower cracks, 0.010 in. deep, required a current density of 10 000 ma/in^2. Deeper cracks were developed with lower current densities and longer charging times. Higher stress levels also produced deeper cracks. For example, 105 000 psi resulted in cracks ranging from 0.035 to 0.050 in. deep. Stress levels higher than 105 000 psi led to the formation of multiple cracks. Stress levels lower than 85 000 psi required a notch or surface scratch to nucleate a crack.

Figure 6 illustrates the setup for creating hydrogen embrittlement crack specimens. The ground specimen is subjected to a uniform bending stress in the bend fixture. A short section of 6Al-4V titanium alloy tubing that is clamped to the surface protected by lacquer and tape surrounds the exposed area to be charged. The tube section becomes the anode

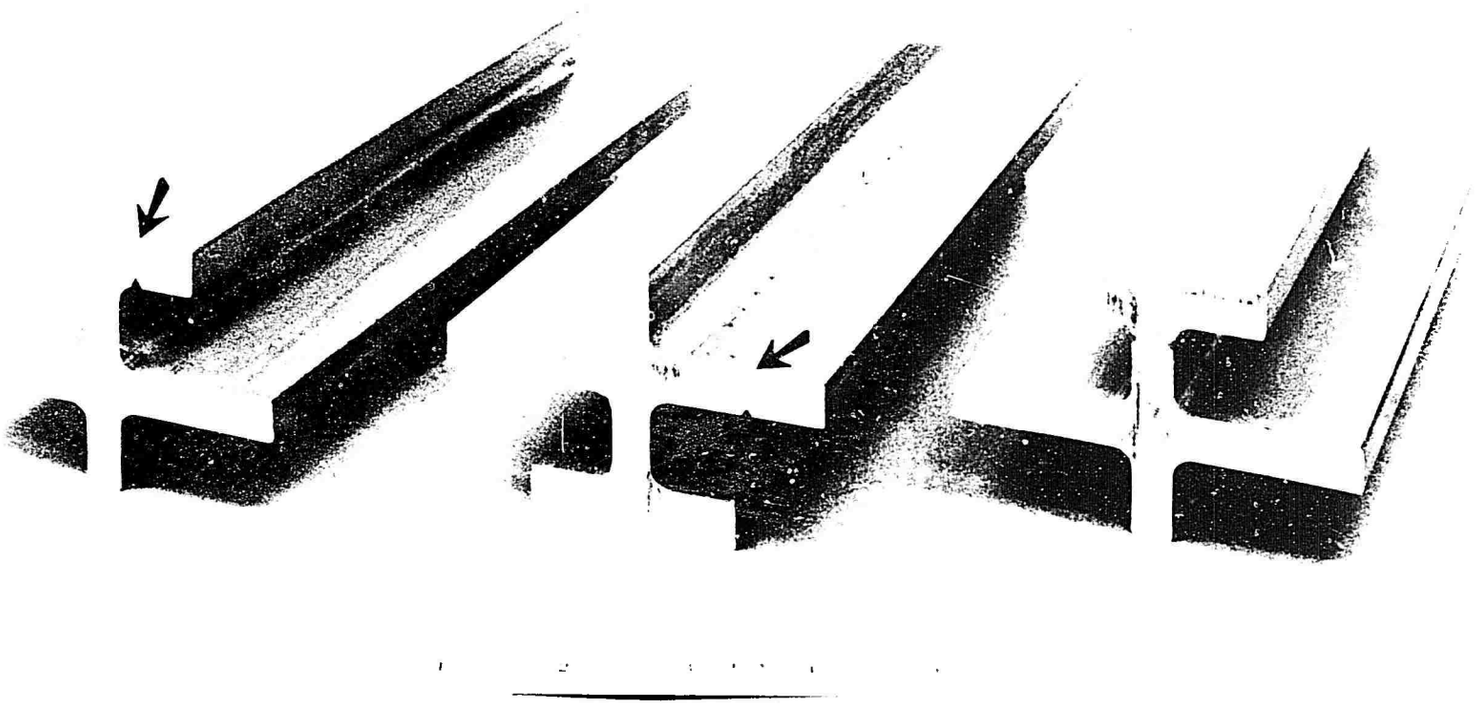
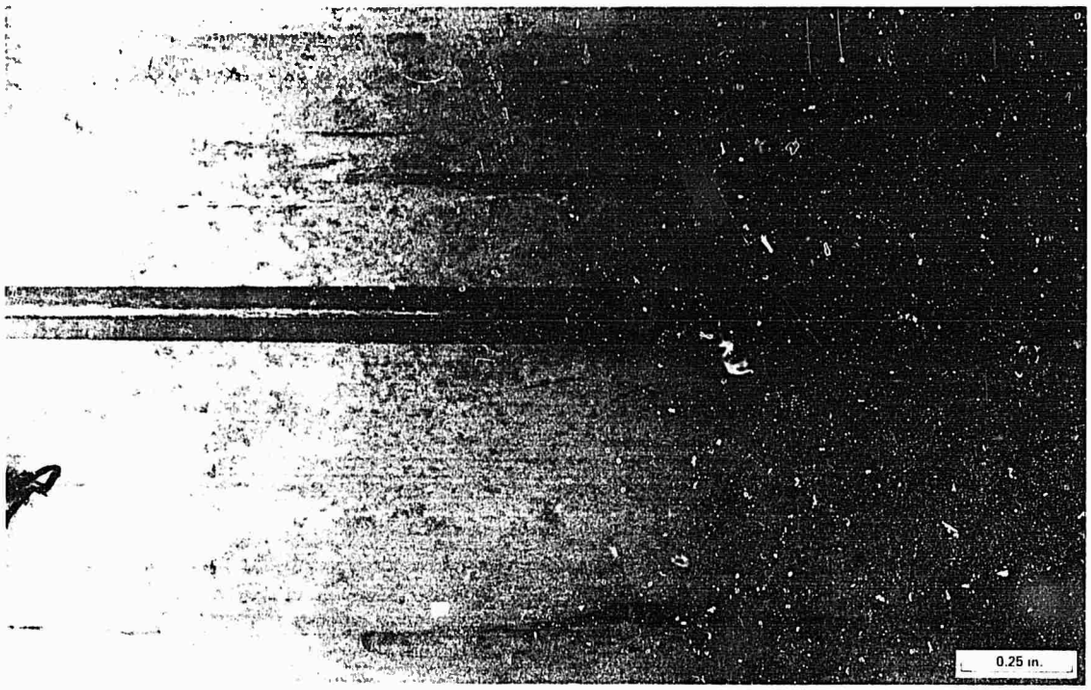
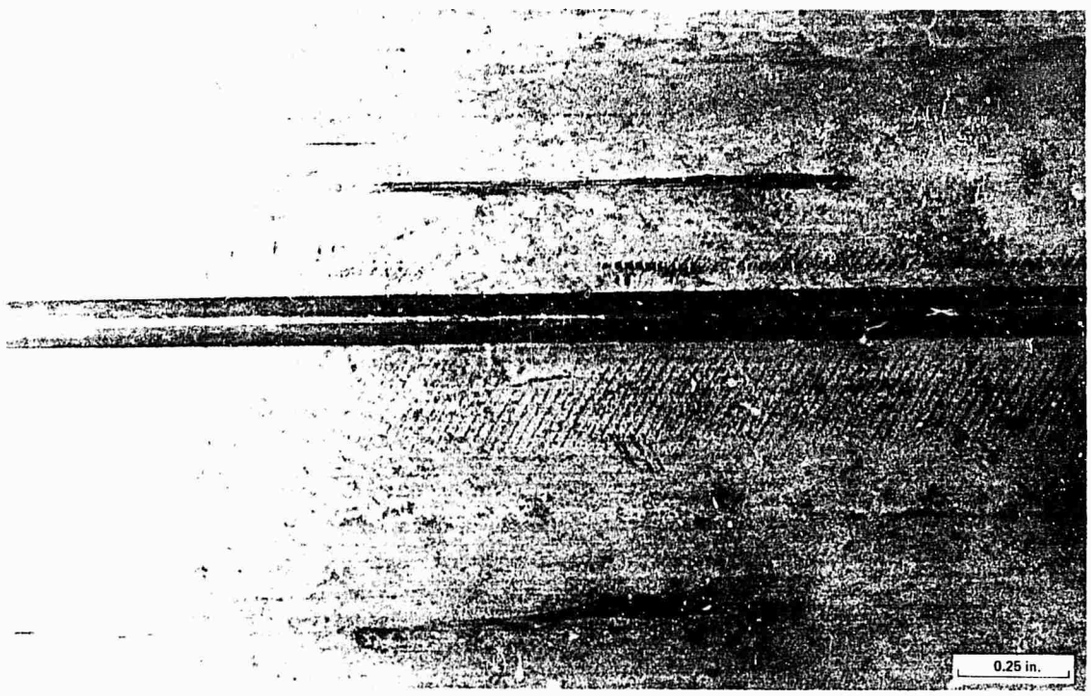


Figure 4.—Three Sections of BAC 1520-1168 Extrusion With Pairs of Grooves in Three Locations Before Compression



a. Before Compression



b. After Compression

Figure 5.–EDM Notch in Aluminum Blank

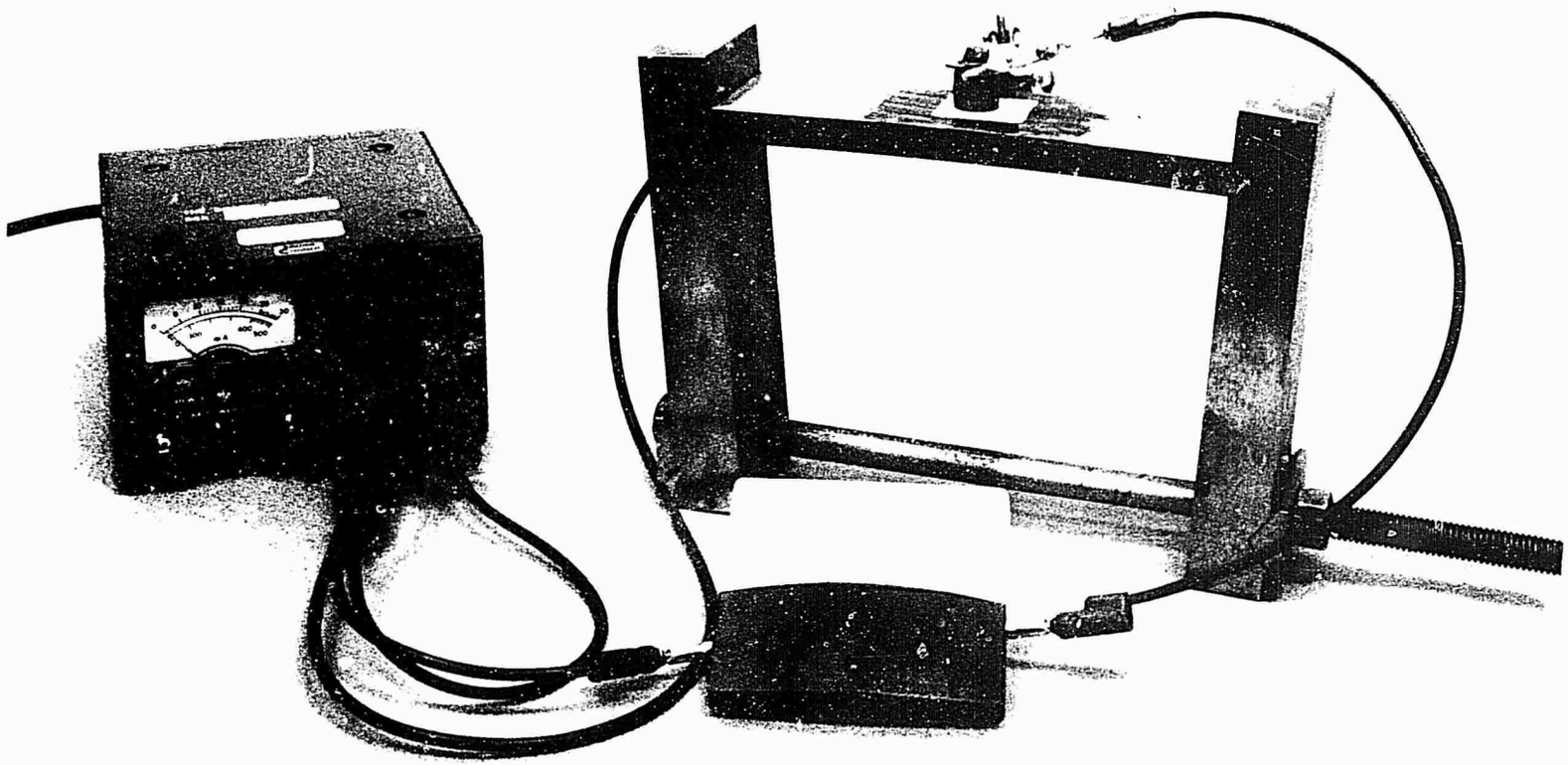


Figure 6.—Electrolytic Charging at a Local Area of a Flat Bar Specimen Under Sustained Bending Stress

and the specimen is the cathode. The electrolyte placed in the tube section is 4% H_2SO_4 plus a trace amount of phosphorous pentasulphide.

When martensitic steel components are the cathode in an electrolytic cell as in electroplating, cathodic cleaning, or electrolytic machining, cations of hydrogen are liberated at the steel surface. The free atoms or charged ions of hydrogen can exist only briefly at the surface, and they either enter the metal lattice in solid solution or they combine to form hydrogen molecules which are too large to penetrate the lattice structure. The net effect is to cause a high concentration of hydrogen in the steel upon prolonged charging. Furthermore, certain elements and compounds present in the electrolyte have been found to greatly increase the amount of hydrogen entering the steel. Studies have shown that the amounts of hydrogen introduced can be increased by as much as ten times (reference 1). These materials are termed "cathodic poisons" and are commonly used in laboratory studies of the effects of hydrogen in steels.

Electrolytic charging, with or without the aid of poisons, is the most widely used method for charging specimens for purposes of studing hydrogen embrittlement and delayed cracking tendencies. With a selected standard electrolyte, usually acidic, the resulting hydrogen content can be varied by changing the charging current density, by using different charging times, or by holding for different times after charging (aging) but before applying stress.

A possible mechanism for the cathodic evolution of hydrogen on metals proposes two occurrences (reference 2).

1. The discharge of hydrated protons (hydronium ion) and adsorption of neutral hydrogen atoms

$$H_3O^+ + e \longrightarrow H_{ads} + H_2O$$

2. Detachment and combination of hydrogen atoms to form molecular hydrogen

$$H_{ads} + H_{ads} \longrightarrow H_2$$

or discharge of a hydrated proton near an adsorbed hydrogen to create molecular hydrogen as follows:

$$H_{ads} + H_3O^+ + e \longrightarrow H_2O + H_2$$

The role of poisons is believed to inhibit the recombination of adsorbed hydrogen ions to form molecules and to increase the lifetime of hydrogen atoms, thereby increasing the probability of their entering the metal.

GRINDING CRACKS

Flat bar specimens (0.5 by 2.0 by 8.0 in.) were heat-treated to 270 to 300 ksi strength level and subjected to varied grinding procedures to achieve surface cracking. Grinding

parameters investigated included types of wheels, rate of coolant (and no coolant), depth of grind, cross feed per pass, rate of dressing feed, and rate of table feed. Wheel speed was esentially constant. Although the procedures followed were judged to be quite abusive, grinding cracks did not develop during the initial trials.

The sensitivity of martensitic steels to the formation of grinding cracks has been known by manufacturing process engineers to be greatly enhanced by the presence of hydrogen within the material. This effect has been demonstrated both when the hydrogen was present in solid solution at the time of grinding and when it was introduced immediately afterward during pickling or plating. Therefore, further effort to induce grinding cracks included the use of electrolytic charging of hydrogen into the specimen surface first after grinding, and later, before grinding. Cracking was achieved and the greater successes were experienced when charging preceded grinding.

Previously described methods of hydrogen embrittlement cracking were applied, except that bending moments were not imposed and residual grinding stresses were the sole source of stress. Again, hydrogen was charged into small areas in attempting to generate small and perhaps single cracks. It was found necessary to charge the surface for much longer periods of time (2 hr) and to refrigerate the specimens by packing in dry ice for the interval of time between charging and grinding. At this state of development, cracking was obtainable and was fairly well confined to the area that was charged with hydrogen. However, multiple crack patterns (typical of natural grinding cracks) were occurring, and the cracks were tending to grow beyond the charged area. In order to restrict the extension of the cracks, it appeared necessary to restrict both the region of high residual stress as well as the charged area. This was accomplished by grinding the surface in a manner leaving rectangular islands standing 0.002 in. above the surrounding surface. These islands were charged with hydrogen and then ground off in one pass with a 0.002 in. grind depth. In this manner, only the area charged was subjected to the abusive grinding. This provided improved control of the area of cracking. However, since multiple cracking still occurred it was necessary to curtail development at this stage and use multiple cracks over a range of sizes.

SECTION IV
SPECIMEN FABRICATION

INTRODUCTION

Final fabrication and design details were established during the development of the flawed specimens and during fabrication of initial specimens to confirm the capability for creating the test articles required for the program. These details were not changed during the program unless absolutely necessary to avoid introducing a source of difference among the finished flaws.

Methods for creating the types of flaws in varied locations within differing specimen configurations and achieving the final flaw sizes desired were not developed previously, and the scope of this program did not include extensive investigation and development of fabrication techniques. Consequently, the procedures described herein and used to produce the program test specimens have not been proven optimum. Particularly, further investigation would improve the reproducibility and control in creating grinding cracks. Also, from the standpoint of economy in subsequent investigations, it would not be necessary to use a large instrumented test machine (fig. 7) to compress the notched specimen blanks. Shop presses with sufficient throat opening to receive the specimens and with 250 tons or greater capacity could be used. The compressive strain could be limited by placing properly dimensioned stop blocks alongside the specimen blanks.

FINAL FABRICATION PROCEDURES

COMPRESSED NOTCHES–STEEL

The strength level of the as-received 4340M material was not completely uniform as determined during compression of the first few trial specimens and subsequently the material was given a subcritical annealing treatment at 1275 to 1325°F for 5 hours prior to machining. This lowered the average hardness to about Rockwell C 25 and improved the strength uniformity.

Specimen blanks for both solid and hollow specimens were lathe turned (figs. 8 and 9). The grooves machined for placement of EDM notches were ground to a 0.020-in. radius in all cases. A compromise width of EDM notches of 0.005 to 0.008 in. was specified. Although narrower slots are attainable, other difficulties arose if lesser widths were required, particularly with the deeper notches. Warpage of the electrodes resulted in irregular slots and the thinner electrodes burned away too rapidly.

After the EDM notches were made, the blanks were subjected to axial compression loading of sufficient magnitude to close the notches by permanent, plastic deformation. This was accomplished with a 1 200 000-lb test machine as shown in figure 7. The machine was instrumented to graphically record the load applied versus the crosshead travel. The amount of strain beyond the approximate proportional limit was monitored and the loading halted

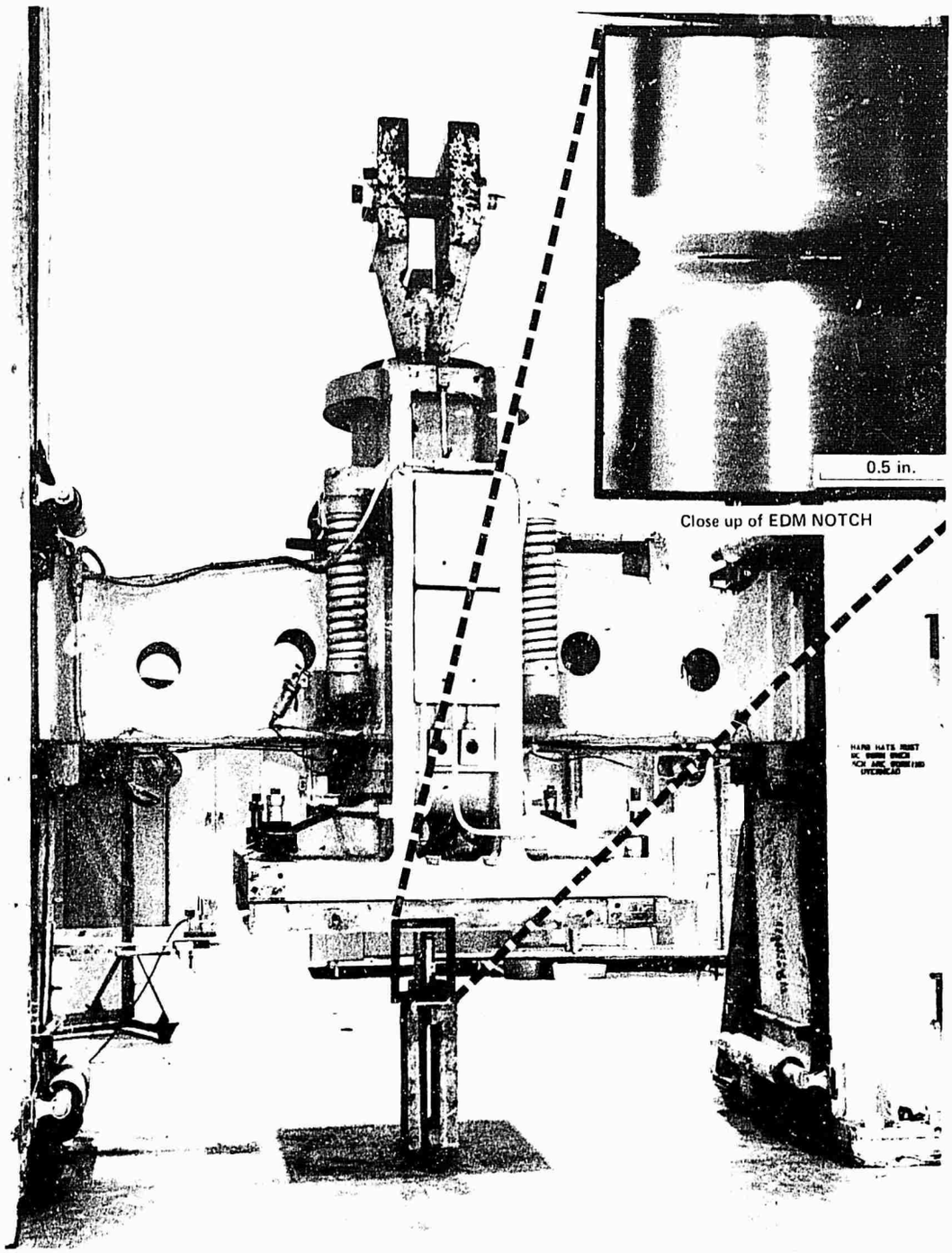


Figure 7.—Compression of Externally Notched Steel Specimen in 1 200 000-lb Test Machine

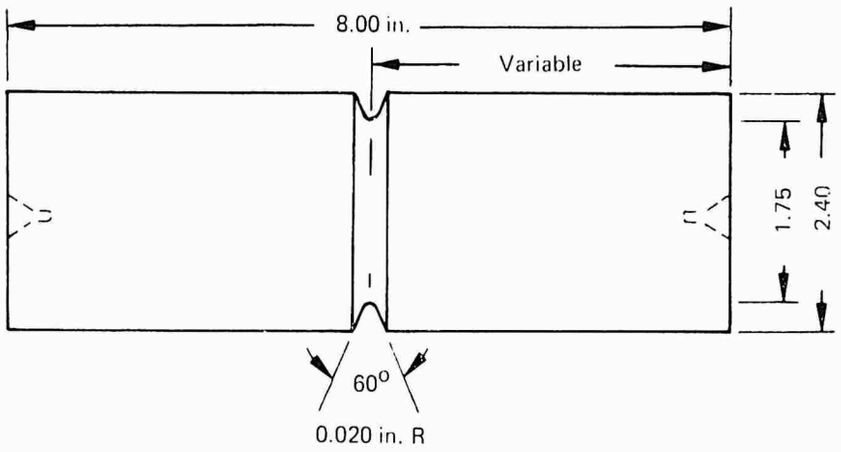


Figure 8.—Drawing of Grooved Blank for Externally Flawed Specimens

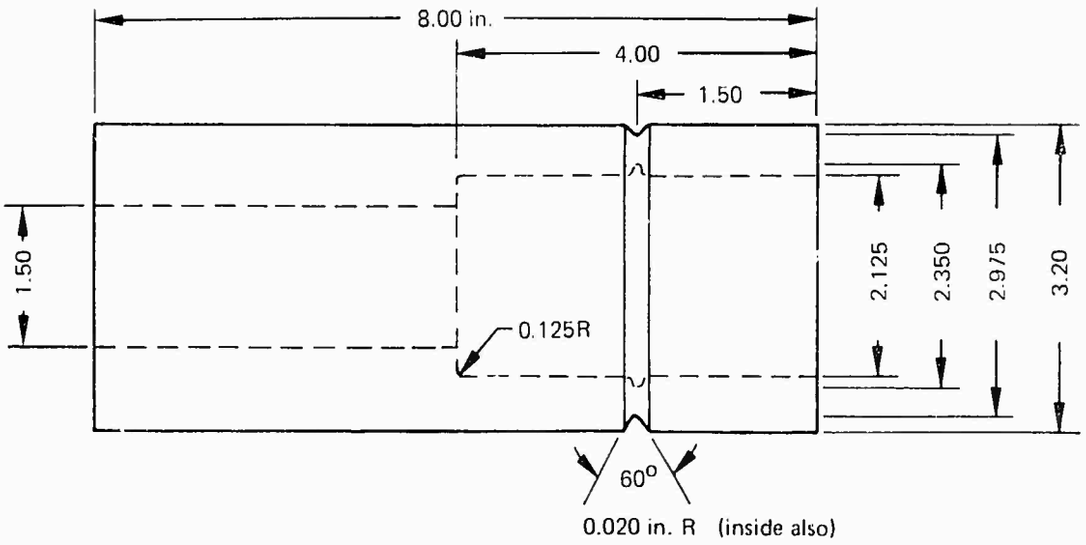


Figure 9.—Drawing of Grooved Blank for Internal Surface Flawed Specimens

at 0.10 in. total plastic strain. The loads varied sufficiently that each specimen required monitoring of its load-strain curve. However, blocks shorter than the specimens by an amount equal to the total elastic plus 0.10 in. plastic compression, placed next to the specimens, could be used in future lots to gage the proper amount of permanent deformation. Figure 10 contains load-strain diagrams typical of compression of the solid steel blanks and figure 11 shows diagrams typical of compression of the hollow steel blanks.

Following compression, the specimen blanks were machined to their intended final configuration. It was then necessary to establish the ultrahigh tensile strength level of 270 to 300 ksi that this alloy commonly exhibits in critical aircraft applications. This was accomplished by a marquenching procedure in order to minimize the potential of cracking these severely notched specimens during heat treatment. For these specimens, the procedure involved austenitizing at 1600°F, quenching in *Mar-Temp* oil at 300°F to 400°F, and then double tempering at 575°F. The fully heat treated specimens were then finish ground to remove the discoloration that occurred during the heat treatment.

COMPRESSED NOTCHES—ALUMINUM

Fabrication of the compressed flaws in the aluminum specimens involved the same fundamental approach as for the steel specimens. However, the starting material required only the milling of the necessary grooves and placement of the EDM notches. In this specimen configuration it was advantageous to machine longitudinal grooves rather than transverse. A cross section of the standard extrusion with typical groove locations is shown in figure 12.

As in the prior experience with the steel specimens, a thermal softening treatment was required to facilitate the compression operation. The initial trial specimens demonstrated that the as-received temper (T3811) had too high a yield strength for the amount of deformation required. The blanks were annealed at 800°F, and all subsequent blanks were successfully compressed.

Typical load-strain curves developed during compression are shown in figure 13. As expected, the 10-in. long sections of annealed extrusion required much less load to achieve closure of the EDM notches than did the steel blanks. The loads of less than 125 000 lb are within the capacity of many laboratory tensile testing machines as well as small shop presses.

Following compression, the specimens were solution heat-treated and artificially aged to the T6 temper. The blanks were then milled to remove the grooves and established smoothly machined surfaces in the finished configuration.

GRINDING AND HYDROGEN EMBRITTLEMENT CRACKS

Fabrication procedures were varied throughout the development of methods of achieving cracks in ground surfaces. While numerous cracks of varied sizes were created, optimum standard procedures were not derived within the limits of the variations investigated. The general procedures for creating ground surface cracks are referred to in section III.

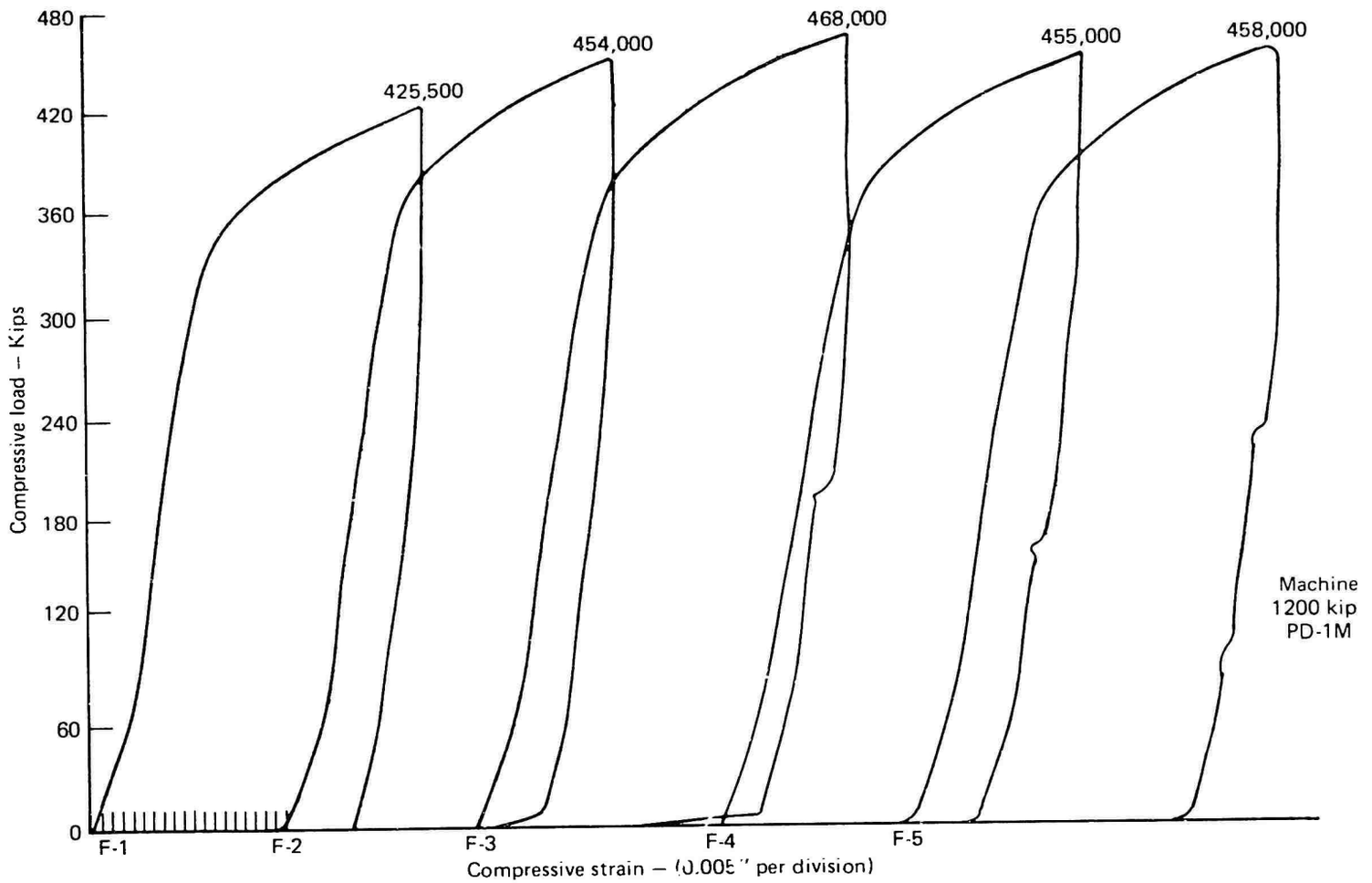


Figure 10.—Load-Strain Diagrams of Compression of Solid Steel Specimen Blanks

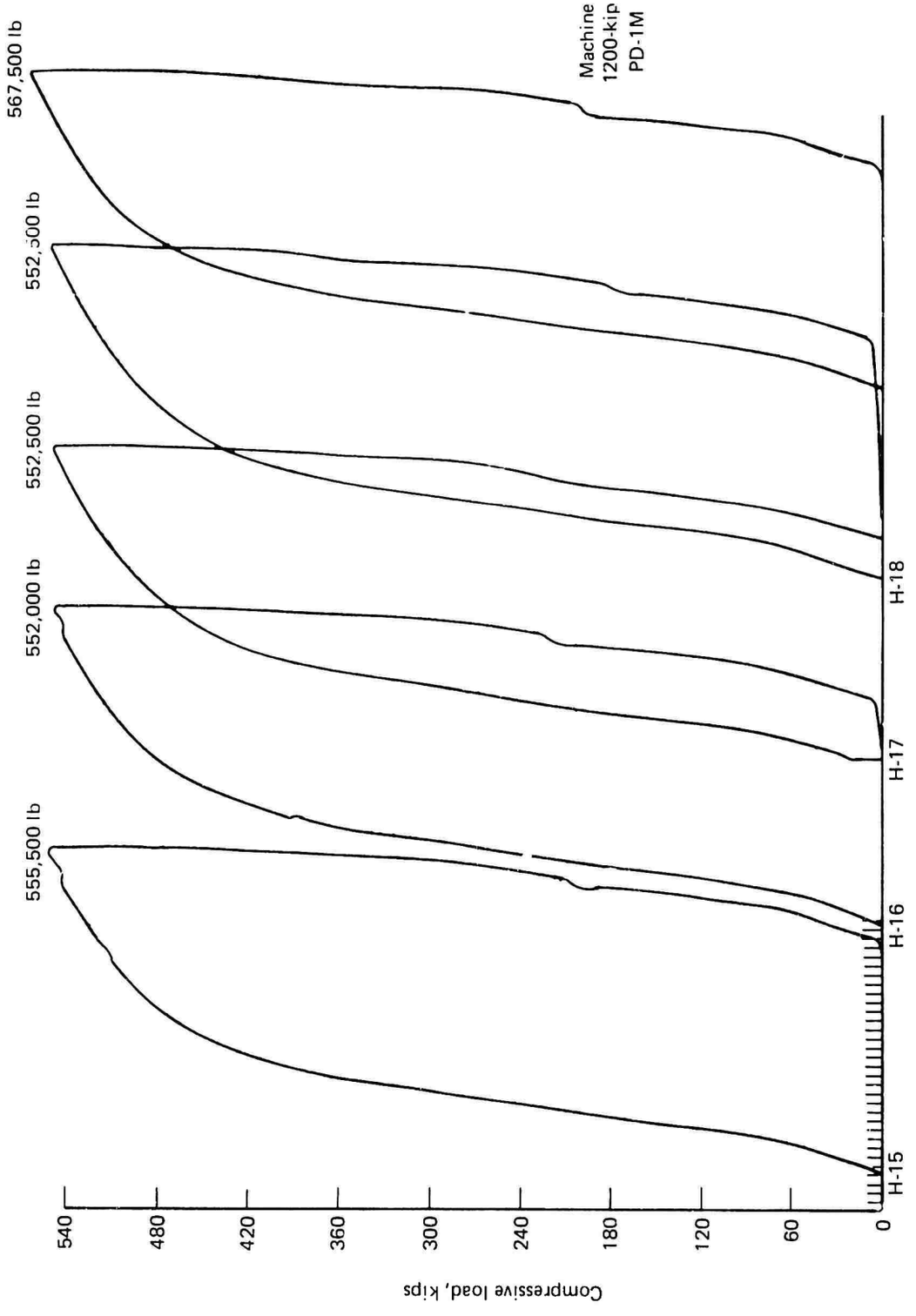


Figure 11.--Load Strain Diagrams of Compression of Hollow Steel Specimen Blanks

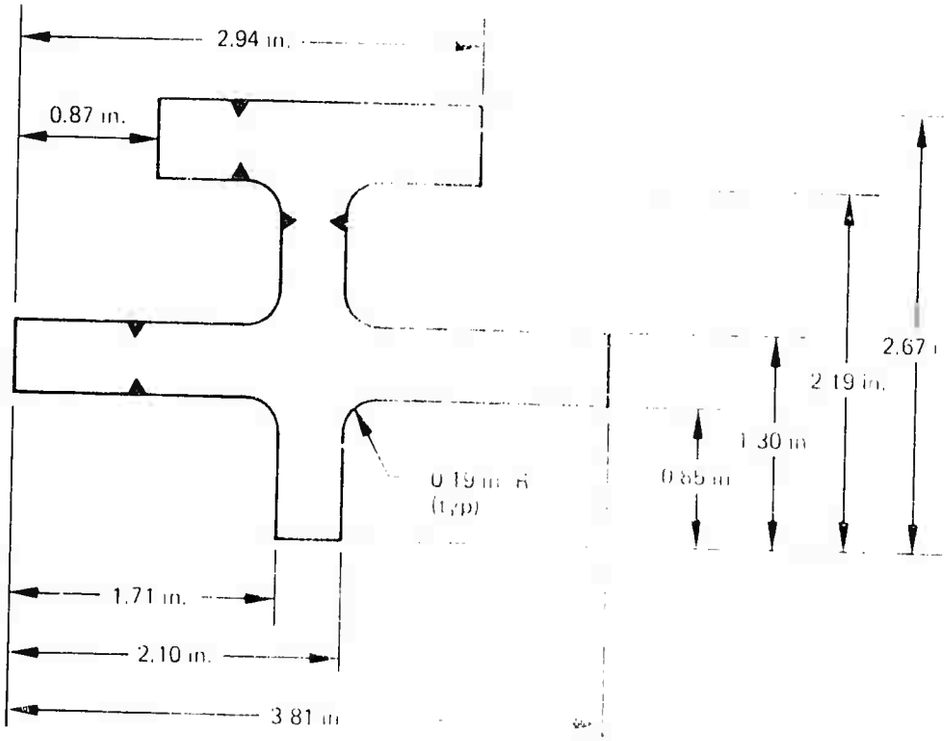


Figure 12.– Cross Section of [illegible] Locations

CONTAMINATED FLAW SPECIMENS

Compressed notch flawed specimens of [illegible] were thermally treated as representative of those having small- and medium [illegible] thermal treatments that would cause significant [illegible] and oxide contamination within the flaws. These prolonged [illegible] exposures were also applied in air atmosphere laboratory furnaces.

Four externally flawed steel specimens were oxidized [illegible] for 25 hours. (Higher temperature treatments [illegible] atmospheres.) This exposure simulated several subtractive operations that possibly could be performed on a production part. Following [illegible] parts were also heat-treated to the 270- 300-ksi strength level and [illegible] machined appearance.

Two of the aluminum cruciform specimens were also [illegible] oxidizing atmosphere in a furnace operated at 800°F. [illegible] 33 hours, which is equivalent to 10 or more anodizing operations. The parts were then solution treated, water quenched, and aged at room temperature.

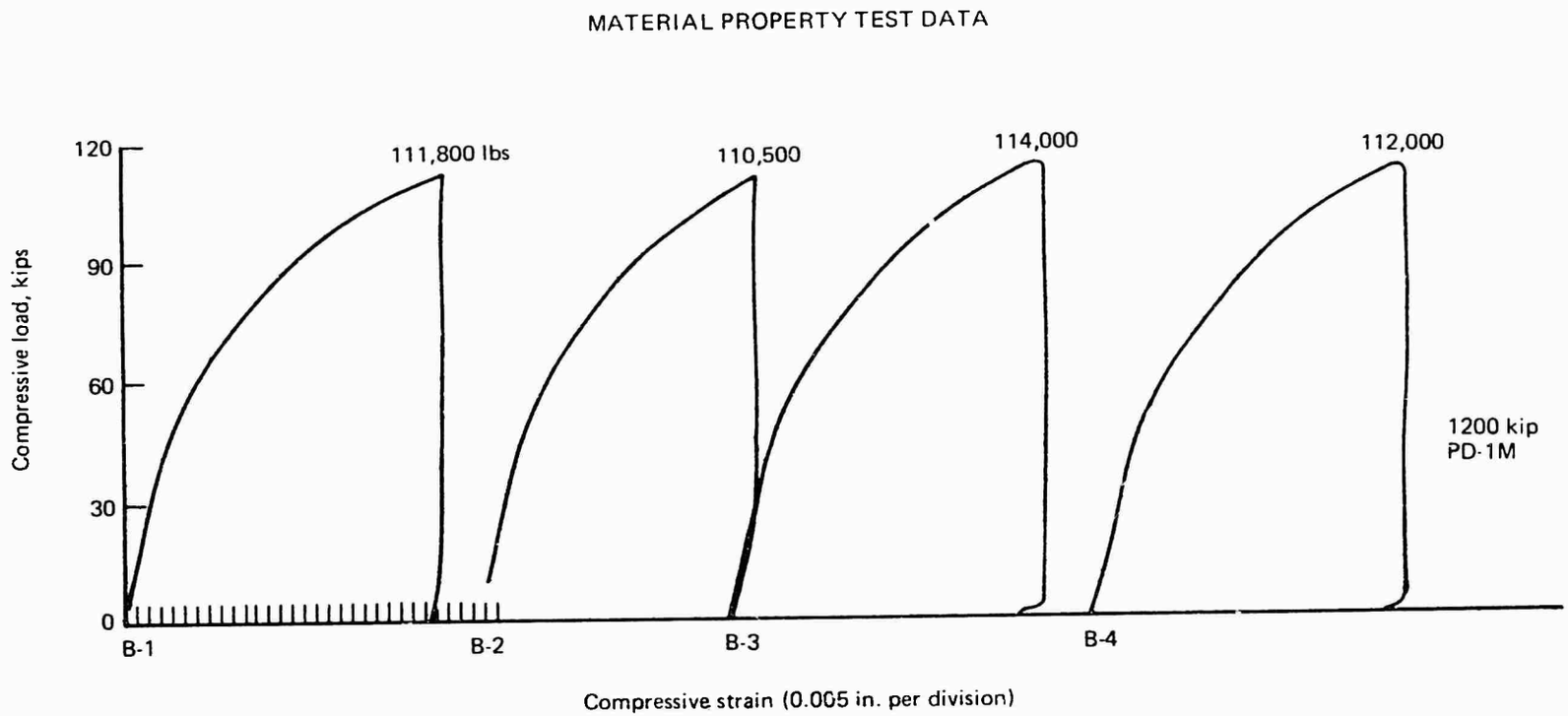


Figure 13.—Load-Strain Diagrams of Compression of Extruded Aluminum Specimen Blanks

FINAL SPECIMEN CONFIGURATIONS

The final specimen configurations have incorporated design features commonly found in production parts. They contain flaws in both critical locations and in regions presenting some difficulties for each of the five NDT methods. The specimens contain changes of section with internal and external fillets. They have both plane and compound curved surfaces. Flaws were located both in and away from stress concentration features and on external and internal surfaces. While the major emphasis was on the externally flawed, compressed notch specimens of steel and aluminum, the other design modifications and flaw types provided bases for comparing such things as the effects of location of flaws on probability of detection by visual versus instrumented probe methods. Such comparisons would indicate the importance of certain human factors in reliability of inspection methods.

Figures 14, 15, and 16 show the specimen blanks and the finished specimen configurations for the externally flawed, compressed notch steel cylinders and two more complex variations. Figures 17 and 18 are hollow specimens and their prenotched blanks. The first is a straight, uniform thickness hollow cylinder. The second contains the visible external square groove and an internal change of thickness as shown in figure 19.

Figure 20 shows a grooved blank and the finish machined aluminum extruded specimen. In this configuration the flaws are orientated longitudinally. The last specimen design, as shown in figure 21, is the simple flat bar with hydrogen embrittlement cracks and hydrogen-induced grinding cracks as variations in flaw types.

FLAW CHARACTERIZATIONS

In the interest of conserving specimens, few specimens fabricated in this program were destroyed for direct examination of the flaws. However, as determination of final flaw characteristics was important to the validity of the results of this program, flaws were examined as follows:

The EDM notches in the specimen blanks were replicated with a silicone flexible mold compound. This was a room temperature vulcanizing rubber, 630A, manufactured by the General Electric Company. This RTV material was very low shrinkage and provided a highly accurate cast replica as shown in figure 22. Such replicas served to confirm the geometry of the original EDM notches to compression.

Following compression of the EDM notched steel specimens, final machining, heat treatment, and finish grinding, some optical measurements were possible with the aid of a low-power microscope. However, final determinations were often assisted by study of magnetic particle indications where the flaw was not optically discernible. Photographs and pressure-sensitive tape transfers of the particle indications were obtained and retained as permanent records. These procedures were also followed for the ground surface crack specimens. Figure 23 illustrates magnetic particle indications of a typical compressed notch flaw and grinding cracks.

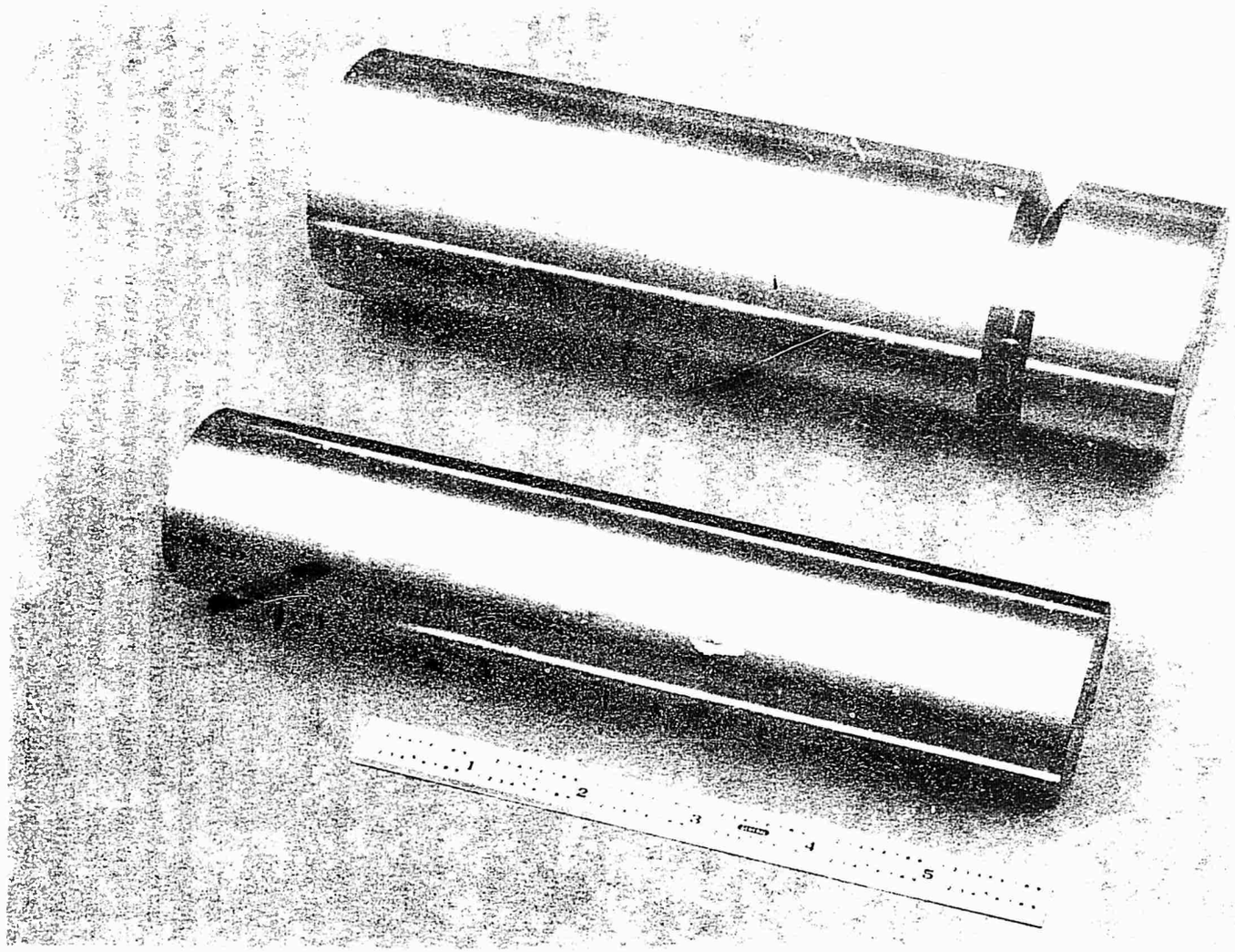


Figure 14.—Straight Cylinder Specimen and Blank

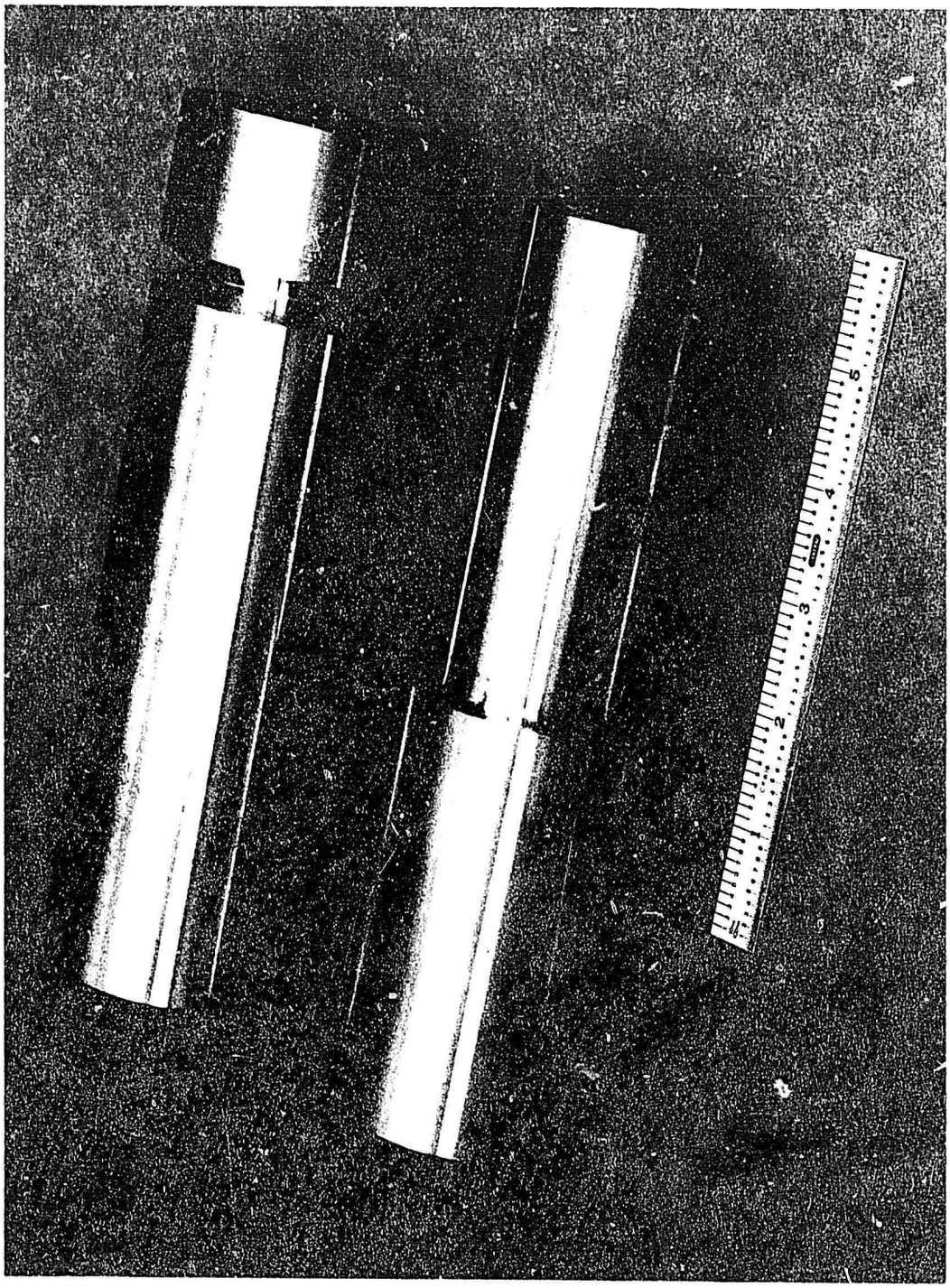


Figure 15.– Filleted Cylinder Specimen and Blank

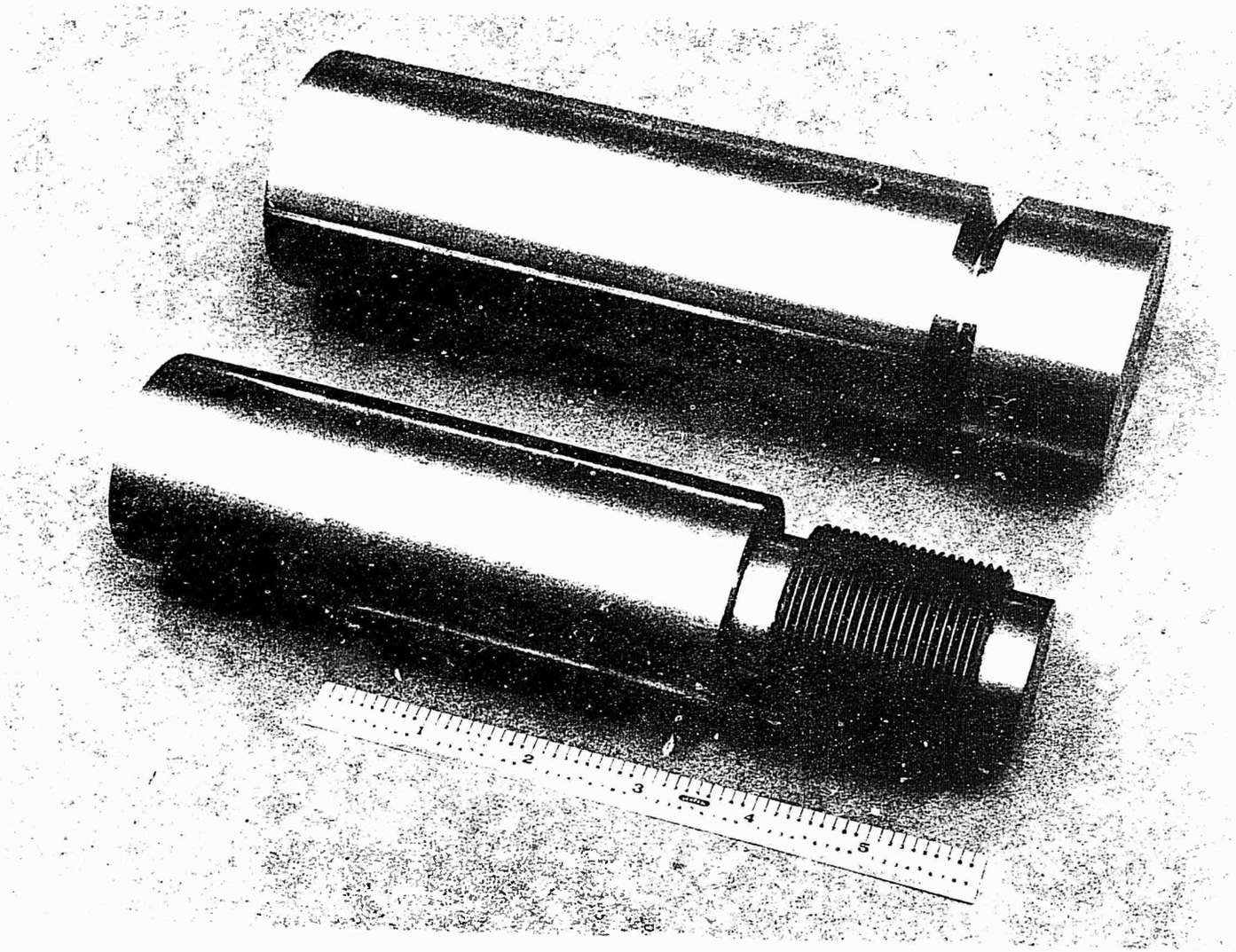


Figure 16.—Threaded Cylinder Specimen and Blank

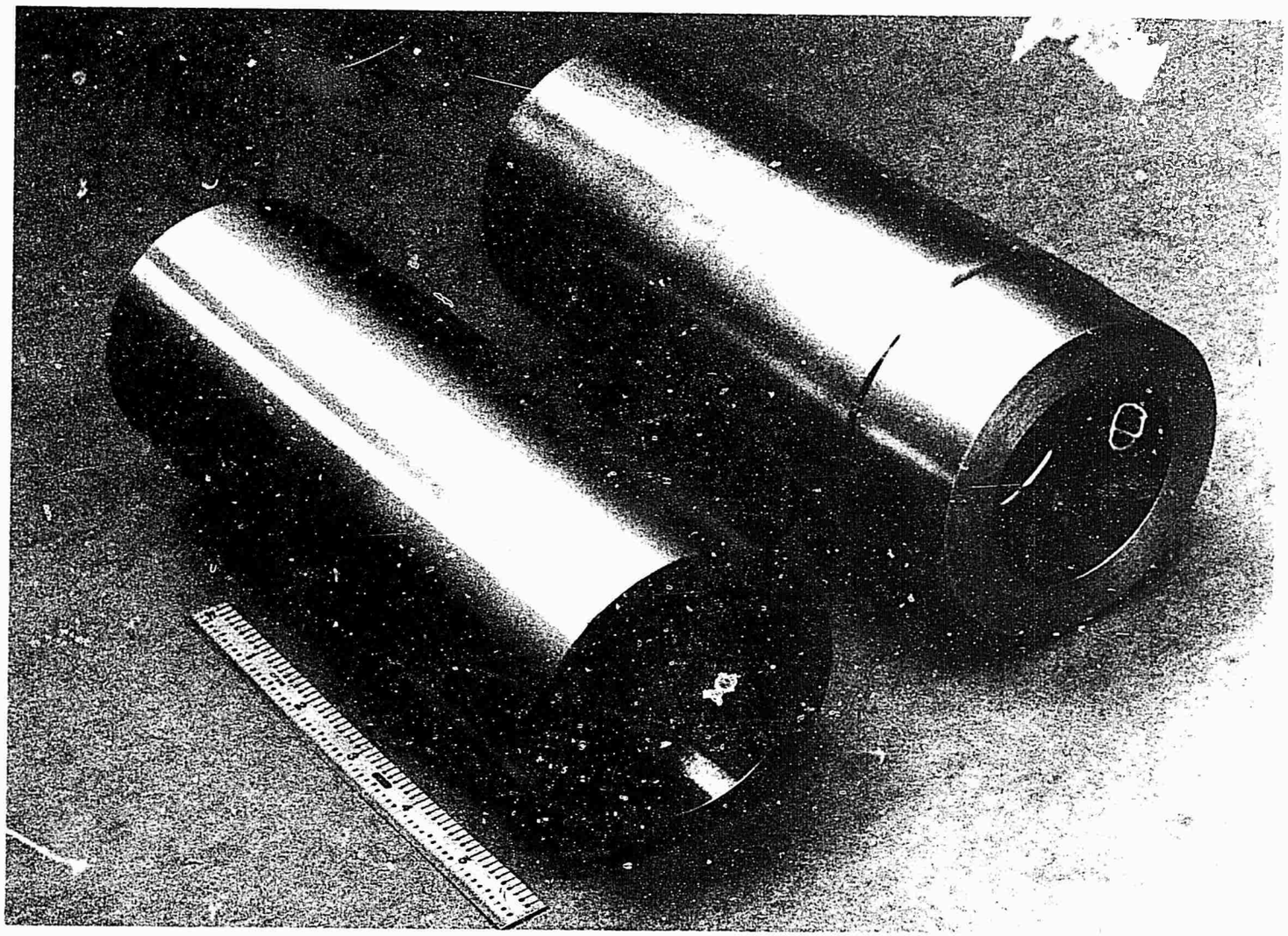


Figure 17.—Straight Hollow Cylinder Specimen and Blank

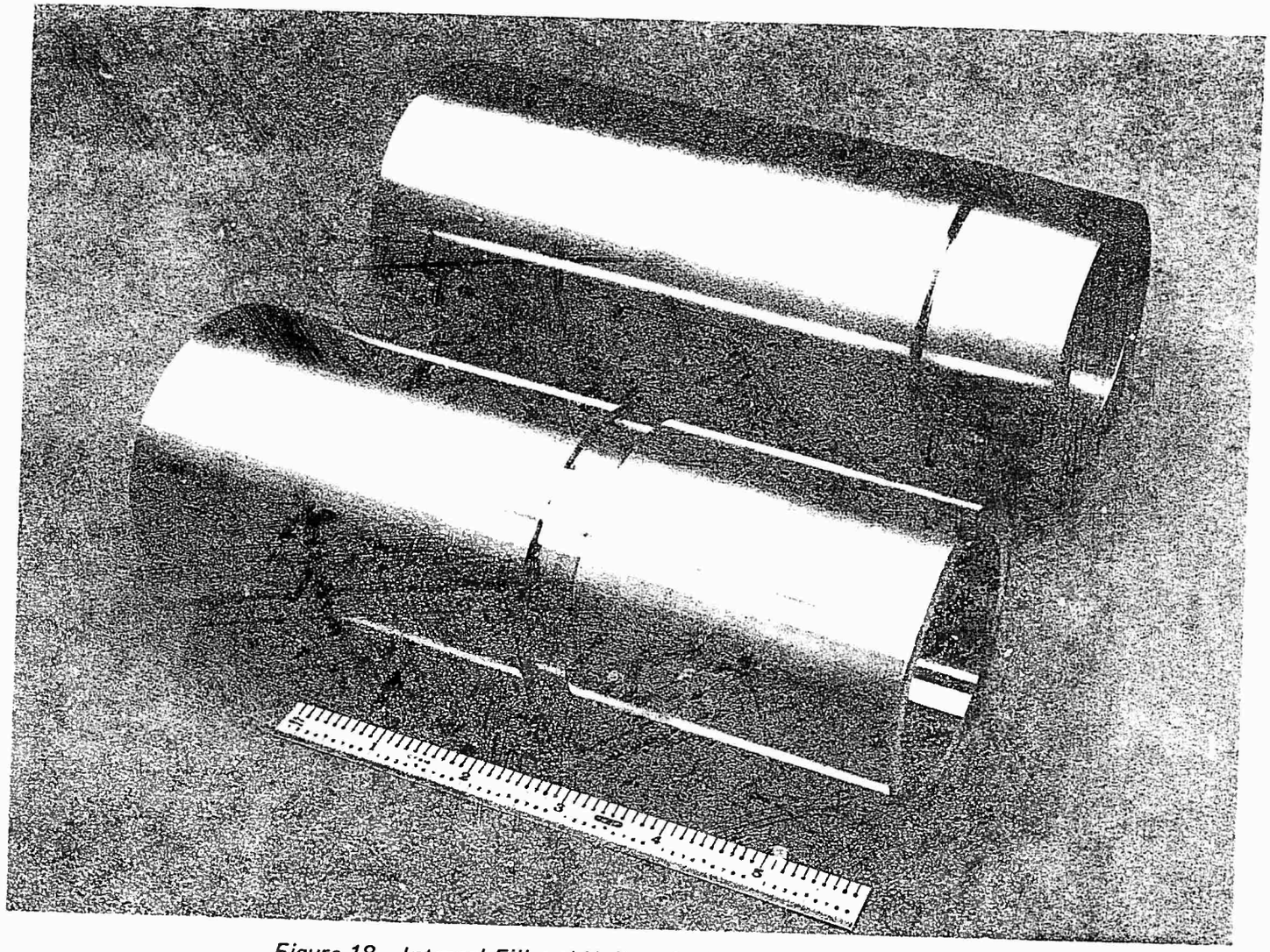


Figure 18.—Internal Filleted Hollow Cylinder Specimen and Blank

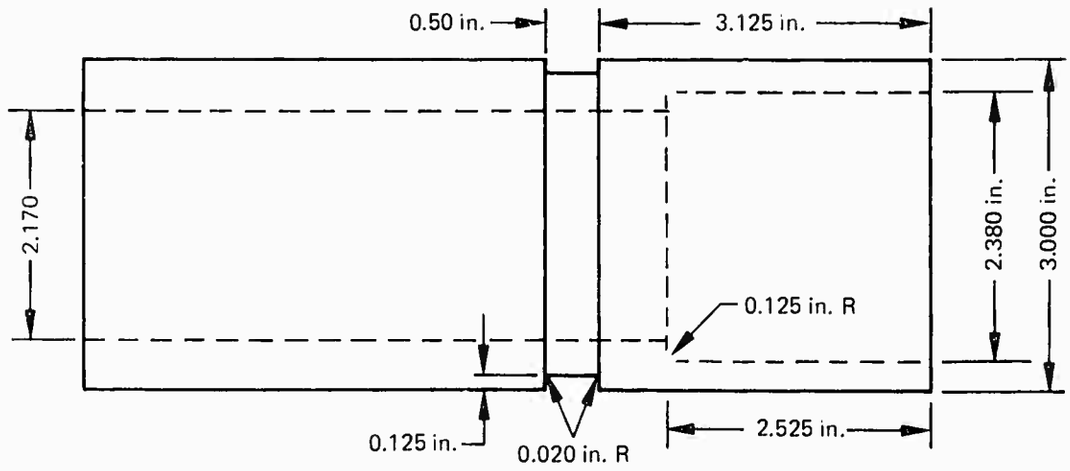


Figure 19.—Sketch of Internal Fillet Hollow Specimen

Similarly, the compressed flaws in the aluminum extruded section were measured following heat treatment and final machining with low-power optical aids where possible and with the help of penetrants to assist in determining the flaw extremities. Photographs of representative penetrant indications were retained and typical penetrant indications are shown in figure 24.

Additional flaws were fabricated for destructive examination to evaluate the stability of the compressed notch dimensions and shape beneath the surfaces during the complete fabrication processes. These flaws were broken open along the flaw planes. Other flaws were carefully sectioned and prepared for metallographic examination in order to determine the widths of the flows at and below the surface and aid in determining if the flaws had extended during heat treatment or other processing. The fractographic and metallographic studies revealed a slight tendency for the compressed notch flaws in steel to grow slightly (9% to 11%) in length at the surface. No similar effect was noted in the aluminum specimens.

In figure 25, views (a) and (b) show the faces of typical compressed notch flaws in hollow and solid specimens. Slight growth beyond the original EDM notch is evident at the ends of the flaw in view (b). This and some rounding of the bottoms of the flaws are the only changes from the original 90°, 0.010 in. radius contour of the EDM electrode.

Photomicrographs of sections through two compressed notch flaws in hollow and solid steel specimens are shown in figure 26. The flaw widths are of the order of 0.0005 to 0.0007 in.

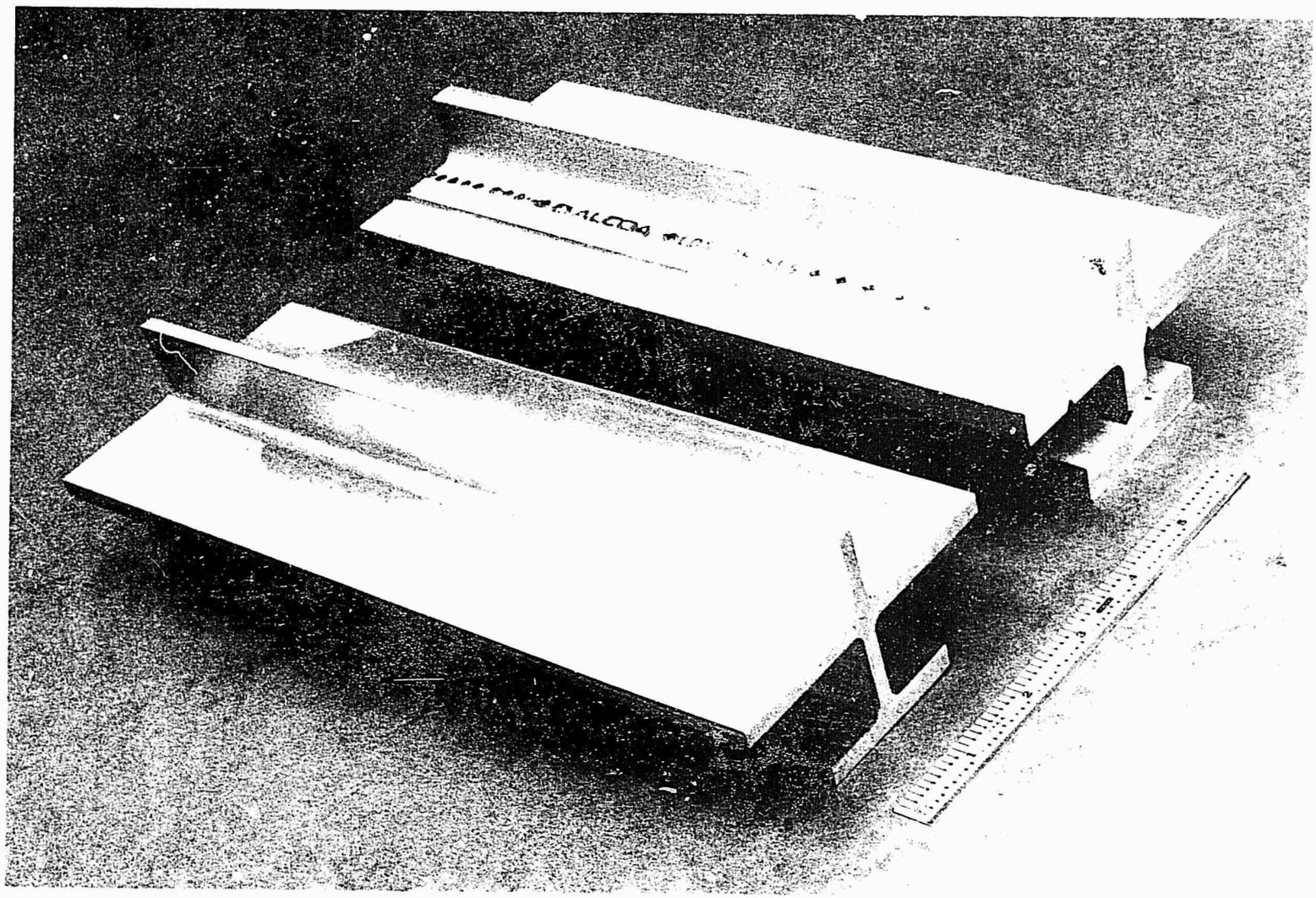


Figure 20.—Extruded Aluminum Specimen and Blank

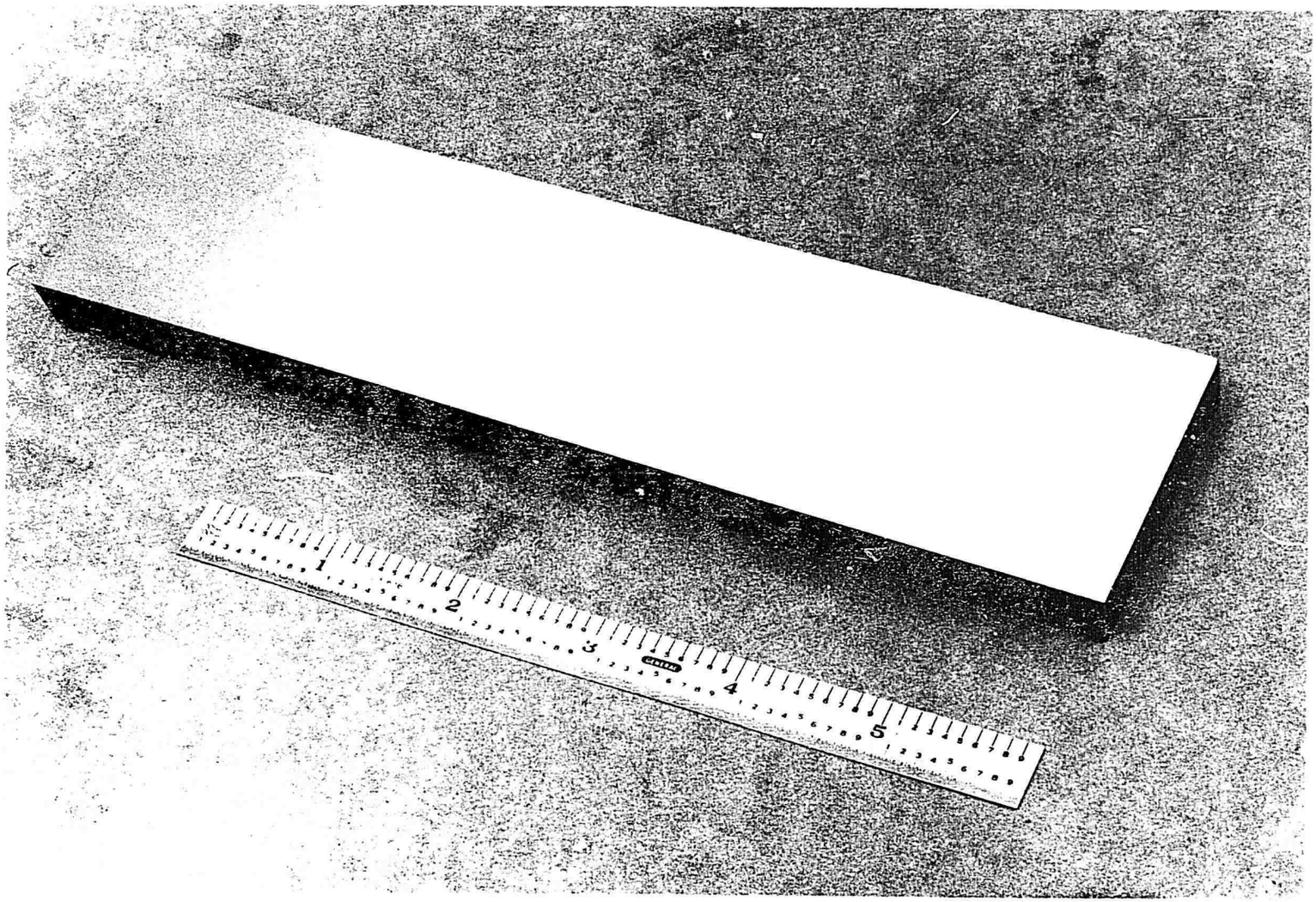


Figure 21.—Hydrogen and Grinding Crack Specimen

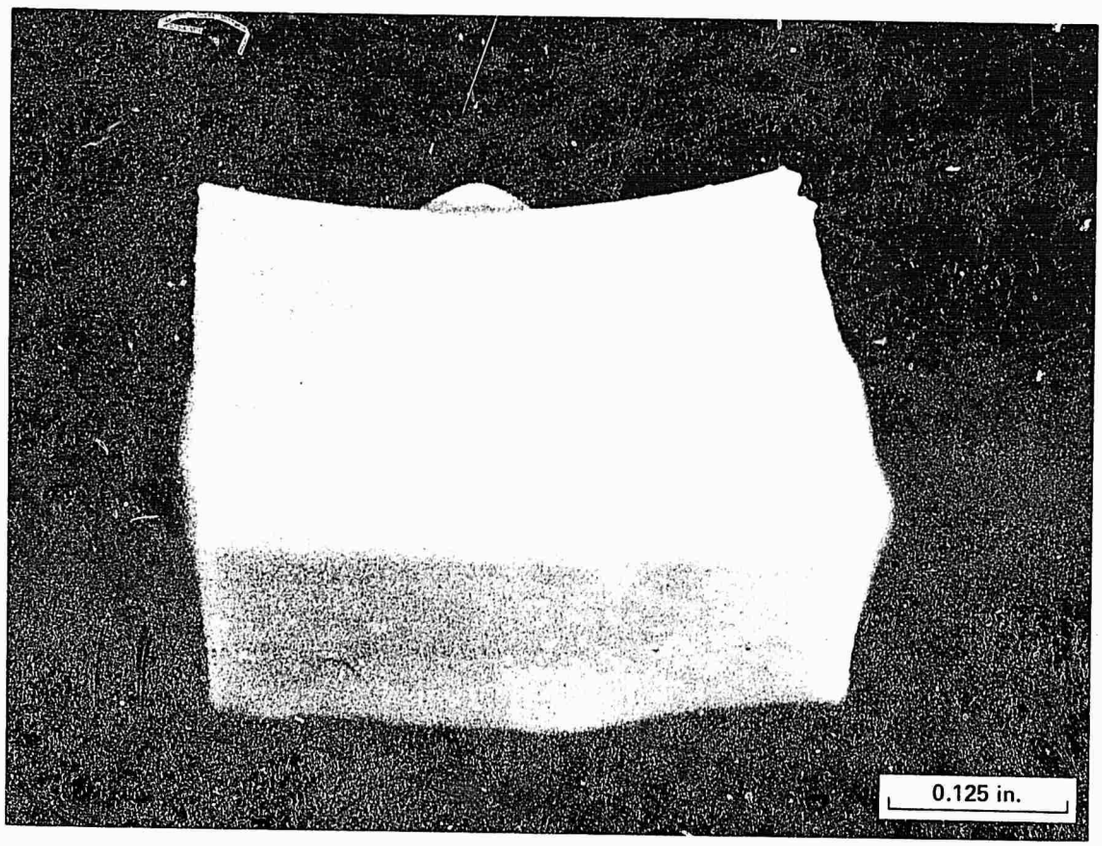
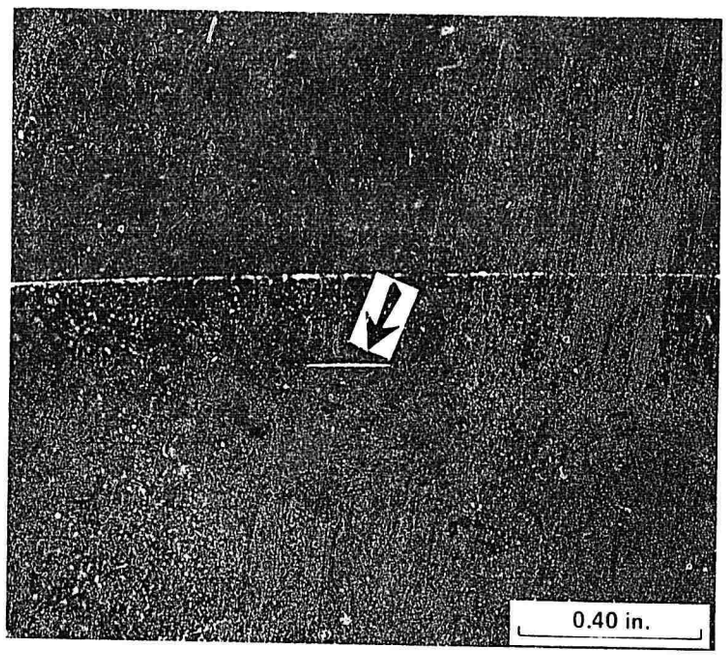
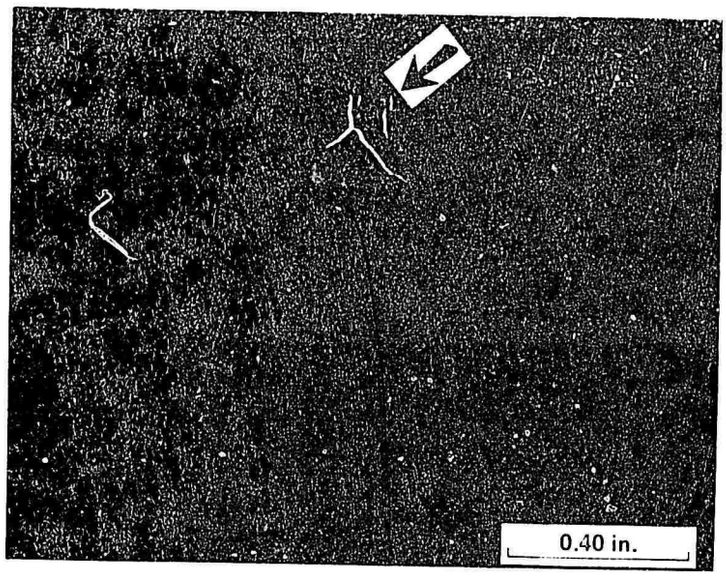


Figure 22.—Typical Liquid RTV Rubber Replica of an EDM Notch in an External Groove Specimen Blank (8X)



a. Compressed Notch Flaw



b. Grinding Cracks

Figure 23. Fluorescent Magnetic Particle Flaw Indications (2.5X)

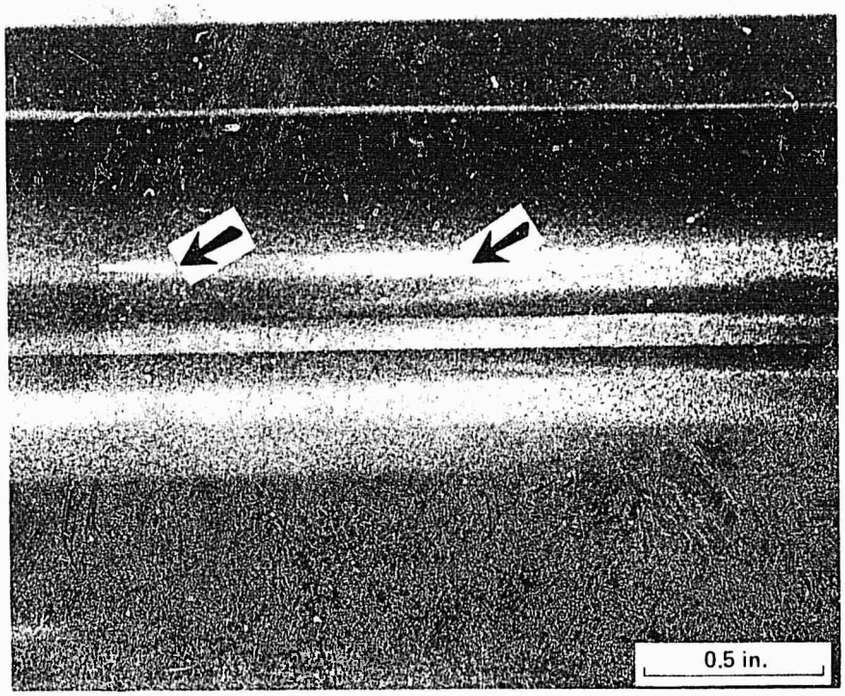
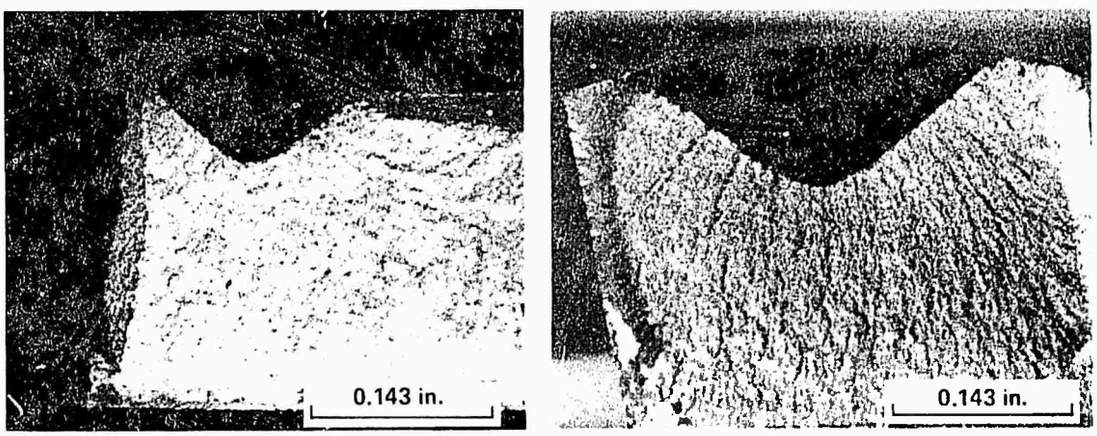


Figure 24.—Two Typical Fluorescent Penetrant Indications of Compressed Notch Flaws in an Aluminum Specimen (2X)



a. Hollow Steel Specimen **b. Solid Steel Specimen**

Figure 25.—Two Fractures Exposing Compressed Notch Flaws in a Hollow Specimen and in a Solid Steel Specimen (7X)

Fractographs of hydrogen embrittlement cracks in figure 27 show two different length/depth ratios obtained by varying the stress level and rate of hydrogen charging. In general, the shallower cracks were obtained with low levels of bending stress and high charging rates as discussed in section III.

Metallographic sections through hydrogen embrittlement cracks and hydrogen-induced grinding cracks are shown in figure 28. These cracks are quite narrow, measuring 0.0001 to 0.00015 in. in width.

Figure 29 presents fractographs of the compressed EDM notches in the aluminum cruciform extrusion specimens revealed very faithful retention of the contour of the EDM electrode having a 90^{0} included angle and a 0.010-in. tip radius.

Photomicrographs of sections through two compressed notch flaws in the extruded aluminum specimens are shown in figure 30. One section was obtained with the groove retained, and the other was made from a specimen with the groove machined away. These flaw widths are of the order of 0.0002-in. wide although the flaw opening at the surface of the specimen from which the groove has been machined away has a constriction that reduced the width to 0.0001 in. or less. This is perhaps evidence of a surface smearing tendency associated with machining of aluminum alloys, which sometimes leads to a requirement of an etch cleaning prior to penetrant inspection.

FABRICATION SUMMARY

The fabricated test specimens contained smaller flaws near the threshold of detectability and larger flaws for each of the NDT methods. Additional specimens of identical designs and appearance contained no flaws and were used in composing inspection lots having a significant but variable percentage of nonflawed specimens. There is a broad range of flaw sizes represented because of the varied capabilities of the five NDT methods. Such a range became a consequence, in part, of the uncertainties in the early predictions of the target sizes. In general, early estimates of sensitivity capabilities proved to be too optimistic, and it was necessary to increase the flaw sizes in the later fabrication lots. This wide distribution of flaw sizes resulted in fewer flaws near a tentative target size that could be gathered in any one inspection lot, and it was necessary to work with relatively small lots.

Table 1 summarizes the specimens, numbers of flaws, and flaw sizes manufactured for the program. These totals were available for inspection in the program but do not include some early trial specimens.

Tables 2 through 6 provide the specific quantities and sizes of flaws in each fabricated specimen and are shown for each original specimen identification number. Typical flaw locations also are indicated on sketches of the specimen configurations on each table.

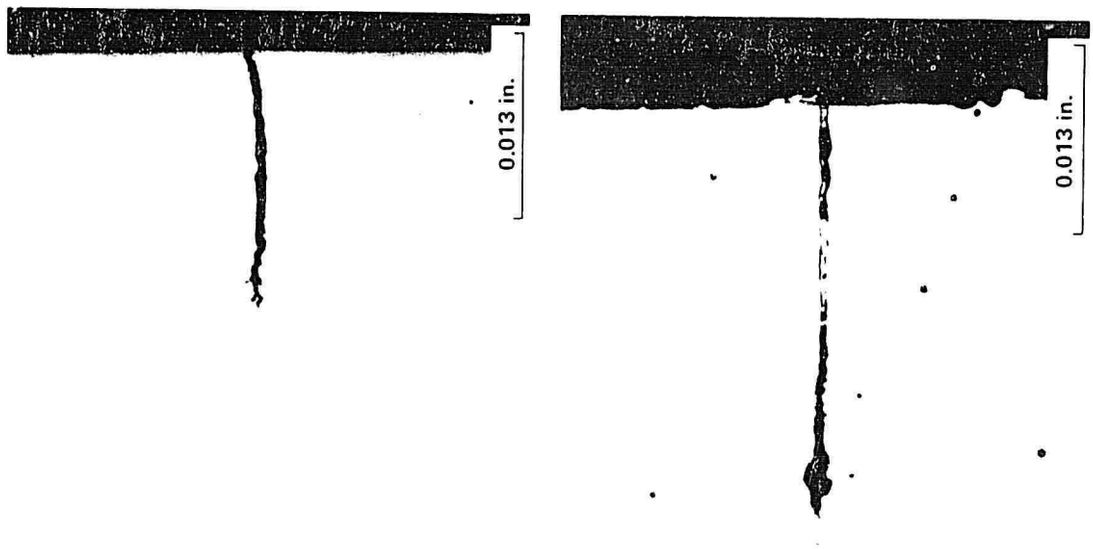


Figure 26.—Metallographic Sections Through Compressed Notch Flaws in Steel Specimens (75X)

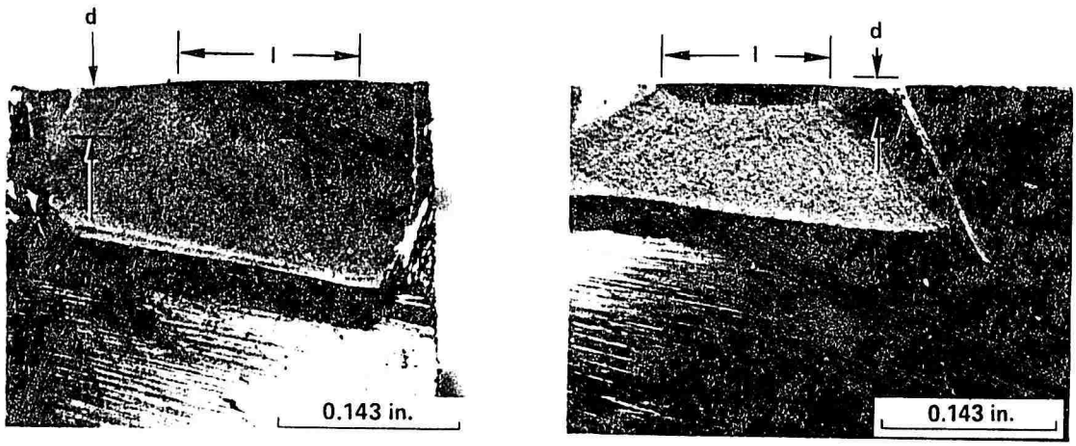


Figure 27.—Fractures Exposing Two Hydrogen Embrittlement Crack Surfaces, Surface Lengths(l) and Depths(d) of Flaws Are Delineated (7X)

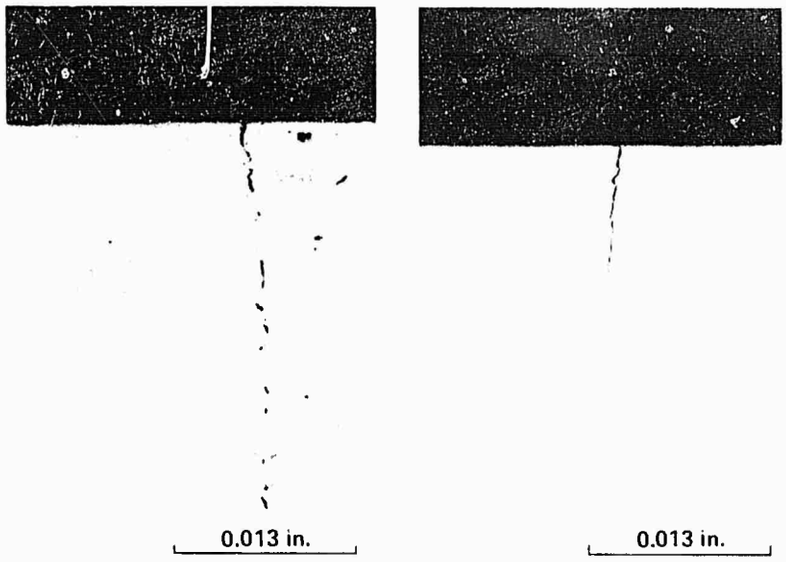


Figure 28.—Metallographic Characterization of Typical Cracks in Ground Steel Surfaces (75X)

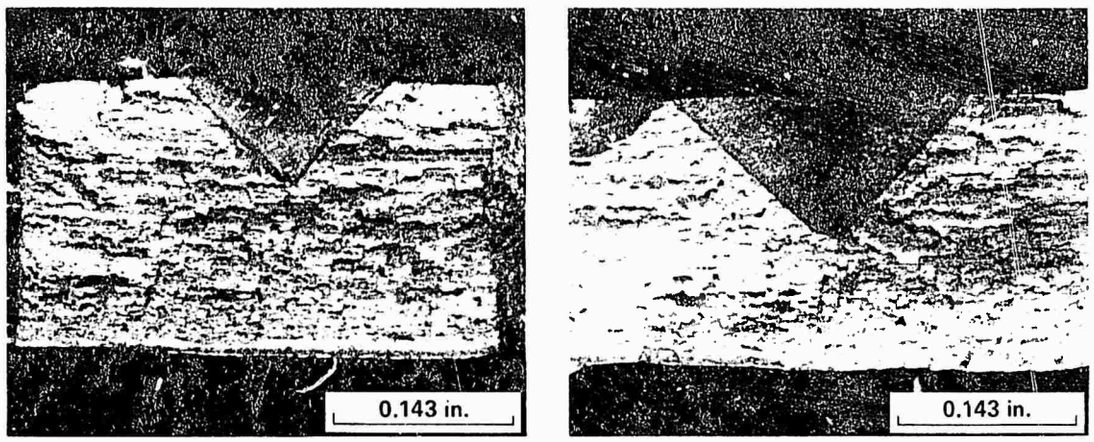


Figure 29.—Two Representative Compressed Notch Flaws in Extruded Aluminum Specimens (7X)

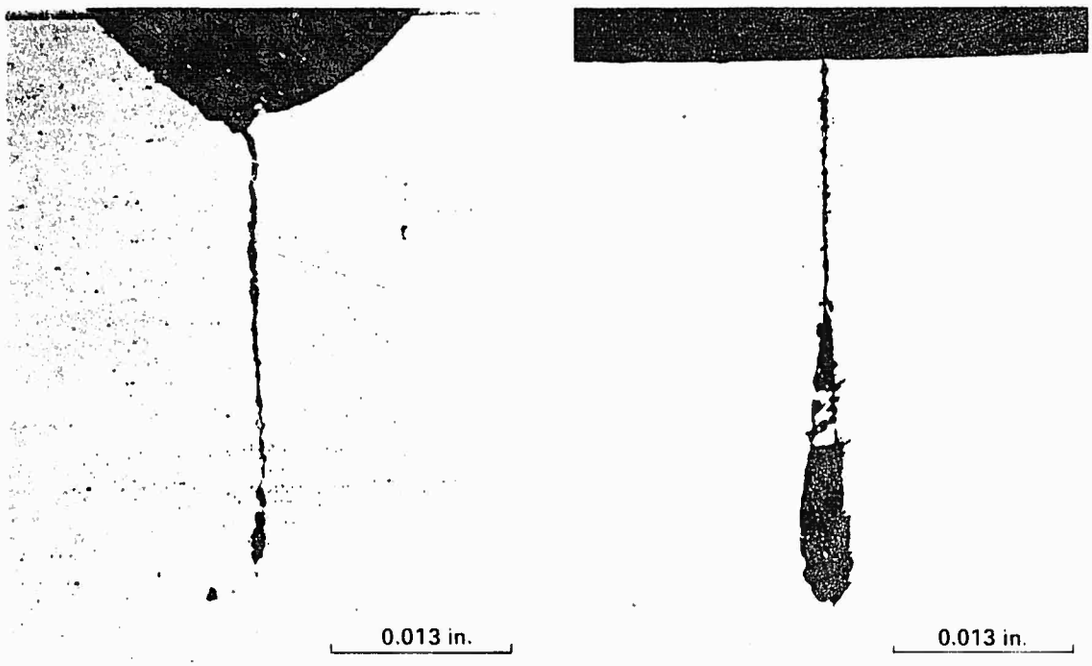


Figure 30.–Metallographic Sections Through Two Compressed Notch Flaws in Aluminum (the Wide Root of the One Flaw is Indicative of Nonuniform Compression Associated With Buckling) (75X)

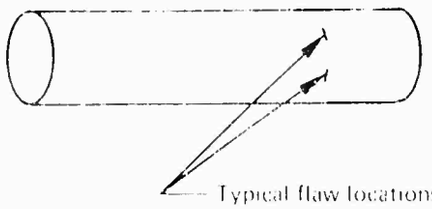
Table 1.—Specimen and Flaw Summary

Quantity	Specimen configuration	Number of flaws	Flaw size range, (length in inches)
	Externally flawed steel:		
14	Solid cylinders, straight	28	0.030 - 0.75
9	Nonflawed dummies	0	
15	Solid cylinders, filleted	30	0.020 - 0.50
7	Nonflawed dummies	0	
20	Aluminum cruciform	47	0.02 - 0.23
6	Nonflawed dummies	0	
	Internally flawed steel:		
13	Hollow cylinder, straight	23	0.060 - 0.57
6	Nonflawed dummies	0	
14	Hollow cylinder, filleted	22	0.070 - 0.46
6	Nonflawed dummies	0	
	Flat bar steel:		
7	Hydrogen embrittled	12	0.050 - 0.54
7	Grinding cracks	10	[1] (0.08 x 0.13) - (0.38 x 0.38)
8	Nonflawed dummies	0	
12	Threaded steel	29	0.04 - 0.65
7	Nonflawed dummies	0	

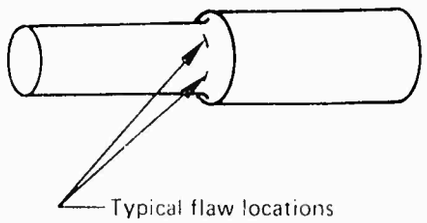
[1] Area of multiple cracks

Table 2. Externally Flawed Steel Specimens

Solid straight

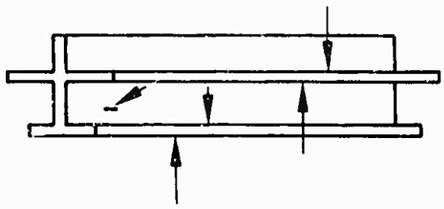


Solid filleted



Specimen number	Flaw length, in.	Specimen number	Flaw length, in.
T 2	0.17, 0.19, 0.19 0.19, 0.20, 0.25	F13 F14	Dummy Dummy
T 3	0.06, 0.14, 0.15	F15	0.03
T 4	0.12, 0.14, 0.16	F16	0.02
T 5	0.75	F17	0.07
S1	Dummy	F18	0.02, 0.07, 0.09
S2	Dummy	F19	0.10
S4	Dummy	F20	0.06, 0.15
S5	0.04	F21	0.14, 0.30
S6	0.03	F22	0.13, 0.37
S7	0.05, 0.14	F23	Dummy
S8	0.05, 0.12	F24	Dummy
S9	0.06, 0.14	F40	0.23, 0.39
S10	0.11, 0.13	F41	0.20, 0.39, 0.41
S11	0.06, 0.20	F42	0.13, 0.24
S12	0.07	F43	0.14, 0.26
S13	0.11	F44	0.13, 0.25, 0.50
S14	0.16	F45	0.15, 0.23, 0.28
S15	Dummy	F46	0.09, 0.38
S16	Dummy	F79	Dummy
S17	Dummy	F80	Dummy
S18	Dummy	F81	Dummy
S60	Dummy		
S61	Dummy		

Table 3.—Aluminum Cruciform Specimens



Typical flaw locations

Specimen number	Flaw length, in.
A1	0.05, 0.04, 0.18
A2	0.05, 0.09
A3	0.10, 0.19
A4	0.17, 0.08, 0.11
81	0.11, 0.16
B2	0.13, 0.17
B3	0.12, 0.22
84	0.09, 0.23, 0.14
C1	0,05, 0.15, 0.15
C2	0.08, 0.18
C3	0.09, 0.15, 0.11
C4	0.10
D1	Dummy
D2	Dummy
D3	Dummy
D4	Dummy
A11	0.17, 0.23, 0.21
A21	0.03, 0.13
A31	0.05, 0.06
A41	0.04, 0.11
811	0.07, 0.23, 0.15
821	0.02, 0.06, 0.05
831	0.04, 0.18
B41	0.11, 0.14
D12	Dummy
D21	Dummy

Table 4.—Internally Flawed Hollow Steel Specimens

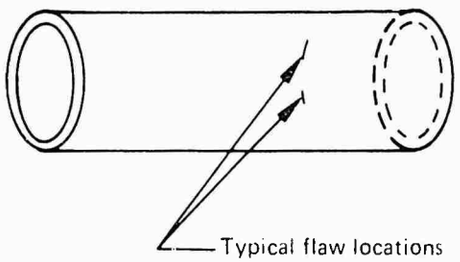
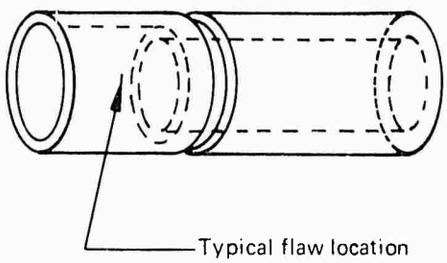
Hollow straight		Hollow fitted	
			
Specimen number	Flaw length, in.	Specimen number	Flaw length, in.
H1	0.10, 0.14	T1-1	0.07, 0.18, 0.30
H2	Dummy	H6	0.08, 0.13
H3	0.12, 0.18	H7	0.11, 0.14
H4	0.10	H8	0.09
H5	0.16	H10	0.14
H9	0.10	HF6	Dummy
H20	Dummy	H12	0.09
H25	Dummy	H14	0.09, 0.30
H11	0.06, 0.10	H16	0.12, 0.31
H13	0.09, 0.14	H18	0.16, 0.45
H15	0.06, 0.13	H22	0.27
H17	0.14, 0.23	H24	0.28, 0.46
H19	0.17, 0.35, 0.51	H26	0.39
H21	0.31, 0.39	H27	0.25
H29	0.35	H28	0.44
H23	0.35, 0.57	HF29	Dummy
H62	Dummy	HF30	Dummy
H63	Dummy	HF24	Dummy
H64	Dummy	HF25	Dummy
		HF26	Dummy

Table 5.—Flat Bar Steel Specimens

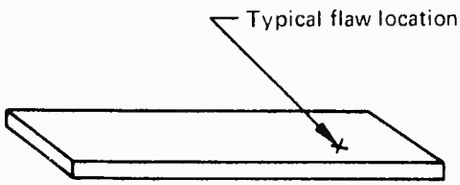
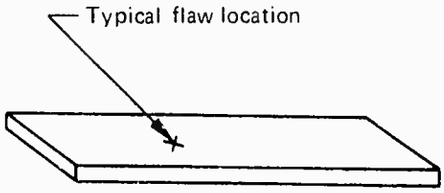
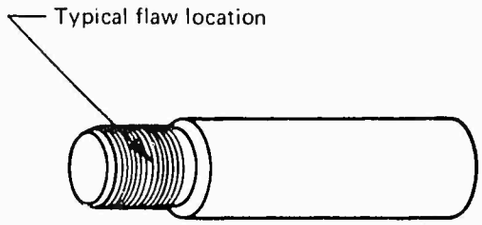
Hydrogen embrittled		Grinding cracks	
			
Specimen number	Flaw length, in.	Specimen number	Flaw area, in.
888132-1	Dummy	SN2	(0.13 x 0.08), (0.25 x 0.16)
888132-3	Dummy	SN4	Dummy
888132-4	Dummy	SN5	(0.35,x0.40)
888132-6	Dummy	SN7	(0.38 x 0.38)
888132-7	Dummy	SN8	(0.18 x 0.14)
888132-8	Dummy	SN10	(0.36 x 0.04)
2	0.20	16	(0.21 x 0.21)
3	0.18+	19	(0.15 x 0.20), (0.22 x 0.16),
4	0.43, 0.50, 0.54		(0.21 x 0.26)
5	0.18, 0.18	20	Dummy
6	0.05, 0.08	27	Dummy
7	0.10, 0.26	SN6	Dummy
8	0.11	SN9	Dummy

Table 6.—Threaded Steel Specimens



Specimen number	Flaw length, in.	
	Root	Crest
T1	0.11, 0.46	0.19
T2	0.11	
T3	0.35	
T4	0.25, 0.38	
T5	0.04, 0.11, ·0.31	
T6	0.10, 0.45, ·0.23	
T7	0.41, 0.13	0.27
T8	0.65	0.10
T9	0.11, 0.25	0.07, 0.21
T10	Dummy	
T11	0.48	
T12	0.30	0.13
T13	0.11, 0.13	0.13, 0.34
T14	Dummy	
T15	Dummy	
T16	Dummy	
Blank	Dummy	
Blank	Dummy	
Blank	Dummy	

SECTION V
NONDESTRUCTIVE INSPECTIONS

INTRODUCTION

Throughout the conduct of the program particular attention was given to obtaining test results based on a broad spectrum of equipment and personnel capabilities. Several different production inspection facilities as well as many individual inspectors were used to assure that a wide range of skill and experience factors were included in the experiment. Involvement of a large number of personnel also served to limit communication of inspection results among inspectors.

In addition to assuring that a diversity of equipment and personnel were used and to allow variations within the normal constraints of the applicable Government and Boeing specifications, detailed inspection techniques were not furnished to the inspectors. The resulting variety in minor technique details was considered more likely to reveal average inspection capabilities and more closely simulate the variable conditions within the total aerospace industry. Also, if detailed procedures were supplied to the inspectors for each of the specimen designs, the test parts would have been identified as special (nonproduction) and would have been treated as such by the inspectors.

INSPECTION FACILITIES AND EQUIPMENT

The nondestructive inspections were accomplished at five different plant locations involving nine different inspection facilities. At least four of these facilities were used for each of the five NDT methods; however, it was impossible to distribute load equally to these facilities because of differences in equipment, available manpower, and fluctuations in production work loads. The facilities used met the requirements of Boeing process specification 5953, *Qualification of Facilities and Personnel - Nondestructive Testing*. Also, the Boeing process specifications for the NDT methods require facilities and equipment compliance with applicable military specifications.

All equipment used are commercially available. No specially designed instruments or accessory items were employed except various minor inspection aids such as probe holders used to facilitate manual scanning. Sensitivity and accuracy capabilities of all systems were representative of current state of the art.

All inspection instruments, whether in use in production or in the laboratories, are regularly maintained on a calibration and recertification schedule. For example, more frequent controls of black light intensities and magnetic particle suspensions are maintained under the applicable inspection process specification. It should be noted that, in general, laboratory equipment is not superior to that available to production inspectors. In many instances the contrary is true, particularly in accessory items designed to facilitate automatic or semiautomatic handling and inspection of large numbers of parts. Also, production magnetic particle and penetrant inspection facilities are designed for large parts and more controlled,

uniform processing. On the other hand Laboratory equipment of this type, is such that inspection processing is much more dependent on skillful processing of each individual part under more awkward conditions.

PERSONNEL

More than 30 individuals actively participated in the laboratory and production inspections. Production inspectors were required to be currently qualified and certified under BAC 5953, *Qualification of Facilities and Personnel Nondestructive Testing*. Those performing laboratory inspections in many cases were similarly certified, but there were no formal requirements that all inspectors be qualified and certified under the same specification. Many of those supporting the laboratory portion of the program had extensive prior production inspection experience.

Experience levels of participating inspectors extended from individuals in training under the guidance of lead inspectors to veteran inspectors with upwards of 30 years' experience.

While the engineering level personnel performing the laboratory inspections have superior educational backgrounds and basic understanding of the NDT methods, it should be noted that the skill levels of the production inspectors may be equal to or exceed that of the laboratory personnel because of their 8-hour-a-day, 5-day-a-week use of a given NDT method.

INSPECTION LOTS

Inspection lots were composed of flawed and unflawed specimens, and the ratios were purposely varied. In the earlier inspections the lots consisted of 60% to 80% flawed specimens. Toward the end of the program the percentage defective was reduced to as low as 25% to 40% in order to approximate the infrequent occurrence of flaws.

The number of flawed and unflawed specimens in the typical lots most frequently ranged from 8 to 12. Larger lots would have promoted greater efficiency in performing inspections and associated tasks, such as transporting the lots, recording results, and renumbering specimens. However, the lot sizes were limited by the quantities of nonflawed specimens, available (less than 30% of the total) and the need to maintain an appreciable percentage of nonflawed specimens in each inspection lot. Also, the large number of different flaw sizes required to assess the varied capabilities of the five NDT methods resulted in fewer specimens in each flaw size range.

ROUTING OF INSPECTION LOTS

The inspection lots were rotated among the participating inspection facilities and plant locations. In most instances the lots passed through the focal point laboratory when going from one location to another. At these times laboratory inspections were accomplished, all inspection results were recorded, specimens were given new numbers as necessary, new protective wrappings were provided, periodic thorough cleanings were accomplished, and new

inspection lots were made up. Lot sizes were varied, percent of defectives changed, and specimens interchanged among lots to further avoid inspection familiarization and recognition of specimens.

SPECIMEN CLEANING AND PRESERVATION

Specimen cleaning is a very important operation in assessing penetrant inspection capability. Since residue in a defect may prevent penetrants from entering the defect, it is necessary that thorough cleaning be accomplished after each penetrant inspection. It is also necessary to avoid any possibility that penetrant indications may result from entrapped penetrant materials carried over from a preceding inspection.

Ultrasonic cleaning is the customary practice at Boeing during laboratory investigations of penetrant capabilities on tight fatigue crack specimens. Vapor degreasing has also been employed. Cleaning requirements by either method have exhibited strong dependence on the nature of the flaws retaining the penetrants. Very tight cracks (fatigue cracks) and very deep cracks (quench cracks) normally require prolonged cleaning. Immersion for 30 minutes in acetone in a 6 to 11 w/in^2 ultrasonic cleaning tank has provided adequate cleaning for most cracks. Application of a nonaqueous developer, such as Sherwin D-100, without reappearance of the penetrant indication within a normal development time has been the criterion for adequate cleaning.

An initial investigation was conducted to determine the effectiveness of ultrasonic cleaning. Figure 31 illustrates three specimens in the laboratory ultrasonic cleaner. Five cleaning solutions were evaluated: acetone, methyl-ethyl-ketone, trichlorethylene, Stoddard's solvent, and a 10% solution of Sherwin penetrant remover ER-82 in water. Cleaning procedures were evaluated on thermally cracked aluminum blocks, compressed notch steel specimens, and the hydrogen and grinding crack specimens. For most specimens, 30 minutes of ultrasonic cleaning in acetone was adequate. Additional cleanings between inspections were accomplished when possible by utilizing vapor degreasing facilities available both in production and in the laboratory.

Close-fitting protective sleeves were made for each specimen from asphalt-barrier, vapor-phase corrosion inhibitor paper (MIL-P-3420B, type I, classes 1 and 2, style F). Plastic bagging was also used to provide further protection. Those methods of preservation reduced handling damage, surface wear, and corrosion. The use of corrosion inhibiting oils and other fluid compounds was avoided so as to prevent contamination of the flaws and subsequent cleaning difficulties with possible adverse effects on penetrant inspections.

REFERENCE STANDARDS

Specimens were provided and identified as reference standards in each inspection lot submitted for ultrasonic and eddy current inspections. In most cases the reference flaw was the smallest in the lot. The sizes of the standard reference flaws varied from 0.03 to 0.11 in. and were selected according to the range of sizes in the particular lot and the inspection method. In general, technique instructions required standardizing to 80% of maximum response and rejecting at 50%. Reference flaw specimens were not permanently identified as standards because they were also used as test specimens.

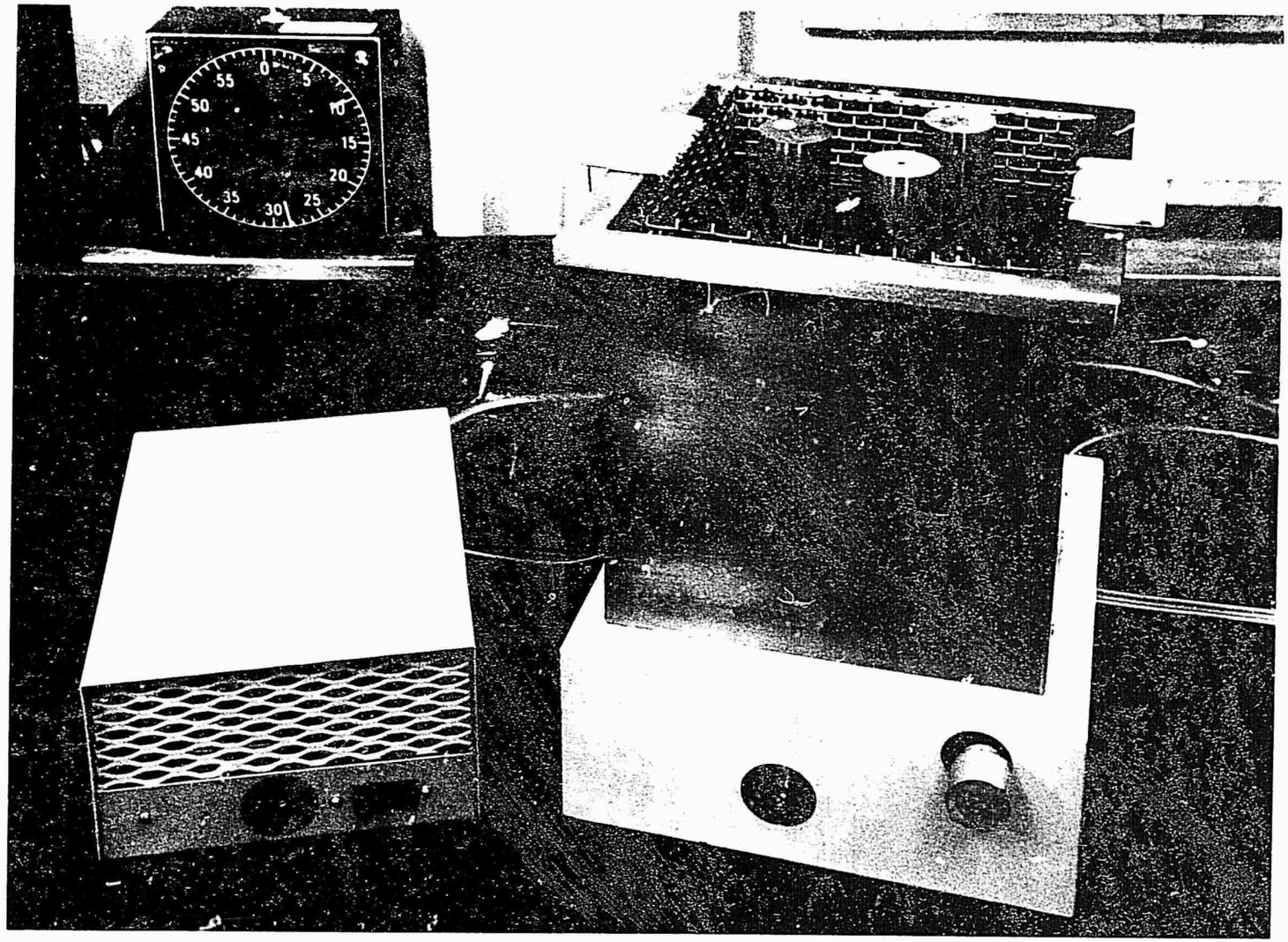


Figure 31.—Laboratory Ultrasonic Cleaning Equipment

It was necessary to provide reference standards for the instrumented inspection methods, ultrasonic and eddy-current, to assure standardization of instrument settings and to promote uniformity in other technique parameters. Industry reference standards such as ASTM E 127-64 and HW Standards for longitudinal and shear wave ultrasonic inspection were not suited for the surface inspection requirements of the program. Also, ultrasonic or eddy-current reference standards for inspection for surface discontinuities have not yet received industry acceptance. When uncommon inspection requirements are encountered it is common practice to create special reference standards by developing artificial defects in actual parts or by machining sections closely simulating the geometries of actual parts. Ultrasonic and eddy-current inspections for surface flaws were not commonly performed on production parts, and the need for special reference standards was met by utilizing program specimens containing the smaller flaws. This was in lieu of developing and fabricating special standards for each of the specimen designs. The flaw sizes detected near the program objective of 0.90 probability and 95% confidence were so much larger than the smaller flaws used as standards and the ultimate sensitivities of the methods that the small variations in standards did not significantly influence the saturation responses from the relatively large flaws detected with 0.90 probability and 95% confidence.

MAGNETIC PARTICLE INSPECTION

Magnetic particle inspections in the laboratory were conducted primarily with a Parker Research Company, model DA-200, contour probe. A Magnaflux Corporation portable model P-90, 750 ampere testing unit also was available and was evaluated in the initial portion of the program. The contour probe was judged to be better suited to the specimen designs and the requirements of the program and was used almost exclusively. Fluorescent magnetic particle suspensions employed were Magnaflux 14AM in prepared bath aerosol cans and 14A powder mixed in oil suspension in the laboratory. All inspections were performed with the wet continuous technique. The Parker probe as applied to inspecting the external fillet, solid cylinder specimens is shown in figure 32.

Production magnetic particle inspections were performed with equipment of types and manufacturers typical of those used throughout the aerospace industry. All were stationary machines operating with rectified three-phase-alternating current and in accordance with Boeing process specification BAC 5424, *Magnetic Particle Inspection.* The technique employed for all inspections was the wet continuous fluorescent procedure. Magnaflux Corporation 14A fluorescent particles were used in both oil and water base suspensions. Inspection procedures under BAC 5424 met the requirements of MIL-I-6868C. *Inspection Process, Magnetic Particle.*

PENETRANT INSPECTION

Both postemulsifiable and water-washable penetrant system materials were used in the laboratory penetrant inspections. Magnaflux postemulsifiable penetrants ZL-2A and ZL-30A were used with ZE-4B emulsifier and ZP-9B developer. These were equivalent in sensitivity to MIL-I-25135 group V and group VI, respectively. High sensitivity water-washable penetrants (Magnaflux ZL-60B, Uresco P133 and P134, and Sherwin HM-405 and HM-3) were also used. These are rated as equivalent in sensitivity to MIL-I-25135 group V or higher. Developers used in conjunction with these penetrants were Magnafluz ZP-9B,

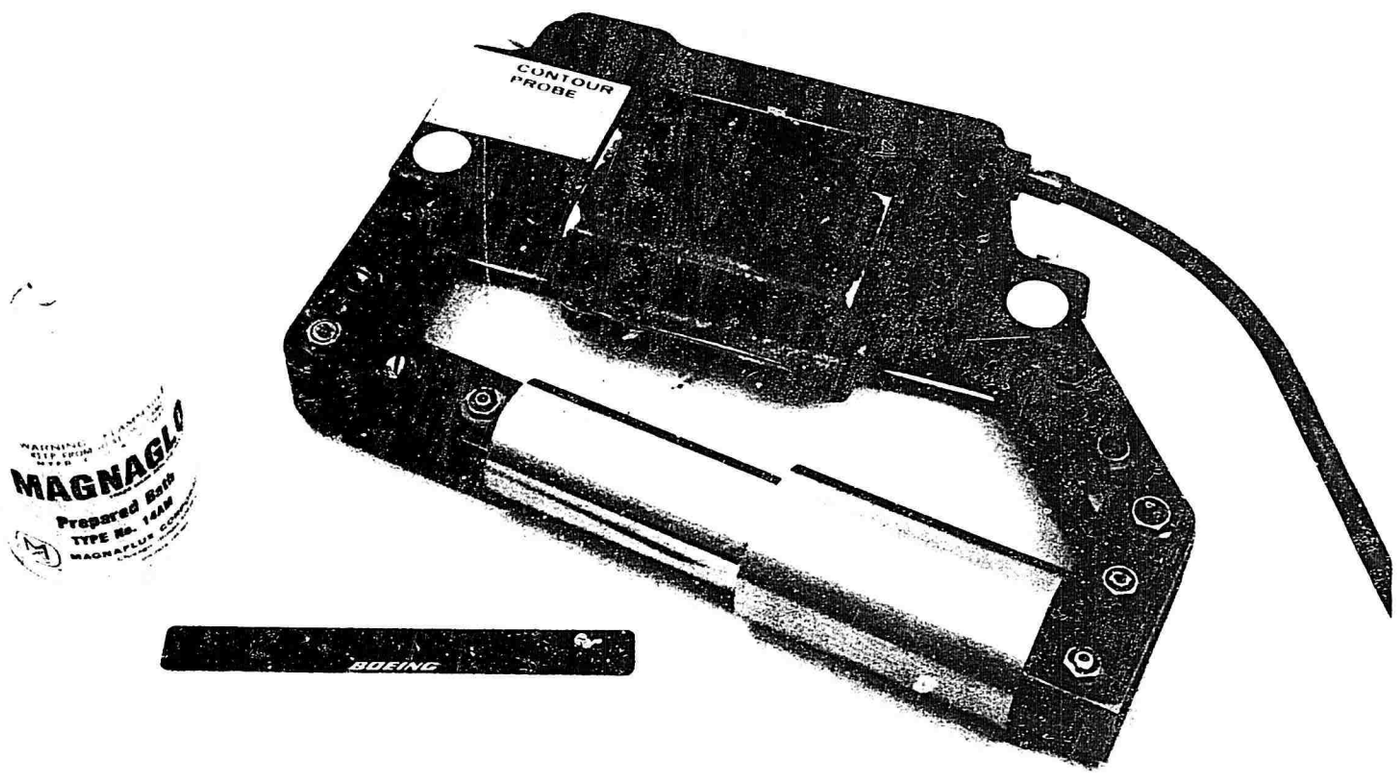


Figure 32.—Laboratory Magnetization of Test Specimen for Magnetic Particle Inspection

Uresco D-495A and D499C, and Sherwin D-100. This wide variety of well-known high sensitivity Air Force approved penetrant materials was utilized to approach an average, high sensitivity penetrant system capability. In this way, a biasing influence of any particular family of materials was avoided.

To assure that the laboratory penetrant inspections were accomplished with a high degree of sensitivity, nonaqueous developers in spray applications were relied upon almost exclusively. Additional parameters selected to help achieve results superior to those obtained in production were: (1) longer penetration (dwell) times, (2) similarly longer development times before inspection, and (3) individual part processing. The unrestricted inspection time in the laboratory was also important. While production inspectors were not limited to processing or inspection times, the normal production flow imposed pressure to complete inspections promptly to a degree not usually experienced by laboratory inspectors.

Penetrant inspection materials used on the test specimens in the various production inspection facilities included Magnaflux ZL-2A postemulsifiable penetrant, Magnaflux ZL-17B and ZL-60B water-washable penetrants, Magnaflux ZE-4A and 4B emulsifiers, Magnaflux ZP-4A, -5, and -13 developers, Uresco P-133 and P-134 water-washable penetrants, and Uresco 499B developer. These materials represent sensitivity equivalency to MIL-I-25135 group V or higher. As in the laboratory, this broad selection of penetrant inspection materials served to provide results representative of the average capability attainable with materials extensively utilized in the industry. The procedures used were also considered representative and were governed by Boeing process specification BAC 5423, *Penetrant Methods of Inspection* and MIL-I-6866.

ULTRASONIC INSPECTION

Ultrasonic inspection is predominantly applied as a method of detecting internal, subsurface flaws. Inspection techniques for internal flaws may not be optimum for detection of surface flaws, particularly if they are perpendicular to the inspection surface. However, ultrasonic techniques can be applied which do have a high sensitivity to such flaws if this is understood as a requirement by the inspector. Otherwise, surface discontinuities may be overlooked completely while the inspector conducts his normal search for internal flaws. For this reason laboratory and production ultrasonic inspectors were instructed to determine the presence of surface flaws, and the procedures they employed predominantly involved shear wave and surface wave techniques.

In the laboratory, surface wave inspections were used in preference to shear wave wherever possible because of a greater sensitivity to surface defects. However, the aluminum extruded specimens were additionally inspected for flaws in the web areas using longitudinal waves introduced slightly off-perpendicular. All laboratory inspections were accomplished by immersion testing methods. Instruments used were a Branson model 301 and a small research tank. All elements of the instrumentation and accessory equipment were stock items except for devices needed to facilitate the handling, manipulating, or indexing of parts. Figure 33 illustrates a typical inspection setup with the test specimen placed in a roller cradle. Additional equipment was a Sperry UM700 reflectoscope used in conjunction with an automatic scanning bridge and an Alden Helix (facsimile) recorder. A number of 5 and 10 MHz trans-

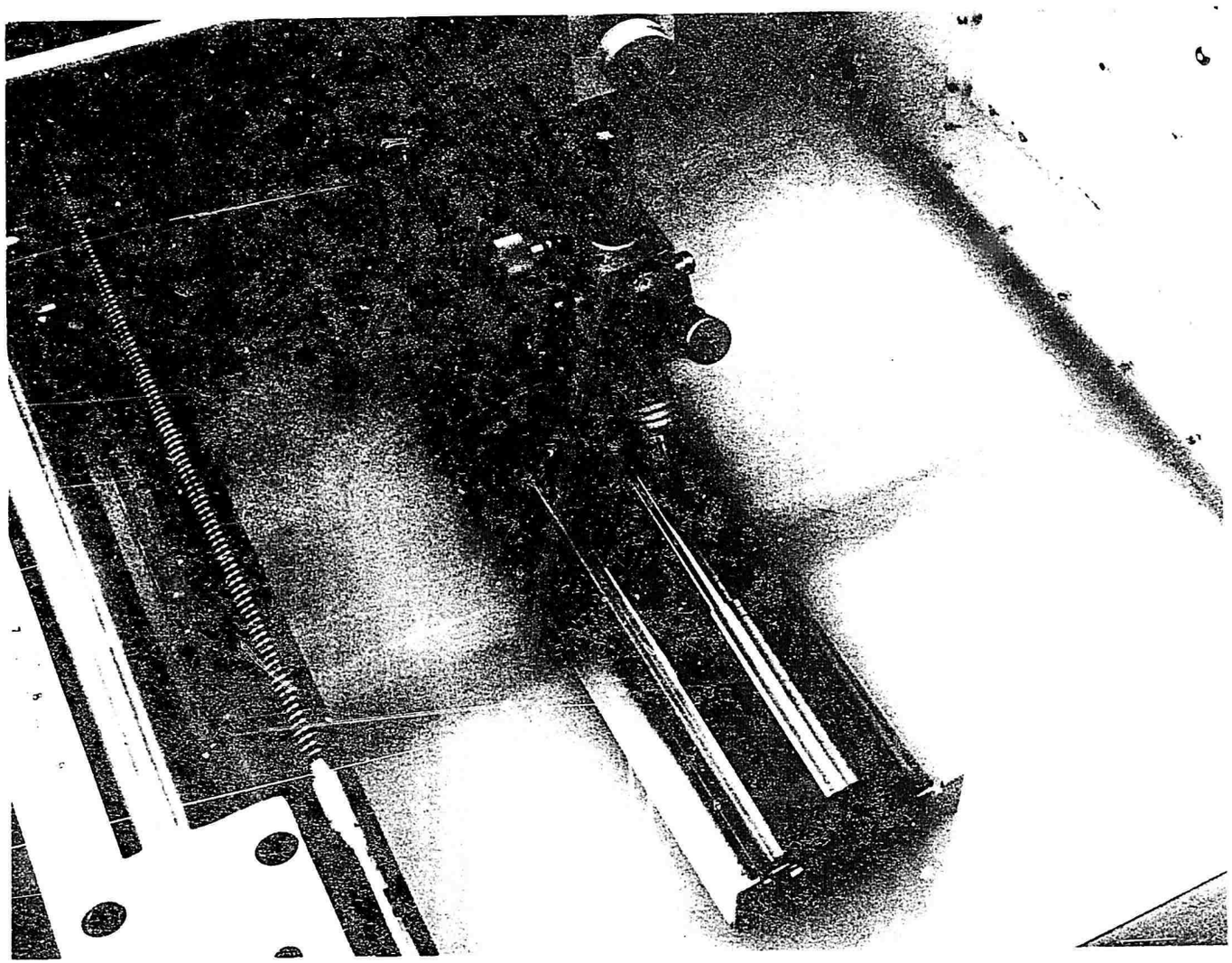


Figure 33.—Laboratory Ultrasonic Inspection of Solid Steel Specimen

ducers of varied sizes and manufacturers were used with major reliance on 5 MHz. Defect specimens were provided and identified as calibration standards for the inspection lots.

Production ultrasonic inspections were conducted by both immersion and contact methods with a wider variation in equipment, personnel, and techniques than in laboratory tests. Instruments used included:

Sonic instruments model Mark I
Krautkramer-Branson USIP 11
Sperry reflectoscopes 715 and UCD
Immerscope 424D

Both shear wave and surface wave modes were used. Most inspections of the web areas of the aluminum extruded specimens also included the longitudinal wave mode. Direct contact, contact with a water filled membrane, and immersion techniques were used. The predominant frequency was 5 MHz with some use of 10 MHz on the threaded specimens. A standard defect was provided for calibration and size reference for each test part configuration. The signal amplitude usually was set to 80% of screen saturation. Overall control of the inspection procedures were governed by Boeing Process Specification, BAC 5439, "Ultrasonic Inspection."

EDDY-CURRENT INSPECTION

At the beginning of the program several available commercial eddy-current instruments and types of probes were comparatively evaluated on the steel test specimens. Based on this preliminary study, past experience, and in consideration of available instruments in production facilities, the Magnatest ED-400 and the ED-520 were selected as well suited to the objectives of the program. The Magnatest ED-400 with a relatively low frequency (100 kHz) and special probe design to suppress permeability and lift-off variations was well suited for the inspection of ferromagnetic specimens. The Magnatest ED-520 was also acceptable on the steel specimens but was better suited to inspecting the aluminum specimens. Bolt hole and surface type probes were used with each instrument. The bolt hole probes allowed inspection of areas such as fillets not accessible to the surface probes.

The configuration of the test specimens and the availability of test fixtures dictated the inspection procedures and the probe scanning directions. Generally, the surfaces of the test specimens were hand scanned. Simple fixtures and probe holders were fabricated to facilitate the inspections. Figure 34 illustrates a roller fixture and a simple probe holder for inspection of cylindrical specimens. Figure 35 shows an expandable holder for a bolt hole probe used in the inspection of the inner surfaces of the hollow specimens.

Little distinction existed between inspections accomplished in the laboratory and those accomplished in production. The Magnatest ED-400 was used more often in the laboratory on the steel specimens than was the case in production where the Magnatest ED-520 was more readily available. Also, some production inspections were performed with the aid of mechanical scanning with X-Y manipulators, whereas laboratory scanning was entirely manual.

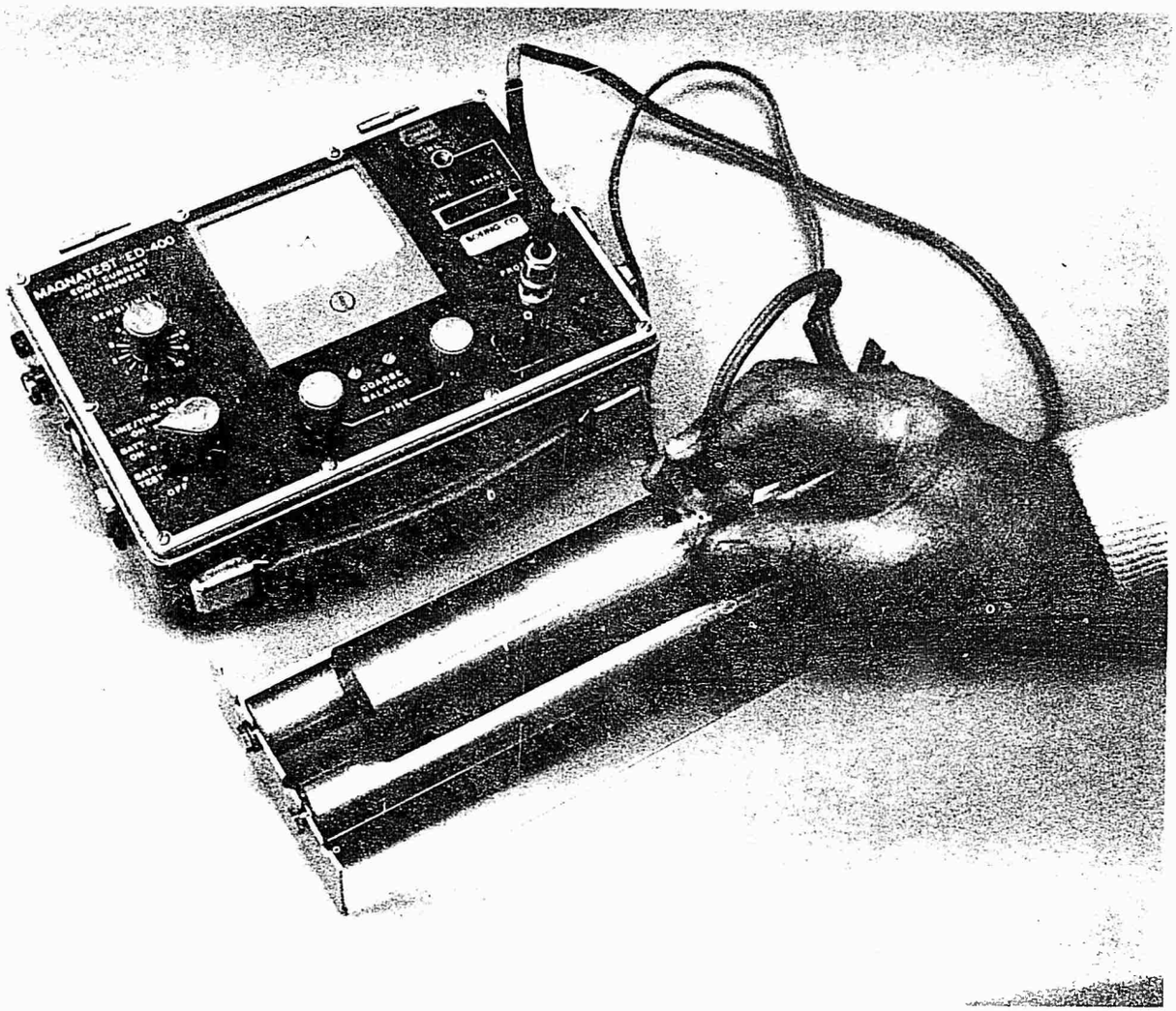


Figure 34.—Laboratory Eddy Current Inspection of Solid Steel Specimens

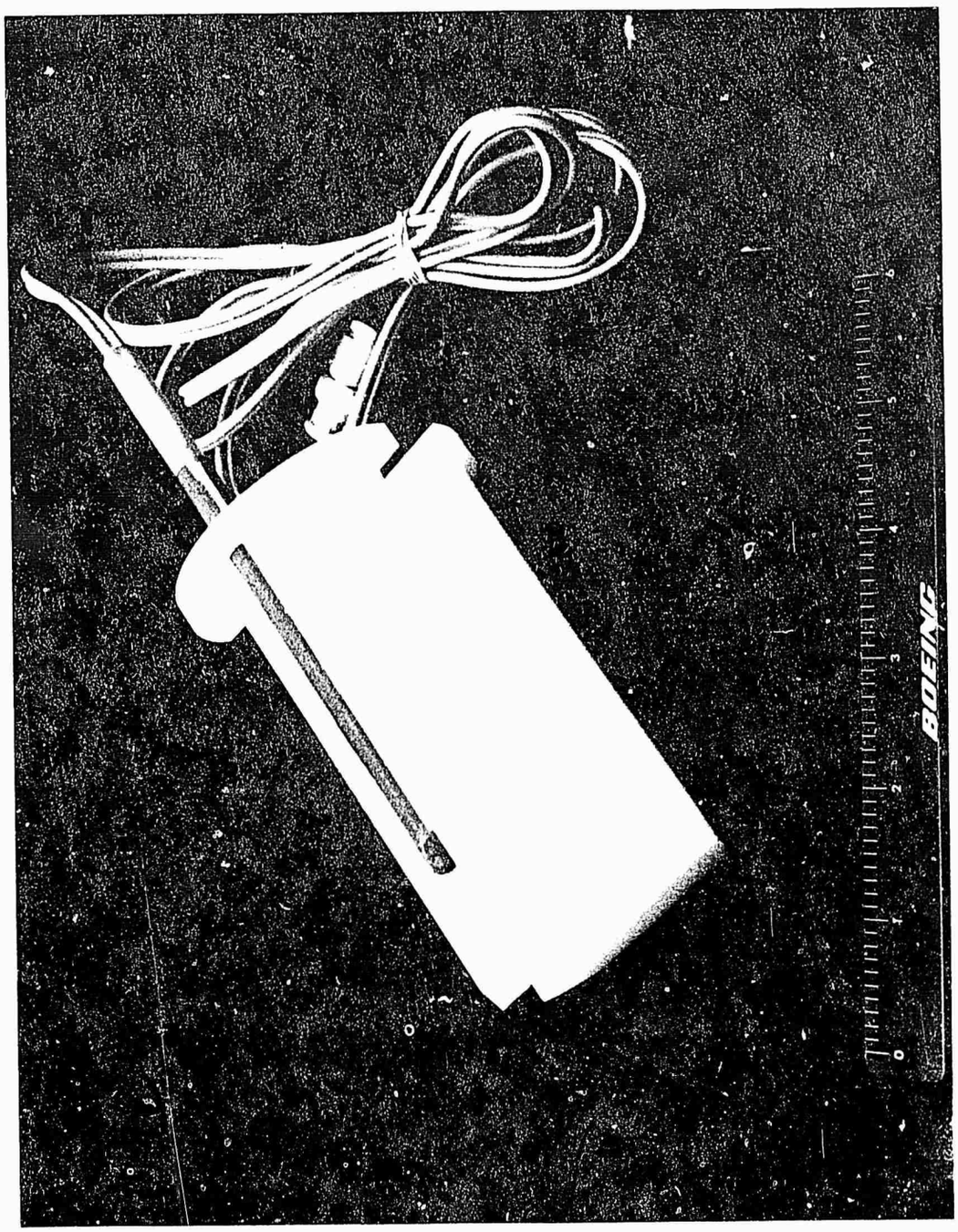


Figure 35.—Expansion Holder for Eddy Current Probe

Inspection procedures were in accordance with Boeing process specification BAC 5963, *Eddy-Current Inspection for Discontinuities*, as applicable. Reference standards were provided with the inspection lots.

RADIOGRAPHIC INSPECTION

Radiographic inspection was expected to exhibit the lowest reliability and sensitivity values of the five methods being evaluated in this program. While radiographic sensitivities to porosity-type voids in weldments, for example, may be of the order of 1% to 2% of the material thickness, cracklike discontinuities present sensitivity problems depending on the orientation of the crack interface to the source of penetrating radiation and the width of the crack. The orientation and width of the crack are so critical that a successful inspection with a normal number of exposures is largely a matter of the change of favorable positioning. Thorough radiographic inspection of the steel specimens requires a large number of views and occasionally lengthy exposures (up to 30 min). Considerable setup time is required to establish necessary shielding for individual parts in reducing scatter and undercutting. Because of the strong element of change and the excessive time required, the inspections were not conducted to establish a 0.90/95% capability but to allow a comparison with the other methods. Based on industry experience, it was expected that radiography would not prove to be a competitive method for detection of surface cracks in the test parts.

There were no obvious differences between radiographic inspections conducted in the laboratory and in production. Inspections were accomplished in accordance with Boeing process specification BAC 5915, *Radiographic Inspection* and MIL-STD-453. As in the ultrasonic tests, it was necessary to instruct both laboratory and production inspectors to inspect for surface cracks. In general, this instruction resulted in more views being exposed and the technique variables being adjusted to obtain maximum radiographic crack image sensitivity. ASTM Class 1 radiographic film was used for greater contrast and greater definition of fine cracks. Laboratory films were hand processed in fresh chemical solutions. Production film processing was manual or automatic, depending on the facility.

Figures 36 and 37 show typical radiographic setups for laboratory inspections of two steel specimen configurations. Exposures were made using a 300 kV, 3 mA Baltospot X-ray generator. Each specimen was shielded with 1/4-in.-thick lead as illustrated to reduce undercut and scatter. The film was hand packed with 0.005-in. lead on the front and 0.010-in. lead on the back side of the film. Films were processed with freshly mixed chemical solutions.

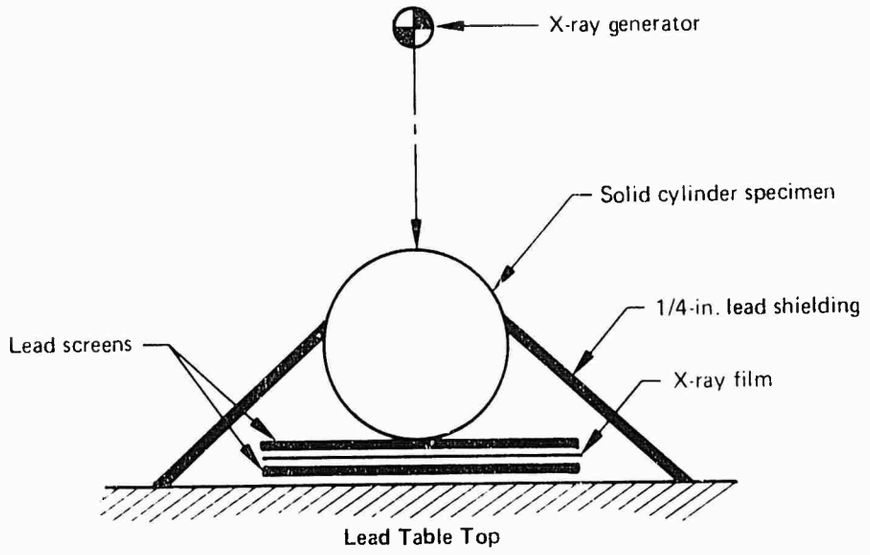


Figure 36.—Radiographic Setup for Solid Cylinder Specimens

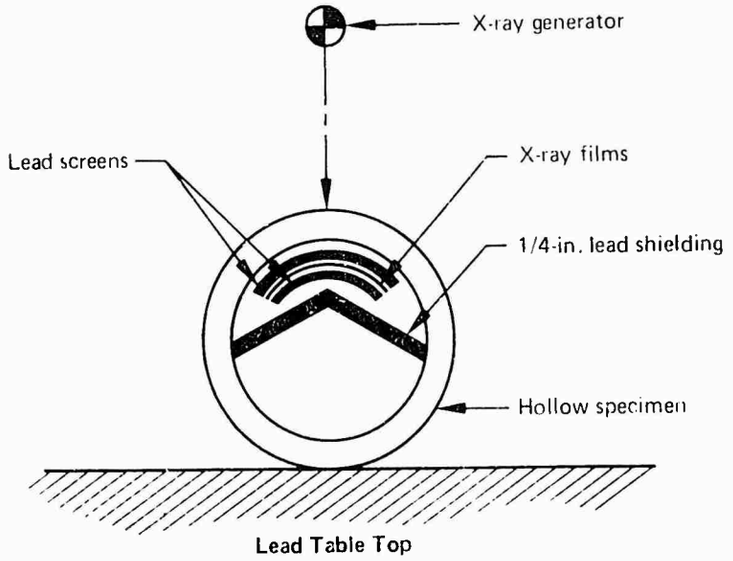


Figure 37.—Radiographic Setup for Hollow Cylinder Specimens

SECTION VI
INSPECTION RESULTS AND EVALUATION

INTRODUCTION

The inspection results are presented in tabular form. Each table concerns one inspection method as applied to one type of specimen. The results of laboratory and production inspections have been listed for each specimen as a ratio of the number of detections over the number of inspections. The original specimen identification is given and the flaw locations shown where considered pertinent. Minor variations in designs such as straight or fillleted cylinder designs are also shown. The test results have been grouped within flaw length intervals, which have been set according to practicable measuring capabilities and as required for analysis.

The statistical analyses of the results have been summarized in companion tables following each of the tables of results. Calculations of the observed probability of detection and the probability of detection with 95% confidence are given for each flaw length interval as experienced in the laboratory and in production. Where these capabilities are closely similar, the results also have been used to obtain combined probability values. Finally, the observed probabilities of detection calculated from the detection ratios and the lower probabilities of detection with 95% confidence are plotted on graphs for most of the tables of results.

The appropriate flaw size intervals have been flag-noted in the tables and graphs where the objectives of a 0.90 probability with 95% confidence of detection have been demonstrated. This was done for external surface flaws in aluminum and steel specimens and for inspections performed in both laboratory and production environments.

Results were also analyzed and compared to reveal the effects of flaw location (external versus internal surfaces) and of flaw types (compressed notches versus embrittlement cracks) in selected instances. A limited number of test results were also obtained on intentionally oxidized flaws in selected specimens of aluminum and steel.

STATISTICAL EVALUATION

The statistical approach to the analysis of the program results was relatively straightforward (ref. 3, 4, and 5). Results for each of the specimen types and inspection methods are shown in tabular form with respect to flaw length intervals. This initial grouping into intervals permitted larger sample sizes which reduced the effects of uncertainties in flaw length measurements and reduced effects of not producing multiple specimens with exactly the same flaw size. The flaw length intervals were kept small (0.010 in.) where small changes in flaw length resulted in large changes in detectability. However, large intervals or groupings were used when detectability was high and fairly consistent over the interval. Grouping in this way insured that a point estimate of the true probability of detection for any particular flaw length interval could be calculated by dividing the total number of successful flaw

Preceding page blank

detections by the total number of flaw inspections attempted in that interval. This can be expressed by the following equation:

$$\hat{p} = f/n \qquad (1)$$

where $\hat{p}$ = point estimate of true probability of detection
f = number of successful flaw detections
n = total number of flaw inspections attempted

Note: $\hat{p}$ and f/n are shown in the tables of results under the headings of OBSERVED PROBABILITY and DETECTION RATIO-TOTAL, respectively.

Statistically this was equivalent to treating all data from flaws within a flaw size interval as a random sample from a population of flaw inspections and associating the estimated probability of detection ($\hat{p}$) to that interval.

Since the observed probability of detection ($\hat{p}$) is only an estimate of the true probability of detection (P), it is important that it be accompanied by a statement which describes how precise or how close it may be to (P), the true probability of detection. This may be done with the use of confidence intervals. The upper and lower endpoints of the confidence interval, called upper and lower confidence limits, are established to enclose the desired parameter, in this case (P), with a certain amount of confidence. The probability that the confidence interval will enclose (P) is called the confidence coefficient. Upper and lower confidence limits, which are based on ($\hat{p}$) and the confidence coefficient, also depend on the type of confidence interval desired, either one-sided or two-sided. With the two-sided intervals, ($\hat{p}$) is usually placed in the middle of the confidence interval with half of the confidence interval above ($\hat{p}$) and half below. However, sometimes one-sided confidence intervals are more desirable since the entire confidence interval can be placed below the observed probability. This has its advantages when establishing practical NDT sensitivity limits because it is of little concern whether flaw detecting ability is *better* than what is claimed. It becomes of serious concern if it is *less* than what is expected. Therefore, lower, one-sided confidence intervals were used.

The lower, one-sided confidence limits were calculated for each flaw length interval, considering the point estimated ($\hat{p}$) to be from a binominal population whose parameters, probability of detection, and sample size were related to flaw size. This lower limit (P_L) was a solution for the identity shown in equation (2):

$$\sum_{x=f}^{n} C(n,x)\, P_L^{\,x} (1-P_L)^{n-x} = (1-\gamma) \qquad (2)$$

where f = number of successful flaw detections
n = total number of flaw inspections attempted
γ = confidence coefficient (equals 0.95 for a 95% confidence limit)

$C(n, x)$ = binomial coefficient (number of combinations of n things taken x at a time) =

$$\frac{n!}{x!\,(n-x)!}$$

P_L = lower 95% confidence limit

To facilitate conversion of detection ratio/sample size data to equivalent confidence limits, a Fortran IV computer program was prepared to evaluate equation (2) with three significant figure accuracy.

Use of a binomial as the statistical model is justified because the usual criteria for a binomial experiment were met. The three most important are:

(1) Experiment consists of (n) identical trials, which are statistically independent. In these tests independence was ensured by presenting the specimens for inspection in a way which did not permit an inspector to condition his response to his previous inspection results. For example, specimens were renumbered and the proportion of flawed to unflawed specimens was varied on successive inspection lots. Lot sizes also were varied and flawed specimens were interchanged among lots.

(2) Each trial results in one of two distinct outcomes. Each separate test was either a successful or an unsuccessful flaw detection.

(3) Probability of success on a single trial is equal to (P) and remains the same from trial to trial. This criterion was the most difficult to meet; however, except for the situations where contaminated and/or smeared flaws occurred, inspections did not appear to be influenced by previous handling and inspection.

A major program objective was to determine the flaw size intervals that were detectable with a 0.90 probability of success with 95% confidence. As discussed, the approach was conservative in that the lower, one-sided confidence limit values were determined. In the course of obtaining the test data, many inspections were recorded on flaw sizes considerably smaller and larger than the final 0.90/95% flaw size intervals. This was a natural consequence of not knowing beforehand what the final results would be and the fact that flaws with large size differences existed in individual specimens. All of the data have been utilized and are presented for information in the following tables of results and the graphical presentations. However, it is cautioned that the lower limit probabilities having 95% confidence diminish rapidly where the numbers of tests are small in any flaw-size interval. See figure 38. It should be noted that because of this, the lower 95% confidence limit probabilities are depressed significantly, and in some cases erratically, below the observed probabilities on either side of flaw-size intervals exhibiting probabilities near the target 0.90 value. This is evident in the statistical analysis tables and is more apparent in the graphs and reflects fewer inspections performed on flaws smaller and larger than those found 90% of the time.

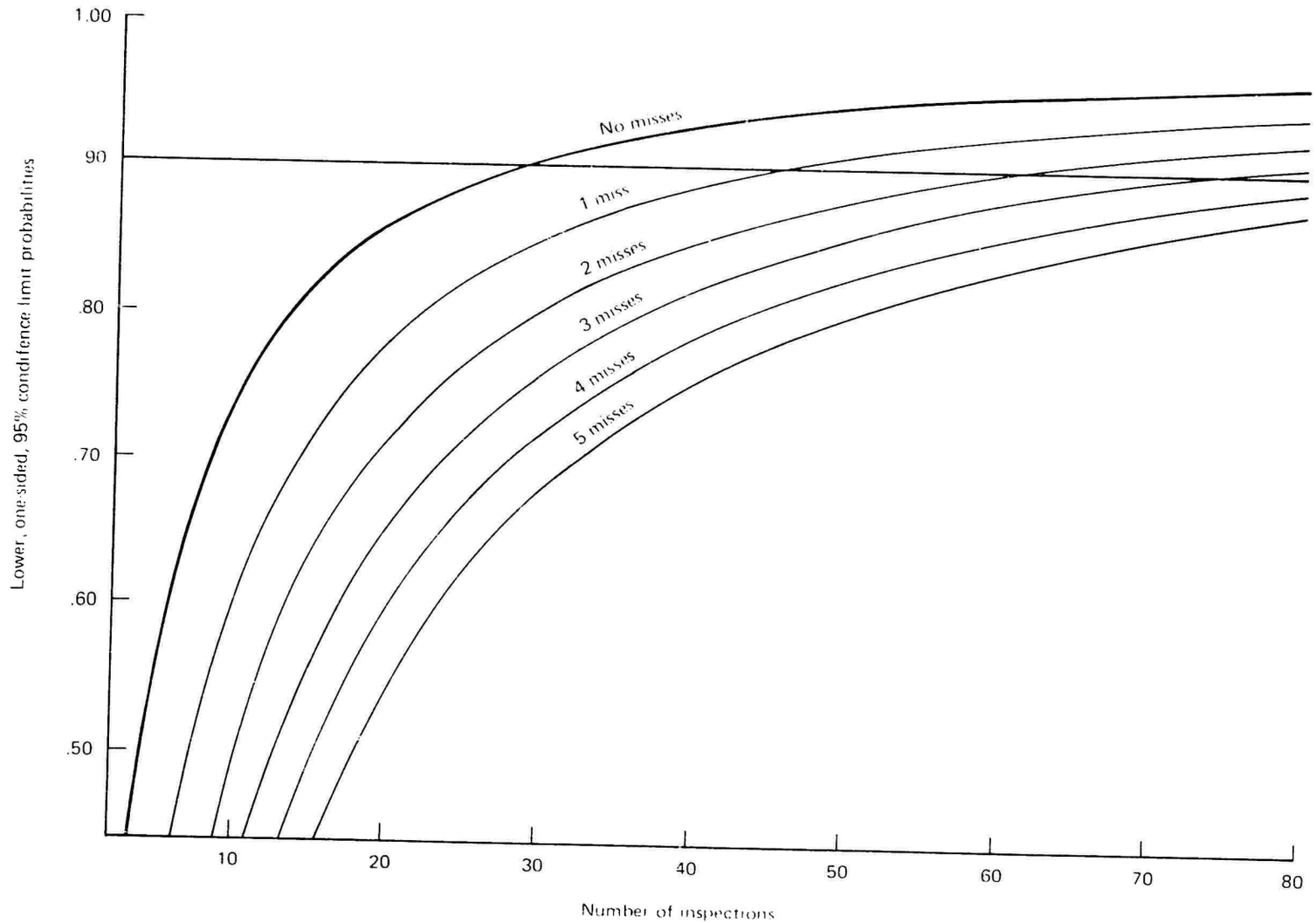


Figure 38.—Effect of Number of Inspections and Misses on 95% Confidence Limit Probabilities

In order to accumulate sufficient test numbers determined from figure 38, adjacent flaw size intervals were grouped in some instances to achieve the 0.90 probability/95% confidence objective. This was done because the initial groupings were small (+0.010 in.), and the percentage differences between flaw sizes in adjacent groups were small. Grouping was done only where the observed probabilities were high and consistent. Also, laboratory and production data were combined in a few cases when technical considerations indicated they should be comparable and there was no statistical difference at the 95% confidence level when tested by the Chi Square procedures.

SUMMARY OF RESULTS

The inspection results contained in the detailed data tabulations and numerous graphs following in this section have been summarized in table 7.

EXTERNALLY FLAWED STEEL SPECIMENS

MAGNETIC PARTICLE INSPECTION

Magnetic particle inspection results on externally flawed steel specimens are shown in tables 8 and 9 and in figure 39. The minimum flaw length interval with at least a 0.90 probability of detection with 95% confidence was demonstrated to be 0.060 to 0.079 in. in the laboratory and 0.060 to 0.099 in. in production. Since the differences between laboratory and production data were very slight, as expected considering the simplicity of the part, combining data was possible. By combining laboratory and production data, an overall flaw length interval of 0.060 to 0.079 in. was determined to have the desired probability and confidence and provided a truer estimate of the method capability.

PENETRANT INSPECTION

Penetrant inspection results are shown in tables 10 and 11, and in figure 40. The minimum flaw length interval with at least a 0.90 probability of detection with 95% confidence was demonstrated in the laboratory to be 0.140 to 0.159 in.; however, the presence of contaminated or smeared flaws later in the program did influence the data. This became more apparent in production where inspections were generally performed later than those in the laboratory and after the flaws experienced repeated inspections and extensive handling. Subsequent laboratory tests confirmed that varying degrees of interference with penetrant inspection had developed. Factors that could account for the diminishing capability of penetrant methods on these specimens are: (1) corrosion and rusting within the flaws as a result of the repeated immersions in water during the ultrasonic inspections, (2) smearing and closure of the flaw openings caused by the scrubbing action of scanning eddy-current or contact ultrasonic probes and, in some instances, the abrasive removal of surface corrosion, and (3) the buildup of penetrant of other residues within the flaws through alternate contaminations and incomplete cleanings. These changes have caused the penetrant method to demonstrate reduced capabilities.

Table 7.--Summary of Results

Specimen Configuration and NDT method	Minimum flaw length intervals with at least 0.90 probability of detection with 95% confidence	
	Laboratory, in.	Production, in.
Steel, externally flawed		
Magnetic particle	0.060 - 0.079	0.060 - 0.099
Penetrant	0.140 - 0.159 (2)	(1) (2)
Eddy current	0.140 - 0.159	0.100 - 0.139
Ultrasonic	0.090 - 0.139	0.070 - 0.089
Radiographic	(3) (1)	(3), (1)
Aluminum, externally flawed		
Penetrant	0.040 - 0.059	(1), (2)
Eddy current	0.160 - 0.239	0.129 - 0.179
Ultrasonic	0.160 - 0.199	(1)
Radiographic	0.060 - 0.119	0.080 - 0.159
Other steel configurations		
Internally flawed hollow specimens		
Magnetic particle	0.060 - 0.079	(4) (1)
Penetrant	0.200 - 0.479(2)	(1) (2)
Eddy current	0.140 - 0.179	0.060 - 0.119
Ultrasonic	0.060 - 0.099	0.080 - 0.119
Radiographic	(1)	(1)
Grinding and embrittlement cracked specimens		
Magnetic particle	0.040 - 0.099	0.040 - 0.099
Penetrant	(1) (2)	(1) (2)
Eddy current	0.360 - 0.559	(5)
Ultrasonic	0.040 - 0.119	(1)
Radiographic	(3) (1)	(3) (1)
Threaded specimens	(6)	(6)

FOOTNOTES:

[1] The minimum flaw length interval with the desired probability and confidence was not obtained; however, results are shown graphically and in tabular form in the data analysis section.

[2] Results were influenced by the presence of contaminated and/or smeared flaws.

[3] Radiographic inspections proved less effective than the other NDT methods for detecting surface cracks in steel and were discontinued.

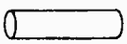
[4] Inattention to interior surfaces during early inspections was encountered.

[5] High background noise due to grinding burn was reported. See figure 53.

[6] Results are shown in table 40-47 for information only.

Table 8.—Results of Magnetic Particle Inspections on Externally Flawed Steel Specimens

Flaw length interval, in.	Specimen configuration ①	Specimen number	Laboratory		Production	
			Detection ratio	Total	Detection ratio	Total
0.020-	F	F16	6/6		1/2	
0.039	F	F18	4/11		5/9	
	S	S-6	5/8		1/4	
	F	F15	6/6	21/31	1/2	8/17
0.040-	S	S-5	4/7		1/3	
0.059	S	S-7	7/8		6/7	
	S	S-8	7/7	18/22	6/7	13/17
0.060-	S	T-3	7/7		9/9	
0.079	S	S-9	8/8		7/7	
	S	S11	3/3		4/5	
	F	F20	10/11		9/9	
	S	S12	8/8		6/6	
	F	F17	7/7		7/7	
	F	F18	11/11	54/55	8/9	50/52
0.080-	F	F18	11/11		9/9	
0.099	F	F46	2/2	13/13	2/2	11/11
0.100-	F	F19	11/11		8/8	
0.119	S	S10	6/6		4/4	
	S	S13	6/6	23/23	5/5	17/17
0.120-	S	T-4	6/6		8/8	
0.139	S	S-8	7/7		7/7	
	S	S10	6/6		4/4	
	F	F22	9/10		4/4	
	F	F42	2/2			
	F	F44	2/2	32/33		23/23
0.140-	S	T-3	7/7		9/9	
0.159	S	T-4	6/6		8/8	
	S	S-7	8/8		7/7	
	S	S-9	8/8		7/7	
	F	F21	10/10		5/5	
	F	F43	2/2			
	S	T-3	7/7		9/9	

① S 

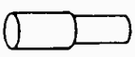
F 

Table 8. – Results of Magnetic Particle Inspections on Externally Flawed Specimens (Continued)

Flaw length interval, in.	Specimen configuration	Specimen number	Laboratory		Production	
			Detection ratio	Total	Detection ratio	Total
Con't	F	F20	11/11		9/9	
	F	F45	2/2	61/61		54/54
0.160	S	T 4	6/6		8/8	
0.199	S	S14	1/1		8/8	
	S	T 2	1/1			
	S	T 2	1/1			
	S	T 2	1/1			
	S	T 2	1/1	11/11		16/16
0.200	S	T 2	1/1			
0.750	S	S 11	3/3		5/5	
	F	F41	2/2			
	F	F40	2/2			
	F	F45	2/2			
	F	F42	2/2			
	S	T 2	1/1			
	F	F44	2/2			
	F	F43	2/2		2/2	
	F	F45	2/2			
	F	F21	10/10		5/5	
	F	F22	10/10		4/4	
	F	F46	2/2		2/2	
	F	F40	2/2			
	F	F41	2/2			
	F	F41	2/2			
	F	F44	2/2			
	S	T 5	6/6	55/55		18/18

Table 8.—Results of Magnetic Particle Inspections on Externally Flawed Specimens (Concluded)

Flaw length interval, in.	Specimen configur-ation	Specimen number	Laboratory		Production	
			Number of inspections	Total	Number of inspections	Total
NONFLAW	S	S1	2		2	
SPECIMENS	S	S2	3		3	
	S	S4	7		5	
	S	S15	1		6	
	S	S16	6		6	
	S	S17	5		6	
	S	S18	5		8	
	S	S60			2	
	S	S61			2	
	F	F13	5		3	
	F	F14	5		3	
	F	F23	10		7	
	F	F24	9		8	
	F	F79			1	
	F	F80			1	
	F	F81		58	1	64

Table 9.—Statistical Analysis of Magnetic Particle Inspection Results on Externally Flawed Steel Specimens

Flaw length interval, in.	Laboratory			Production			Combined		
	Detection ratio	Probability		Detection ratio	Probability		Detection ratio	Probability	
		Observed	Lower 95% conf limit		Observed	Lower 95% conf limit		Observed	Lower 95% conf limit
0.020-0.039	21/31	0.677	0.539	8/17	0.471	0.260	29/48	0.604	0.489
0.040-0.059	18/22	0.818	0.631	13/17	0.765	0.539	31/39	0.795	0.690
0.060-0.079	54/55	0.982	0.917①	50/52	0.968	0.903①	104/107	0.972	0.929①
0.080-0.099	13/13	1.000	0.794	11/11			24/24	1.000	0.883
0.100-0.119	23/23	1.000	0.878	17/17	1.000	0.838	40/40	1.000	0.928
0.120-0.139	32/33	0.970	0.864	23/23	1.000	0.878	66/67	0.985	0.931
0.140-0.159	61/61	1.000	0.952	54/54	1.000	0.946	115/115	1.000	0.974
0.160-0.199	11/11	1.000	0.762	16/16	1.000	0.829	27/27	1.000	0.895
0.200-0.750	55/55	1.000	0.947	18/18	1.000	0.847	73/73	1.000	0.960

① Program objective demonstrated

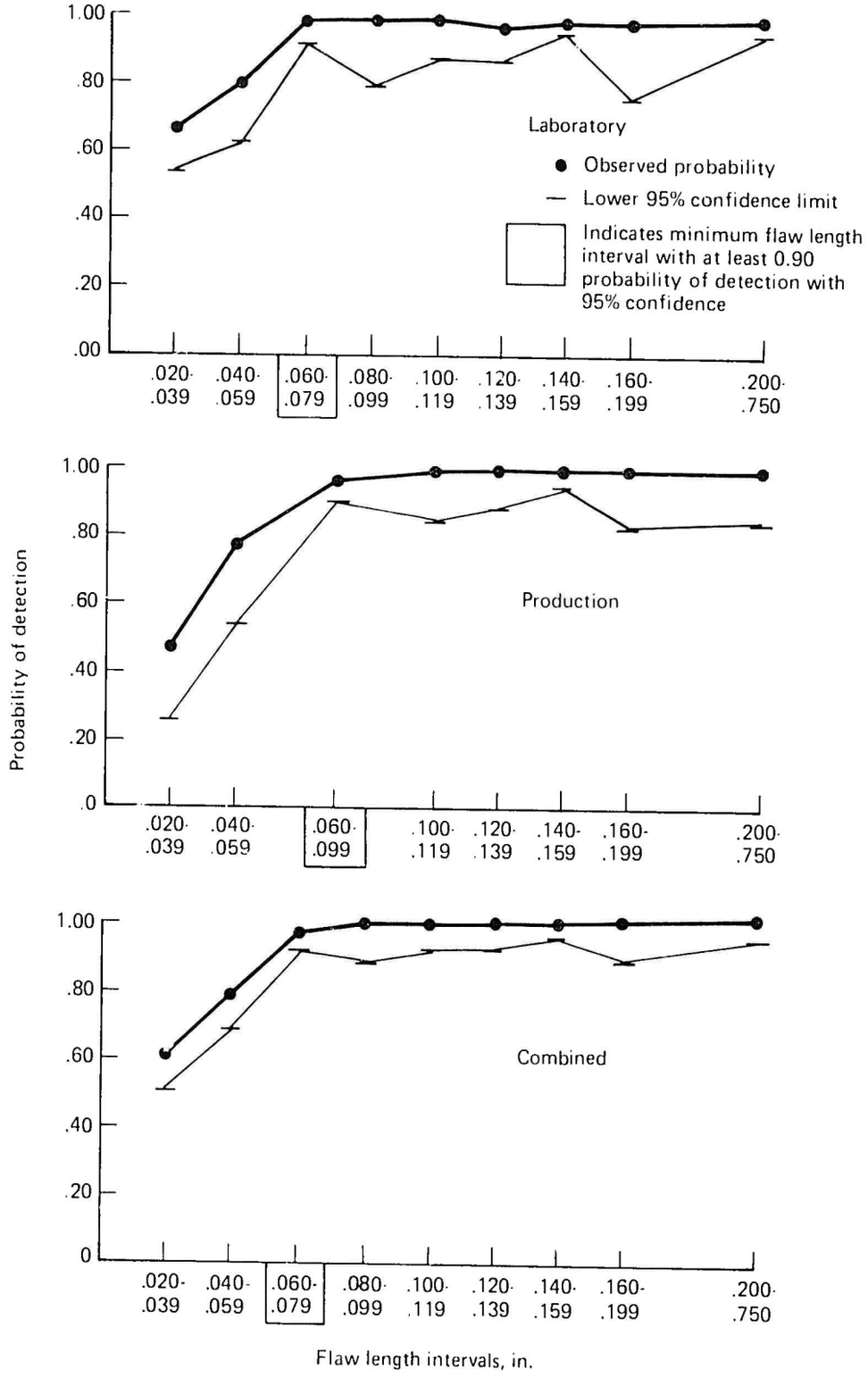
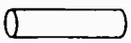
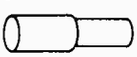


Figure 39.—Magnetic Particle Results on Externally Flawed Steel Specimens

Table 10.—Results of Penetrant Inspections on Externally Flawed Steel Specimens

Flaw length interval, in.	Specimen configuration ①	Specimen number	Laboratory		Production	
			Detection ratio	Total	Detection ratio*	Total
0.020-	F	F16	6/6		6/2	
0.039	F	F18	5/8		4/8	
	S	S-6	1/8		0/2	
	F	F15	6/6	18/28	0/2	4/14
0.040-	S	S-5	2/7		1/2	
0.059	S	S-7	3/6		3/6	
	S	S-8	0/1*	5/14	2/6	6/14
0.060-	S	T-3	7/7		7/8	
0.079	S	S-9	0/1*		1/5	
	S	S11	0/1*		1/3	
	F	F20	7/7		5/7	
	S	S12	5/6		2/5	
	F	F17	7/7		5/5	
	F	F18	8/8	34/37	6/8	27/41
0.080-	F	F18	8/8		7/8	
0.099	F	F46		8/8	2/2	9/10
0.100-	F	F19	5/5		6/6	
0.119	S	S10			3/3	
	S	S13	4/5	9/10	3/5	12/14
0.120-	S	T-4	7/7		7/7	
0.139	S	S-8	0/1*		3/5	
	S	S10			3/3	
	F	F22	6/6		3/4	
	F	F42				
	F	F44		13/14		16/19
0.140-	S	T-3	7/7		8/8	
0.159	S	T-4	7/7		7/7	
	S	S-7	6/6		5/6	
	S	S-9	1/1		3/5	
	F	F21	6/6		3/3	
	F	F43			0/1	
	S	T-3	7/7		8/8	

① S 

F 

* Includes Contaminated and/or Smeared Flaws

Table 10.–Results of Penetrant Inspections on Externally Flawed Steel Specimens (Continued)

Flaw length interval, in.	Specimen configur-ation	Specimen number	Laboratory		Production	
			Detection ratio	Total	Detection ratio*	Total
Con't.	F	F20	7/7		6/7	
	F	F45		41/41		40/45
0.160-	S	T-4	7/7		7/7	
0.179	S	S14			5/6	
	S	T-2		7/7		12/13
0.180-	S	T-2				
0.199	S	T-2				
	S	T-2				
0.200-	S	T-?				
0.219	S	S-11	1/1		3/3	
	F	F41		1/1		3/3
0.220-	F	F40				
0.750	F	F45				
	F	F42				
	S	T 2				
	F	F44				
	F	F43	1/1		1/1	
	F	F45				
	F	F21	6/6		3/3	
	F	F22	6/6		4/4	
	F	F46			2/2	
	F	F40				
	F	F41				
	F	F41				
	F	F44				
	S	T-5	7/7	20/20	2/2	12/12

Table 10.—Results of Penetrant Inspections on Externally Flawed Steel Specimens (Concluded)

Flaw length interval, in.	Specimen configur-ation	Specimen number	Laboratory		Production	
			Number of inspections	Total	Number of inspections	Total
NON	S	S1	2		2	
FLAW	S	S2	3		2	
SPECI-	S	S4	7		4	
MENS	S	S15	1		4	
	S	S16	6		5	
	S	S17	5		6	
	S	S18			7	
	S	S60			2	
	S	S61			2	
	F	F13	5		2	
	F	F14	7		2	
	F	F23	6		6	
	F	F24	6		7	
	F	F79	2		1	
	F	F80	2		1	
	F	F81	2	54	1	54

Table 11. Statistical Analysis of Penetrant Inspections Results on Externally Flawed Steel Specimens

Flaw length interval, in.	Laboratory			Production			Combined		
	Detection ratio ②	Probability		Detection ratio ②	Probability		Detection ratio	Probability	
		Observed	Lower 95% conf limit		Observed	Lower 95% conf limit			
0.000-0.019				—	—				
0.020-0.039	18/28	0.643	0.470	4/14	0.286	0.142			
0.040-0.059	5/14	0.357	0.153	6/14	0.429	0.206			
0.060-0.079	34/37	0.919	0.803	27/41	0.659	0.538	DATA CANNOT		
0.080-0.099	8/8	1.000	0.688	9/10	0.900	0.606	BE COMBINED		
0.100-0.119	9/10	0.900	0.606	12/14	0.857	0.615			
0.120-0.139	13/14	0.929	0.703	16/19	0.842	0.641			
0.140-0.159	41/41	1.000	0.930 ①	40/45	0.889	0.810			
0.160-0.179	7/7	1.000	0.652	12/13	0.923	0.684			
0.180-0.199				—	—				
0.200-0.219	1/1	1.000	—	3/3	1.000	0.368			
0.220-0.750	20/20	1.000	0.861	12/12	1.000	0.779			

① Program objective demonstrated

② Includes inspections on contaminated and/or smeared flaws

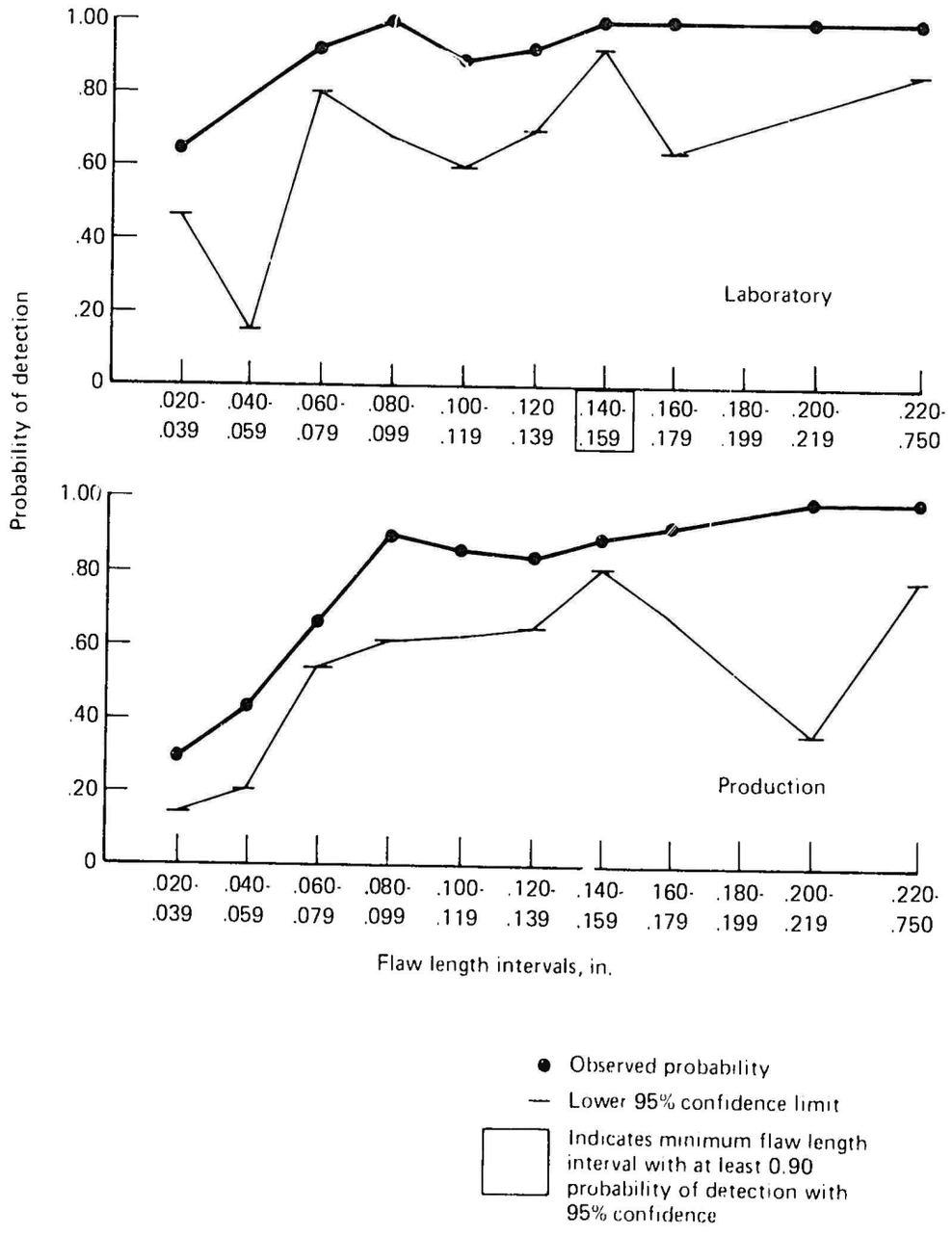


Figure 40.—Penetrant Results on Externally Flawed Steel Specimens

EDDY-CURRENT INSPECTION

Eddy-current inspection results on externally flawed steel specimens are shown in tables 12 and 13 and figure 41. The demonstrated minimum flaw length intervals with at least 0.90 probability of detection with 95% confidence are shown to be 0.140 to 0.159 in. and 0.100 to 0.139 in. in the laboratory and production, respectively. However, since the laboratory and production data are not statistically different, as shown in figure 41, data was combined and an overall minimum flaw length with the desired probability and confidence was considered to be 0.100 to 0.119 in.

ULTRASONIC INSPECTION

Ultrasonic inspection results on externally flawed steel specimens are shown in tables 14 and 15 and in figure 42. As shown in table 15, the minimum flaw length interval with at least 0.90 probability of detection with 95% confidence was demonstrated to be 0.090 to 0.139 in. in the laboratory and 0.070 to 0.089 in. in production. Although production inspections appeared to detect slightly smaller flaws more consistently, the difference between laboratory and production data was so slight that combining the data was possible and 0.060 to 0.069 in. is more likely a truer estimate of the minimum flaw length interval with the desired probability and confidence.

RADIOGRAPHIC INSPECTION

Radiographic inspection results in externally flawed steel specimens are shown in tables 16 and 17, and in figure 43. The minimum flaw length interval with at least 0.90 probability of detection with 95% confidence was not demonstrated for any of the flaw length intervals considered. Even the longest flaw interval (0.40 to 0.75 in.) was detected with only 0.57 probability with 95% confidence, and it was doubtful whether additional inspections would have brought this figure up to obtain the 0.90 probability with 95% confidence. Radiographic inspection cannot be considered a reliable method for detection of tight surface flaws in steel in comparison to the other conventional NDI methods.

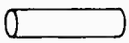
EXTERNALLY FLAWED ALUMINUM SPECIMENS

PENETRANT INSPECTION

Penetrant inspection results are shown in tables 18 and 19, and in figure 44. As with the penetrant inspections on steel specimens, the presence of contaminated and/or smeared flaws later in the program greatly affected the results. These flaws, which were readily found in the laboratory early in the program, became progressively more contaminated and/or smeared after repeated inspections. This was particularly true for those flaws used as eddy-current standards, where repeated probe contact over the specimen surface essentially closed the flaw to further penetrant inspections. Because of this, production results never obtained a flaw length interval with at least 0.90 probability of detection, with 95% confidence. However, in the laboratory 37 out of 37 flaw detections were reported in the flaw length interval 0.040 to 0.059 in., which indicates at least a 0.92 probability of detection with 95% confidence.

Table 12.—Results of Eddy Current Inspections on Externally Flawed Steel Specimens

Flaw length interval, in.	Specimen configuration ①	Specimen number	Laboratory		Production	
			Detection ratio	Total	Detection ratio	Total
0.020-0.039	F	F16	0/4			
	F	F18	1/5		2/4	
	S	S-6	0/2		1/4	
	F	F15	1/1	2/12		3/9
0.040-0.059	S	S-5	0/2		0/4	
	S	S-7	5/6		4/6	
	S	S-8	4/5	9/13	5/7	9/17
0.060-0.079	S	T-3	4/7		7/7	
	S	S-9	8/9		1/2	
	S	S11	3/3		1/2	
	F	F20	3/8		6/7	
	S	S12	2/3		2/4	
	F	F17	1/1		5/6	
	F	F18	4/5	25/36	4/5	26/32
0.080-0.099	F	F18	5/5		4/5	
	F	F46	3/3	8/8	3/3	7/8
0.100-0.119	F	F19	5/5		9/9	
	S	S10	5/5		3/3	
	S	S13	3/3	13/13	3/3	15/15
0.120-0.139	S	T-4	6/7		4/4	
	S	S-8	4/5		7/7	
	S	S10	5/5		3/3	
	F	F22	5/5		1/1	
	F	F42				
	F	F44	2/3	22/25	1/1	16/16
0.140-0.159	S	T-3	6/7		7/7	
	S	T-4	7/7		4/4	
	S	S-7	6/6		5/5	
	S	S-9	8/9		1/2	
	F	F21	7/7		5/5	
	F	F43	5/5		2/2	
	S	T-3	7/7		7/7	

① S 

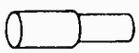
F 

Table 12.—Results of Eddy Current Inspections on Externally Flawed Steel Specimens (Continued)

Flaw length interval, in.	Specimen configuration	Specimen number	Laboratory		Production	
			Detection ratio	Total	Detection ratio	Total
	F	F20	8/8		7/7	
	F	F45	3/3	57/59		38/39
0.160-	S	T-4	7/7		4/4	
0.750	S	S14	3/3		2/2	
	S	T-2	5/5			
	S	T-2	5/5			
	S	T-2	5/5			
	S	T-2	5/5			
	S	T-2	5/5			
	S	S-11	3/3		2/2	
	F	F41				
	F	F40				
	F	F45	3/3			
	F	F42				
	S	T-2	5/5			
	F	F44	3/3		1/1	
	F	F43	5/5		2/2	
	F	F45	3/3			
	F	F21	7/7		5/5	
	F	F22	5/5		1/1	
	F	F46	3/3		3/3	
	F	F40				
	F	F41				
	F	F41				
	F	F44	3/3		1/1	
	S	T-5	2/2	76/76	4/4	25/25

Table 12. Results of Eddy Current Inspections on Externally Flawed Steel Specimens (Concluded)

Flaw length interval, in.	Specimen configuration	Specimen number	Laboratory		Production	
			Number of inspections	Total	Number of inspections	Total
NONFLAW	S	S1	5		3	
SPECIMENS	S	S2	1		5	
	S	S4	2		4	
	S	S15	5		4	
	S	S16	4		3	
	S	S17	4		3	
	S	S18	7		2	
	S	S60				
	S	S61				
	F	F13	3		2	
	F	F14	1		2	
	F	F23	5		4	
	F	F24	5		2	
	F	F79	3		2	
	F	F80	3		2	
	F	F81	3	48	1	39

Table 13.–Statistical Analysis of Eddy Current Inspection Results on Externally Flawed Steel Specimens

Flaw length interval, in.	Laboratory			Production			Combined		
	Detection ratio	Probability		Detection ratio	Probability		Detection ratio	Probability	
		Observed	Lower 95% conf limit		Observed	Lower 95% conf limit		Observed	Lower 95% conf limit
0.020-0.039	2/12	0.167	0.030	3/9	0.333	0.098	5/21	0.238	0.099
0.040-0.059	9/13	0.692	0.427	9/17	0.529	0.311	18/30	0.600	0.453
0.060-0.079	25/36	0.694	0.569	26/32	0.812	0.698	51/68	0.750	0.663
0.080-0.099	8/8	1.000	0.688	7/8	0.875	0.529	15/16	0.938	0.736
0.100-0.119	13/13	1.000	0.794	15/15	1.000	0.908①	28/28	1.000	0.899①
0.120-0.139	22/25	0.880	0.718	16/16			38/41	0.927	0.822
0.140-0.159	57/59	0.966	0.897①	38/39	0.974	0.884	95/98	0.969	0.923
0.160-0.750	76/76	1.000	0.956	25/25	1.000	0.887	101/101	1.000	0.971

① Program objective demonstrated

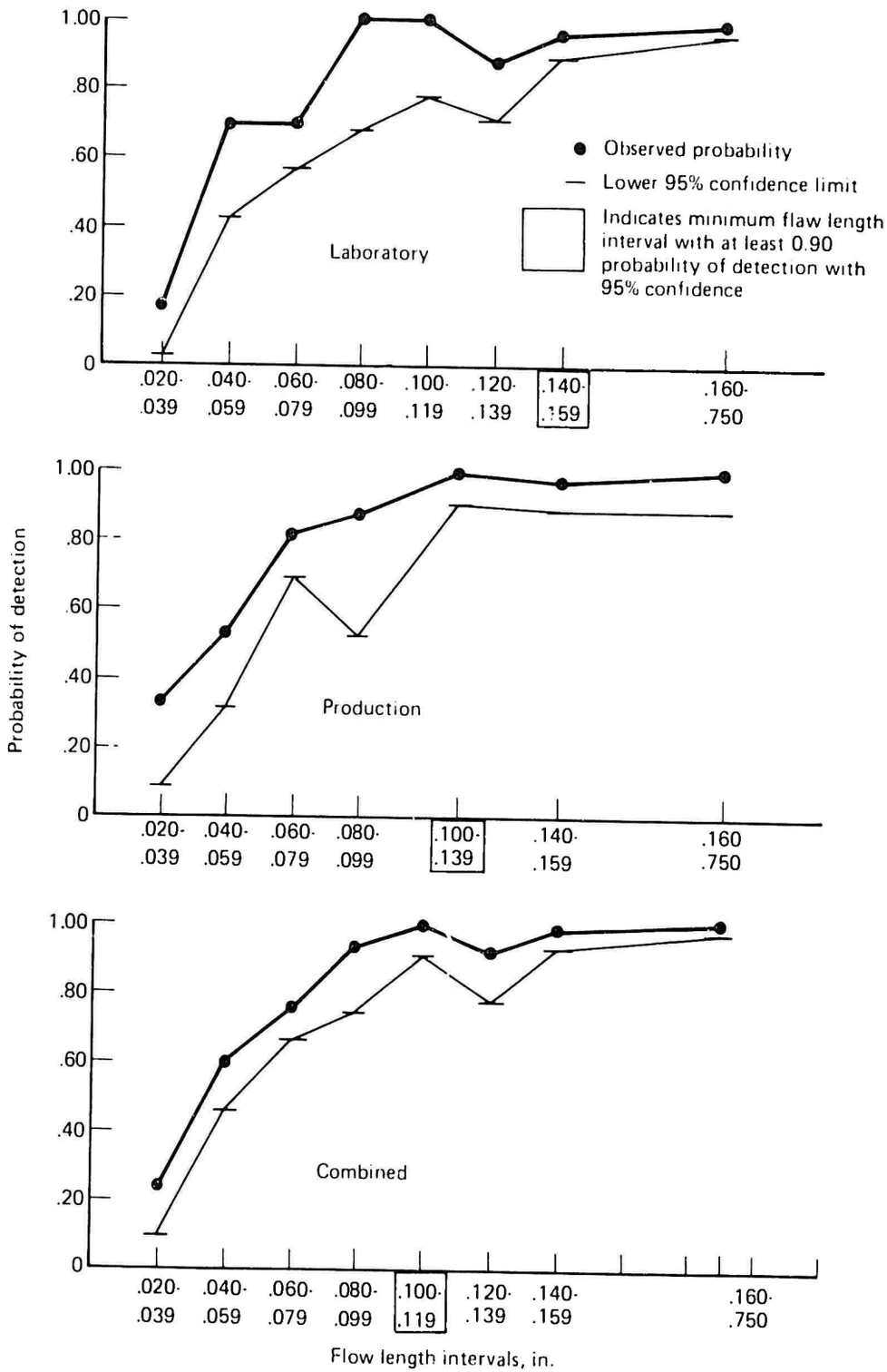
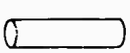


Figure 41.—Eddy Current Results on Externally Flawed Steel Specimens

Table 14.—Results of Ultrasonic Inspections on Externally Flawed Steel Specimens

Flaw length interval, in.	Specimen configuration (1)	Specimen number	Laboratory		Production	
			Detection ratio	Total	Detection ratio	Total
0.020-	F	F16	1/4		1/1	
0.039	F	F18	6/10		6/8	
	S	S-6	2/3		2/3	
	F	F15	1/1	10/18	1/1	10/13
0.040-	S	S-5	0/1		2/3	
0.059	S	S-7	9/10		5/5	
	S	S-8	12/12	21/23	6/6	13/14
0.060-	S	T-3	9/9		9/9	
0.069	S	S-9	8/9		8/9	
	S	S11	11/11		7/8	
	F	F20	7/7	35/36	12/12	36/38
0.070-	S	S12	12/13		9/9	
0.089	F	F17	6/7		11/11	
	F	F18	10/10	28/30	10/10	30/30
0.090-	F	F18	10/10		10/10	
0.109	F	F46	4/4		2/2	
	F	F19	6/6	20/20	11/11	23/23
0.110	S	S10	1/1			
0.139	S	S13	2/2		2/2	
	S	T-4	3/3		5/5	
	S	S-8	12/12		7/7	
	S	S10	1/1			
	F	F22	2/2		1/1	
	F	F42	1/1			
	F	F44	1/1	23/23		15/15
0.140-	S	T-3	9/9		9/9	
0.159	S	T-4	3/3		5/5	
	S	S-7	10/10		3/3	
	S	S-9	9/9		9/9	
	F	F21	2/2		3/3	
	F	F43	1/1			
	S	T-3	9/9		9/9	

(1) S 

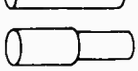
F 

Table 14.–Results of Ultrasonic Inspections on Externally Flawed Steel Specimens (Continued)

Flaw length interval, in.	Specimen configuration	Specimen number	Laboratory		Production	
			Detection ratio	Total	Detection ratio	Total
Con't	F	F20	7/7		12/12	
	F	F45	1/1	51/51		50/50
0.160	S	T-4	3/3		5/5	
0.219	S	S14	2/2		1/1	
	S	T-2				
	S	T-2				
	S	T-2				
	S	T-2				
	S	T-2				
	S	S-11	11/11		8/8	
	F	F41	1/1	17/17		14/14
0.220	F	F40	1/1			
0.750	F	F45	1/1			
	F	F42	1/1			
	S	T-2				
	F	F44	1/1			
	F	F43	1/1			
	F	F45	1/1			
	F	F21	2/2		3/3	
	F	F22	2/2		1/1	
	F	F46	4/4		2/2	
	F	F40	1/1			
	F	F41	1/1			
	F	F41	1/1			
	F	F44	1/1			
	S	T-5	2/2	20/20	3/3	9/9

Table 14. Results of Ultrasonic Inspections on Externally Flawed Steel Specimens (Concluded)

Flaw length interval, in.	Specimen configuration	Specimen number	Laboratory		Production	
			Number of inspections	Total	Number of inspections	Total
NONFLAW	S	S1	10		4	
SPECIMENS	S	S2	1		6	
	S	S4	1		3	
	S	S15	11		7	
	S	S16	4		7	
	S	S17	3		4	
	S	S18	2		4	
	S	S60	3			
	S	S61	3			
	F	F13	1		2	
	F	F14	3		3	
	F	F23	5		3	
	F	F24	2		2	
	F	F79	3		4	
	F	F80	3		4	
	F	F81	2	57	4	57

Table 15. - Statistical Analysis of Ultrasonic Inspection Results on Externally Flawed Steel Specimens

Flaw length interval, in.	Laboratory			Production			Combined		
	Detection ratio	Probability		Detection ratio	Probability		Detection ratio	Probability	
		Observed	Lower 95% conf limit		Observed	Lower 95% conf limit		Observed	Lower 95% conf limit
0.020-0.039	10/18	0.556	0.341	10/13	0.769	0.505	20/31	0.645	0.504
0.040-0.059	21/23	0.913	0.751	13/14	0.929	0.703	34/37	0.919	0.803
0.060-0.069	35/36	0.972	0.875	36/38	0.947	0.843	71/74	0.959	0.899①
0.070-0.089	28/30	0.933	0.805	30/30	1.000	0.905①	58/60	0.967	0.899
0.090-0.109	20/20	1.000	0.933①	23/23	1.000	0.878	43/43	1.000	0.933
0.110-0.139	23/23			15/15	1.000	0.819	38/38	1.000	0.924
0.140-0.159	51/51	1.000	0.943	50/50	1.000	0.942	101/101	1.000	0.971
0.160-0.219	17/17	1.000	0.838	14/14	1.000	0.807	31/31	1.000	0.908
0.200-0.750	20/20	1.000	0.861	9/9	1.000	0.717	29/29	1.000	0.902

① Program objective demonstrated

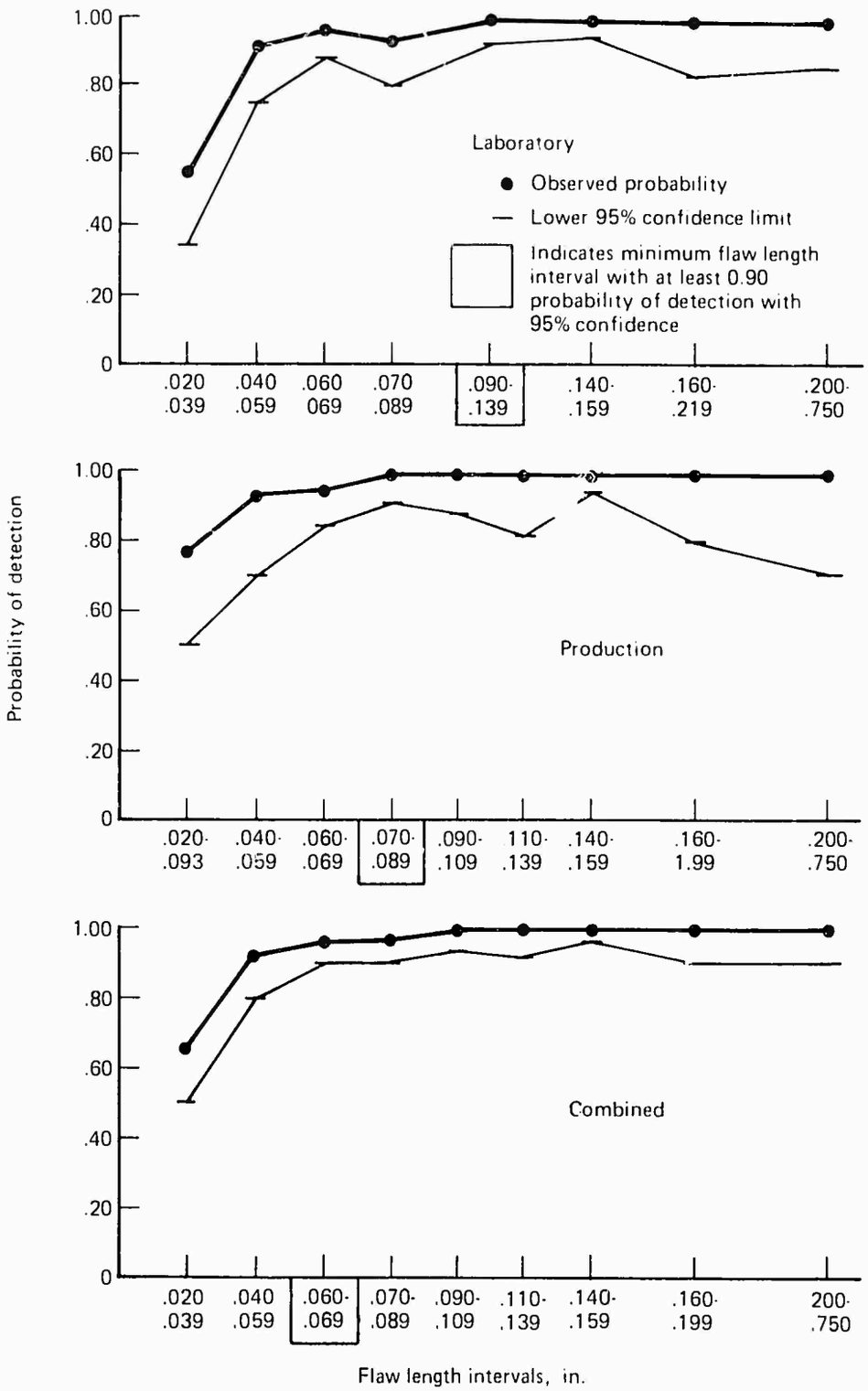
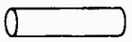


Figure 42.—Ultrasonic Results on Externally Flawed Steel Specimens

Table 16.–Results of Radiographic Inspections on Externally Flawed Steel Specimens

Flaw length interval, in.	Specimen configuration (1)	Specimen number	Laboratory		Production	
			Detection ratio	Total	Detection ratio	Total
0.020	F	F16			0/1	
0.039	F	F18			0/1	
	S	S-6			0/2	
	F	F15			0/2	0/6
0.040	S	S-5			0/3	
0.059	S	S-7	0/1		0/3	
	S	S-8	0/1	0/2	0/3	0/9
0.060	S	T-3	0/1		0/2	
0.079	S	S-9	0/1		0/3	
	S	S11	0/1		0/4	
	F	F20	0/1		0/1	
	S	S12	0/1		0/3	
	F	F17	0/1		0/1	
	F	F18		0/6	0/1	0/15
0.080	F	F18			0/1	
0.099	F	F46	0/1	0/1	0/1	0/2
0.100	F	F19	0/1		0/1	
0.119	S	S10			0/2	
	S	S13	0/1	0/2	0/3	0/6
0.120	S	T-4	0/1			
0.139	S	S-8	0/1		0/3	
	S	S10			0/2	
	F	F22	0/1		0/2	
	F	F42				
	F	F44	0/1	0/4	0/1	0/8
0.140	S	T-3	1/1		0/2	
0.159	S	T-4	0/1			
	S	S-7	0/1		0/3	
	S	S-9	0/1		0/3	
	F	F21	0/1		0/1	
	F	F43				
	S	T-3	1/1		1/2	

(1) S 

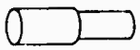
F 

Table 16. - Results of Radiographic Inspections on Externally Flawed Steel Specimens (Continued)

Flaw length interval, in.	Specimen configuration	Specimen number	Laboratory		Production	
			Detection ratio	Total	Detection ratio	Total
Cont'd	F	F20	0/1		0/1	
	F	F45		2/7		1/12
0.160	S	T4	1/1			
0.179	S	S14	0/1		0/4	
	S	T2	0/1	1/3		0/4
0.180	S	T2	0/1			
0.199	S	T2	0/1			
	S	T2	0/1	0/3		
0.200	S	T2	0/1			
0.219	S	S11	0/1		0/1	
	F	F41		0/2	0/1	0/5
0.220	F	F40	0/1		0/1	
0.239	F	F45		0/1		0/1
0.240	F	F42				
0.259	S	T2	0/1			
	F	F44	1/1	1/2	0/1	0/1
0.260	F	F43				
0.299	F	F45				
0.300	F	F21	0/1		1/1	
0.319				0/1		1/1
0.320	F	F22	1/1		1/2	
0.399	F	F46	1/1		0/1	
	F	F40	1/1		1/1	
	F	F41		3/3		2/4
0.400	F	F41				
0.750	F	F44	1/1		1/1	
	S	T5	2/2	3/3	4/4	5/5

Table 16.—Results of Radiographic Inspections on Externally Flawed Steel Specimens (Concluded)

Flaw length interval, in.	Specimen configuration	Specimen number	Laboratory		Production	
			Number of inspections	Total	Number of inspections	Total
NONFLAW	S	S1			1	
SPECIMENS	S	S2			1	
	S	S4			2	
	S	S15	1		3	
	S	S16	1		3	
	S	S17	1		3	
	S	S18	1		3	
	S	S60				
	S	S61				
	F	F13	1		1	
	F	F14	1		1	
	F	F23			1	
	F	F24			1	
	F	F79				
	F	F80				
	F	F81		6		20

Table 17.—Statistical Analysis of Radiographic Inspection Results on Externally Flawed Steel Specimens

Flaw length interval, in.	Laboratory			Production			Combined		
	Detection ratio	Probability		Detection ratio	Probability		Detection ratio	Probability	
		Observed	Lower 95% conf limit		Observed	Lower 95% conf limit		Observed	Lower 95% conf limit
0.020-0.039	–	–	–	0/6	0.000	–	0/6	0.000	–
0.040-0.054	0/2	0.000	–	0/9	0.000	–	0/11	0.000	–
0.060-0.079	0/6	0.000	–	0/15	0.000		0/21	0.000	
0.080-0.099	0/1	0.000	–	0/2	0.000		0/3	0.000	–
0.100-0.119	0/2	0.000	–	0/6	0.000		0/8	0.000	–
0.120-0.139	0/4	0.000	–	0/8	0.000	–	0/12	0.000	–
0.140-0.159	2/7	0.286	0.053	1/12	0.083	0.004	3/19	0.158	0.044
0.160-0.179	1/3	0.333	0.017	0/4	0.000	–	1/7	0.143	0.007
0.180-0.199	0/3	0.000	–	–			0/3	0.000	–
0.200-0.219	0/2	0.000	–	0/5	0.000		0/7	0.000	–
0.220-0.239	0/1	0.000	–	0/1	0.000		0/2	0.000	–
0.240-0.259	1/2	0.500	0.025	0/1	0.000		1/3	0.333	0.017
0.260-0.299	–	–			–			–	–
0.300-0.319	0/1	0.000		1/1	1.000	–	1/2	0.500	0.025
0.320-0.399	3/3	1.000	0.368	2/4	0.500	0.098	5/7	0.714	0.341
0.400-0.750	3/3	1.000	0.368	5/5	1.000	0.549	8/8	1.000	0.688

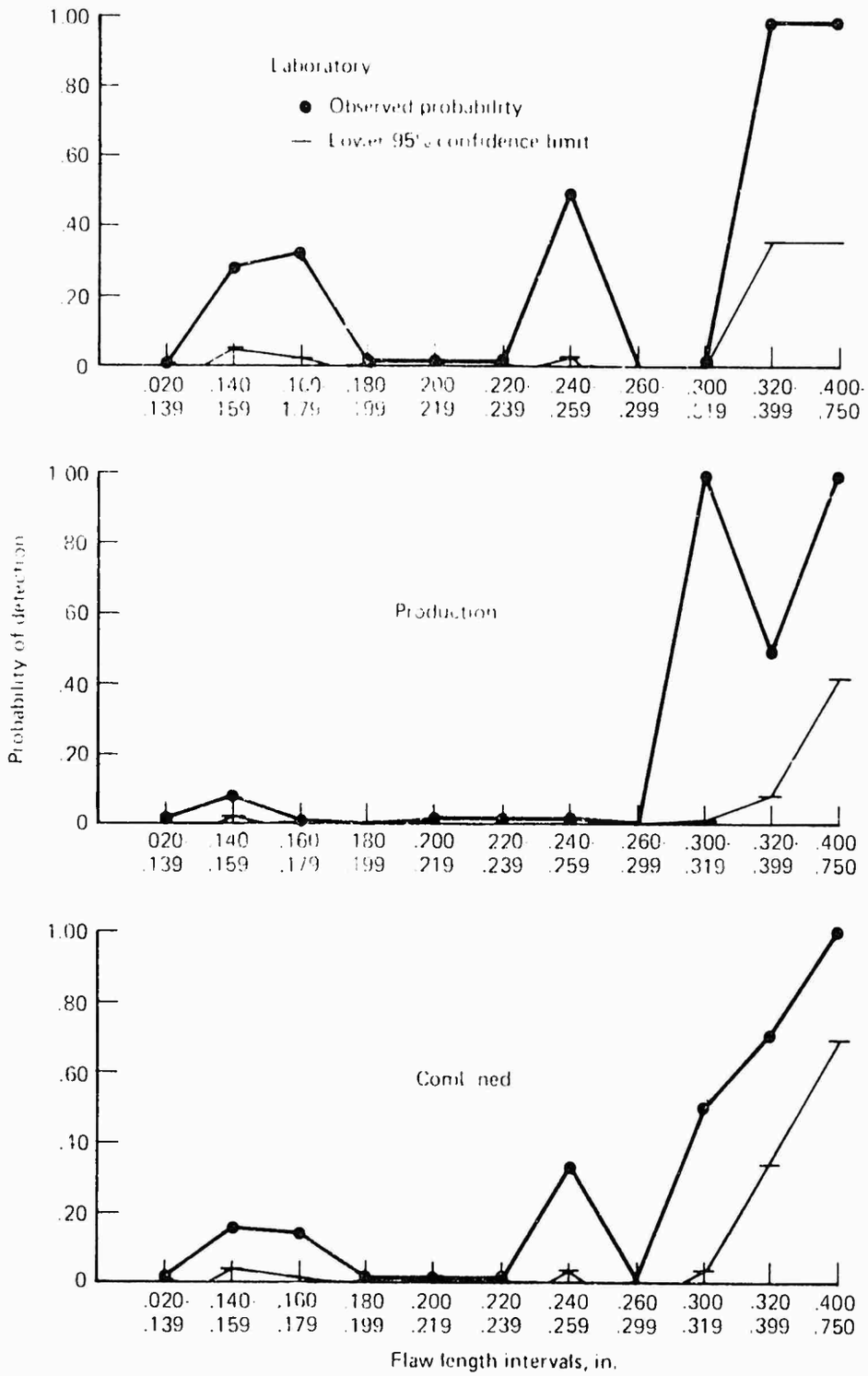
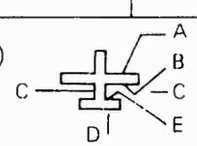


Figure 43.—Radiographic Results on Externally Flawed Steel Specimens

Table 18. Results of Penetrant Inspections on Flawed Aluminum Specimens

Flaw length interval, in.	Flaw location (1)	Specimen number	Laboratory		Production	
			Detection ratio	Total	Detection ratio	Total
0.020	A	B-21	1/6		1/2	
0.039	C	A-21	3/3	4/9	1/5	2/7
0.040	E	A-1	4/4		3/5	
0.059	C	A-41	5/5		3/4	
	B	B-31	4/4		3/3	
	D	A-1	4/4		4/5	
	D	A-2	2/2			
	B	C-1	6/6		0/2	
	C	A-31	6/6		3/4	
	B	B-21	6/6	37/37	1/2	17/25
0.060	C	A-31	6/6		3/4	
0.079	A	B-21	6/6		1/2	
	A	B-11	2/2	14/14	4/6	8/12
0.080	E	A-4	2/2			
0.099	B	C-2	3/3		7/7	
	E	A-2	2/2			
	C	B-4	2/2		5/5	
	B	C-3	4/4	13/13	4/4	16/16
0.100	D	A-3	4/4		7/7	
0.119	A	C-4	1/1		2/6 (1)	
	E	A-4	2/2			
	C	B-1	2/2		5/6 (1)	
	A	C-3	4/4		2/4 (1)	
	C	A-41	5/5		4/4	
	B	B-41	4/4	22/22	4/4	24/31
0.120	C	B-3	2/2		3/3	
0.139	C	B-2	2/5 (1)		0/3 (1)	
	C	A-21	3/3	7/10	2/5 (1)	5/11
0.140	C	B-4	4/4		4/5	
0.159	A	B-41	4/4		4/4	
	A	C-1	6/6		1/2	
	B	C-1	6/6		2/2	

(1)



(1) Includes inspections on contaminated and/or smeared flaws

Table 18. - Results of Penetrant Inspections on Flawed Aluminum Specimens (Continued)

Flaw length interval, in.	Flaw location	Specimen number	Laboratory		Production	
			Detection ratio	Total	Detection ratio	Total
Con't	B	C 3	4 4		4 4	
	B	B 11	2 2	26 26	6 6	21 23
0 160	C	B 1	2 2		6 6	
0 239	D	A 4	2 2			
	C	B 2	5 5		2 3[1]	
	C	A 11	3 3		2 2	
	E	A 1	4 4		5 5	
	B	C 2	3 3		7 7	
	A	B 31	4 4		3 3	
	E	A 3	1 1		7 7	
	C	A 11	3 3		1 2	
	C	P 3	2 2		1 3[1]	
	C	B 4	4 4		5/5	
	C	A 11	3 3		2/2	
	A	B 11	2 2	38 38	6 6	47/51

Flaw length interval, in.	Flaw location	Specimen number	Laboratory		Production	
			Number of inspections	Total	Number of inspections	Total
NONFLAW		D1	4		8	
SPECIMENS		D2	4		6	
		D3	3		4	
		D4	1		3	
		D12	4		5	
		D21	2	18	5	31

Table 19.–Statistical Analysis of Penetrant Inspection Results on Flawed Aluminum Specimens

Flaw length interval, in.	Laboratory (1)			Production (1)			Combined (1)		
	Detection ratio	Probability 0/1		Detection ratio	Probability		Detection ratio	Probability	
		Observed	Lower 95% conf limit		Observed	Lower 95% conf limit			
0.020-0.039	4/9	0.444	0.169	2/7	0.286	0.053			
0.040-0.059	37/37	1.000	0.922 ①	17/25	0.680	0.528			
0.060-0.079	14/14	1.000	0.807	8/12	0.667	0.391			
0.080-0.099	13/13	1.000	0.794	16/16	1.000	0.829	DATA CANNOT		
0.100-0.119	22/22	1.000	0.873	24/31 (1)	0.744 (1)	0.652 (1)	BE COMBINED		
0.120-0.139	7/10 (1)	0.700 (1)	0.393 (1)	5/11 (1)	0.455 (1)	0.200 (1)			
0.140-0.159	26/26	1.000	0.891	21/23 (1)	0.913 (1)	0.751 (1)			
0.160-0.239	38/38	1.000	0.924	47/51 (1)	0.922 (1)	0.829 (1)			

① Program objective demonstrated

(1) Includes inspections on contaminated and/or smeared flaws

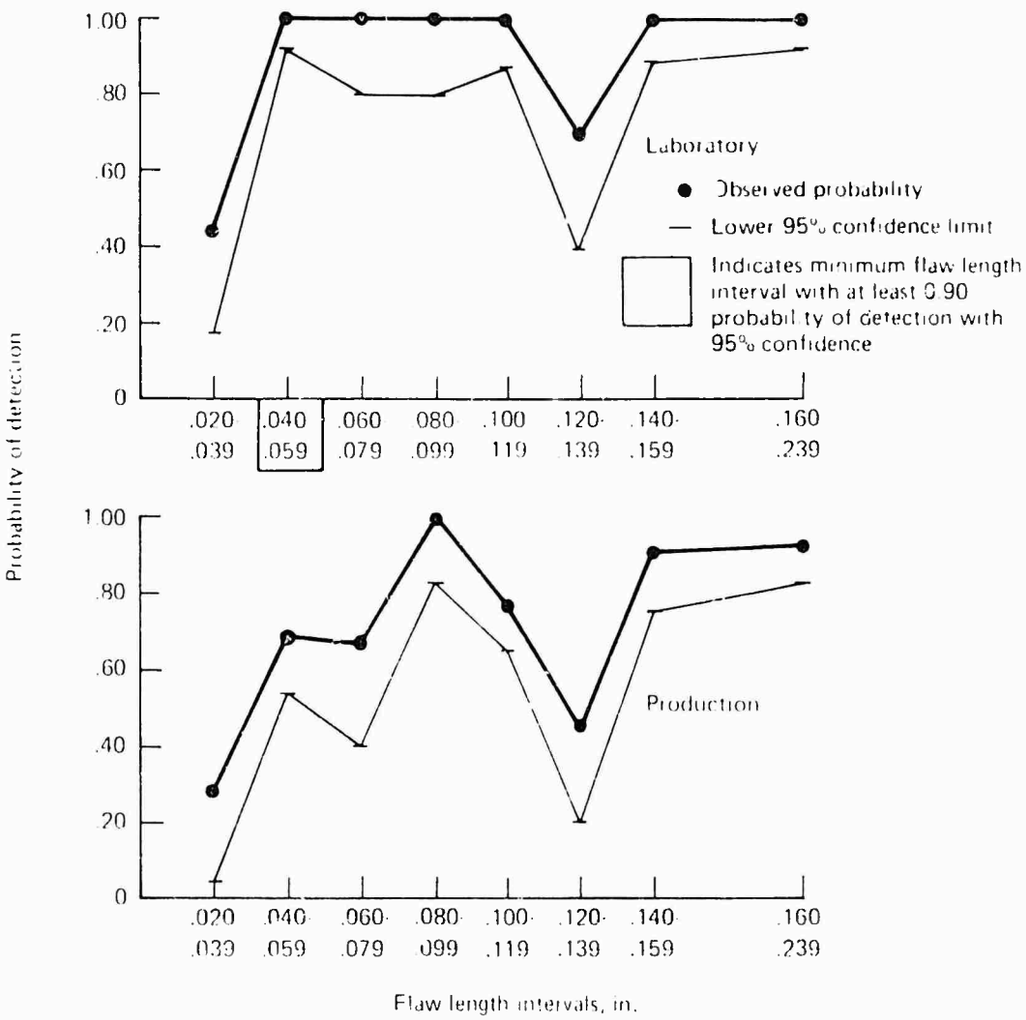


Figure 44. -Penetrant Results on Flawed Aluminum Specimens

Three misses were reported in the laboratory on flaw lengths greater than this. However, the misses were all on the same flaw, which also was used as an eddy-current standard. Further, these misses occurred after two previous successful detections. This is additional support to the conclusion that the detectability of flaws by penetrant methods was changing during the course of the program.

EDDY-CURRENT INSPECTION

Eddy-current inspection results are shown in tables 20 and 21, and in figure 45. The minimum flaw length intervals with at least 0.90 probability of detection with 95% confidence were 0.160 to 0.239 in. and 0.120 to 0.179 in. in the laboratory and production, respectively. Production inspection appeared to find the smaller flaws more consistently, but as figure 45 indicates, the observed probabilities of detection for flaw sizes above 0.120 in. are very similar in the laboratory and production. By combining data, a better estimate of eddy-current capabilities was possible. The combined data showed the desired probability and confidence of detection was essentially obtained for the flaw length interval, 0.160 to 0.199 in. The flaws in this range may be longer than expected by eddy-current methods, but, as table 20 indicates, detectability was influenced by flaw location as well as length for these aluminum specimens.

ULTRASONIC INSPECTION

Ultrasonic inspection results are shown in tables 22 and 23 and in figure 46. The flaw length internal with the desired probability and confidence was demonstrated in the laboratory to be 0.160 to 0.199 in. By recognizing the slight differences between laboratory and production, as figure 46 indicates, a similar interval was demonstrated for the combined production and laboratory data. As with eddy-current inspections on these same aluminum specimens, both flaw location and flaw length were the factors influencing detectability. This was especially true in ultrasonic inspections where a combination of longitudinal, shear and surface waves were used depending on flaw location and the particular inspector. Because of these factors, conclusions based upon flaw length alone should not be applied to other parts unless they are closely similar in design to these unique specimens.

RADIOGRAPHIC INSPECTION

Radiographic inspection results are shown in tables 24 and 25, and in figure 47. The minimum flaw length intervals detectable with at least 0.90 probability and 95% confidence are shown in table 25 to be 0.060 to 0.119 in. for the laboratory and 0.080 to 0.159 in. for production. These different flaw intervals demonstrated in the laboratory and in production were mostly due to different numbers of tests. A truer estimate of radiographic capability was shown by combining data and calculating an overall flaw length interval of 0.080 to 0.119 in.

INTERNALLY FLAWED HOLLOW STEEL SPECIMENS

Inspection results for the hollow steel specimens are presented in tables 26 to 35, and in figures 48 to 52. As the tables indicate, two hollow configurations, hollow straight and hollow filleted, were used in the program. Since the inspection results were essentially the same for the two hollow configurations, data were combined for analysis.

Table 20. – Results of Eddy Current Inspections on Flawed Aluminum Specimens

Flaw length interval, in.	Flaw location (1)	Specimen number	Laboratory		Production	
			Detection ratio	Total	Detection ratio	Total
0.020-	A	B-21	2/2		0/1	
0.039	C	A-21	0/2	2/4	1/5	1/6
0.040-	E	A-1	0/2		1/2	
0.059	C	A-41	4/4		1/2	
	B	B-31	2/2		0/2	
	D	A-1	0/2		2/2	
	D	A-2			1/1	
	B	C-1	1/2		4/4	
	C	A-31	2/2		1/1	
	B	B-21	2/2	11/16	1/1	11/15
0.060-	C	A-31	2/2		1/1	
0.079	A	B-21	2/2		1/1	
	A	B-11	4/4	8/8	5/6	7/8
0.080-	E	A-4	0/1		1/1	
0.099	B	C-2	6/10		6/6	
	E	A-2			1/1	
	C	B-4	3/8		6/7	
	B	C-3	4/6	13/25	3/3	17/18
0.100-	D	A-3	3/4		5/7	
0.119	A	C-4	4/6		6/7	
	E	A-4	1/1		1/1	
	C	B-1	2/4		10/10	
	A	C-3	5/6		3/3	
	C	A-41	4/4		2/2	
	B	B-41	3/4	22/29	4/4	31/34
0.120-	C	B-3	3/3		9/9	
0.139	C	B-2	2/2		6/6	
	C	A-21	2/2	7/7	5/5	20/20
0.140-	C	B-4	7/8		6/7	
0.159	A	B-41	3/4		5/6	
	A	C-1	2/2		5/5	
	B	C-1	2/2		4/4	

(1)

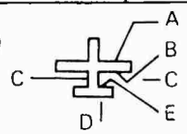


Table 20.—Results of Eddy Current Inspections on Flawed Aluminum Specimens (Continued)

Flaw length interval, in.	Flaw location	Specimen number	Laboratory		Production	
			Detection ratio	Total	Detection ratio	Total
Con't	B	C-3	6/6		3/3	
	B	B-11	3/4	23/26	4/4	27/29
0.160-0.179	C	B-1	4/4		10/10	
	D	A-4	1/1		1/1	
	C	B-2	2/2		7/7	
	C	A-11	2/2	9/9	2/2	20/20
0.180-0.199	E	A-1	2/2		2/2	
	B	C-2	10/10		6/6	
	A	B-31	2/2		3/3	
	E	A-3	3/4	17/18	6/6	17/17
0.200-0.219	C	A-11	2/2	2/2	2/2	2/2
0.220-0.239	C	B-3	3/3		9/9	
	C	B-4	B/B		7/7	
	C	A-11	2/2		2/2	
	A	B-11	4/4	17/17	6/6	24/24

Flaw length interval, in.	Flaw location	Specimen number	Laboratory		Production	
			Number of inspections	Total	Number of inspections	Total
NONFLAW SPECIMENS		D1	5		6	
		D2	10		5	
		D3	3		6	
		D4	3		9	
		D12			3	
		121		21	5	34

Table 21 —Statistical Analysis of Eddy Current Inspection Results on Flawed Aluminum Specimens

Flaw length interval, in.	Laboratory			Production			Combined		
	Detection ratio	Probability		Detection ratio	Probability		Detection ratio	Probability	
		Observed	Lower 95% conf limit		Observed	Lower 95% conf limit		Observed	Lower 95% conf limit
0.020-0.039	2/4	0.500	0.098	1/6	0.167	0.009	3/10	0.300	0.087
0.040-0.059	11/16	0.688	0.452	11/15	0.733	0.489	22/31	0.710	0.577
0.060-0.079	8/8	1.000	0.688	7/8	0.875	0.529	15/16	0.938	0.736
0.080-0.099	13/25	0.520	0.355	17/18	0.944	0.762	30/43	0.698	0.573
0.100-0.119	22/29	0.759	0.594	31/34	0.912	0.787	53/63	0.841	0.765
0.120-0.139	7/7	1.000	0.652	20/20	0.971	0.914①	27/27	1.000	0.895①
0.140-0.159	23/26	0.885	0.728	27/29			50/55	0.909	0.818
0.160-0.179	9/9	0.978	0.903①	20/20			29/29	1.000	0.902
0.180-0.199	17/18			17/17	1.000	0.838	34/35	0.971	0.872
0.200-0.219	2/2			2/2	1.000	0.224	4/4	1.000	0.473
0.220-0.239	17/17			24/24	1.000	0.883	41/41	1.000	0.930

① Program objective demonstrated

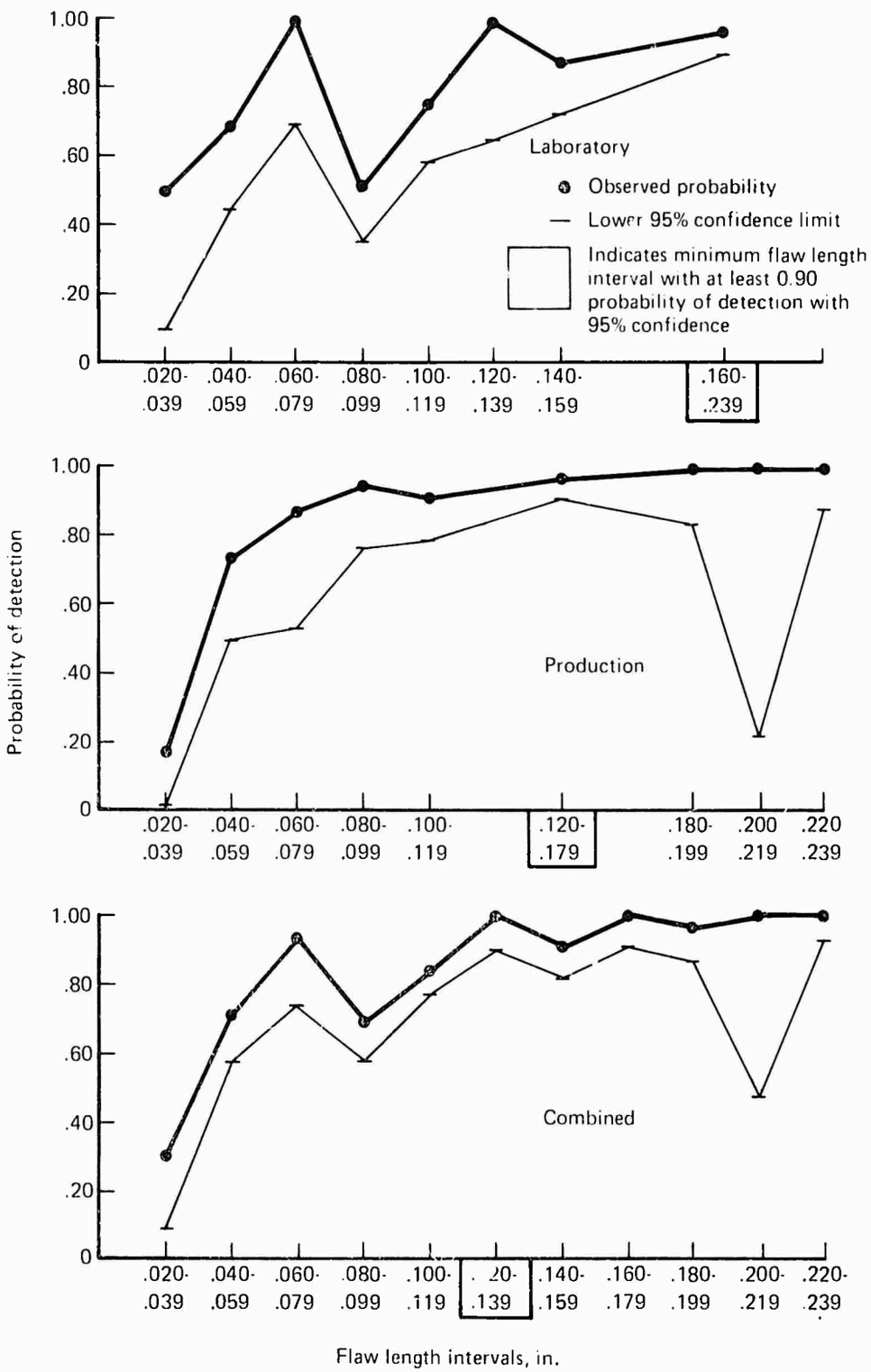


Figure 45.—Eddy Current Results on Flawed Aluminum Specimens

Table 22.—Results on Ultrasonic Inspections on Flawed Aluminum Specimens

Flaw length interval, in.	Flaw location ①	Specimen number	Laboratory		Production	
			Detection ratio	Total	Detection ratio	Total
0.020-	A	B-21	4/6			
0.039	C	A-21	0/3	4/9	1/2	1/2
0.040-	E	A-1	2/3		1/2	
0.059	C	A-41	1/5		2/2	
	B	B-31	5/5		2/3	
	D	A-1	3/3		1/2	
	D	A-2			2/2	
	B	C-1	0/4		3/4	
	C	A-31	1/5			
	B	B-21	5/6	17/31		11/15
0.060-	C	A-31	2/5			
0.079	A	B-21	6/6			
	A	B-11	6/6	14/17	4/4	4/4
0.080-	E	A-4			2/2	
0.099	B	C-2	6/6		3/3	
	E	A-2			2/2	
	C	B-4	1/4		3/5	
	B	C-3	7/7	14/17	5/5	15/17
0.100-	D	A-3	5/5		4/4	
0.119	A	C-4	4/4		4/5	
	E	A-4			2/2	
	C	B-1	4/4		5/6	
	A	C-3	7/7		5/5	
	C	A-41	3/5		2/2	
	B	B-41	5/6	28/31	2/2	24/26
0.120-	C	B-3	1/2		9/9	
0.139	C	B-2	6/6		5/5	
	C	A-21	3/3	10/11	2/2	16/16
0.140-	C	B-4	2/4		5/6	
0.159	A	B-41	6/6		2/2	
	A	C-1	4/4		3/4	
	B	C-1	4/4		3/4	

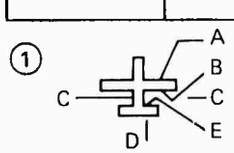


Table 22.–Results on Ultrasonic Inspections on Flawed Aluminum Specimens (Continued)

Flaw length interval, in.	Flaw location	Specimen number	Laboratory		Production	
			Detection ratio	Total	Detection ratio	Total
Con't.	B	C-3	7/7		5/5	
	B	B-11	5/5	28/30	4/4	22/25
0.160-0.179	C	B-1	4/4		5/6	
	D	A-4			2/2	
	C	B-2	6/6		4/4	
	C	A-11	1/1	11/11	2/2	13/14
0.180-0.199	E	A-1	3/3		2/2	
	B	C-2	6/6		3/3	
	A	B-31	5/5		3/3	
	E	A-3	5/5	19/19	4/4	12/12
0.200-0.219	C	A-11	1/1	1/1	2/2	2/2
0.220-0.239	C	B-3	2/2		9/9	
	C	B-4	2/4		4/5	
	C	A-11	1/1		2/2	
	A	B-11	6/6	11/13	4/4	19/20

Flaw length interval, in.	Flaw location	Specimen number	Laboratory		Production	
			Number of inspections	Total	Number of inspections	Total
NONFLAW SPECIMENS		D1	7		6	
		D2	6		3	
		D3	5		5	
		D4	2		7	
		D12	7		3	
		D21	3	30	4	28

Table 23.–Statistical Analysis of Ultrasonic Inspection Results on Flawed Aluminum Specimens

Flaw length interval, in.	Laboratory			Production			Combined		
	Detection ratio	Probability		Detection ratio	Probability		Detection ratio	Probability	
		Observed	Lower 95% conf limit		Observed	Lower 95% conf limit		Observed	Lower 95% conf limit
0.020-0.039	4/9	0.444	0.169	1/2	0.500	0.025	5/11	0.455	0.200
0.040-0.059	17/31	0.548	0.388	11/15	0.733	0.489	28/46	0.609	0.482
0.060-0.079	14/17	0.824	0.604	4/4	1.000	0.473	18/21	0.857	0.671
0.080-0.099	14/17	0.824	0.604	15/17	0.882	0.674	29/34	0.853	0.715
0.100-0.119	28/31	0.903	0.769	24/26	0.923	0.777	52/57	0.912	0.849
0.120-0.139	10/11	0.909	0.636	16/16	1.000	0.829	26/27	0.963	0.836
0.140-0.159	28/30	0.933	0.805	22/25	0.880	0.718	50/55	0.909	0.845
0.160-0.179	11/11	1.000	0.905①	13/14	0.929	0.703	24/25	0.982	0.918①
0.180-0.199	19/19			12/12	1.000	0.779	31/31		
0.200-0.219	1/1	1.000		2/2	1.000	0.224	3/3	1.000	0.368
0.220-0.239	11/13	0.846	0.590	12/20	0.950	0.784	30/33	0.909	0.782

① Program objective demonstrated

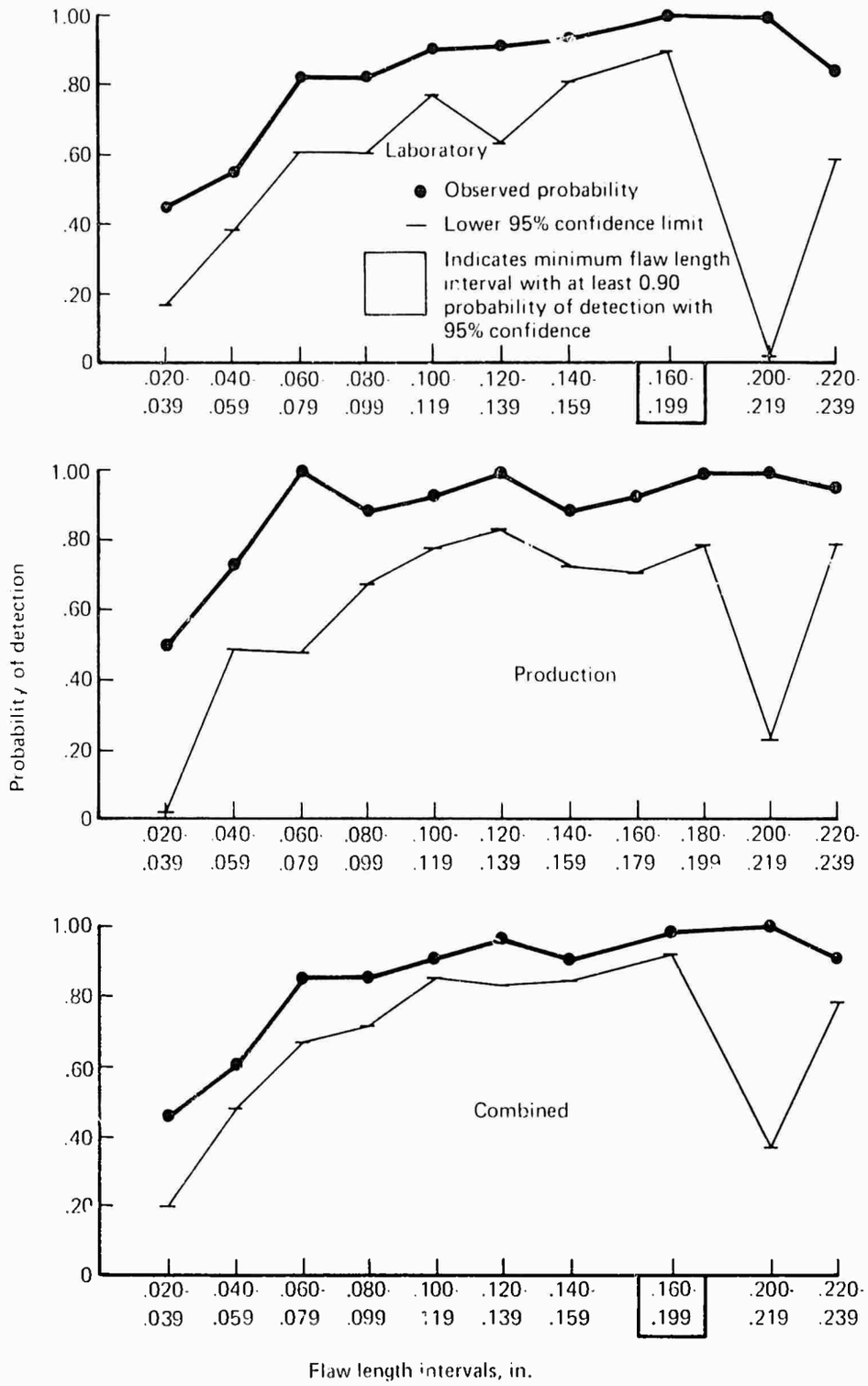


Figure 46 – Ultrasonic Results on Flawed Aluminum Specimens

Table 24.—Results of Radiographic Inspections on Flawed Aluminum Specimens

Flaw length interval, in.	Flaw location (1)	Specimen number	Laboratory		Production	
			Detection ratio	Total	Detection ratio	Total
0.020-	A	B-21	0/5		0/5	
0.039	C	A-21	1/2	1/7	3/3	3/8
0.040-	E	A-1	5/6		4/4	
0.059	C	A-41	3/3		2/2	
	B	B-31	0/2		0/3	
	D	A-1	6/6		4/4	
	D	A-2	3/3		1/1	
	B	C-1	4/4		4/4	
	C	A-31	5/5		3/3	
	B	B-21	4/5	30/34	3/5	21/26
0.060-	C	A-31	5/5		3/3	
0.079	A	B-21	5/5		4/5	
	A	B-11	1/1	11/11	3/3	10/11
0.080-	E	A-4	2/2		1/1	
0.099	B	C-2	3/3		1/1	
	E	A-2	3/3		1/1	
	C	B-4	4/4		1/1	
	B	C-3	2/2	14/14	2/2	6/6
0.100-	D	A-3	4/4			
0.119	A	C-4	1/1		2/2	
	E	A-4	2/2		1/1	
	C	B-1	2/2			
	A	C-3	2/2		2/2	
	C	A-41	3/3		2/2	
	B	B-41	2/2	16/16		7/7
0.120-	C	B-3	2/2		3/3	
0.139	C	B-2	2/2		1/1	
	C	A-21	2/2	6/6	3/3	7/7
0.140-	C	B-4	4/4		1/1	
0.159	A	B-41	2/2			
	A	C-1	4/4		4/4	
	B	C-1	4/4		4/4	

(1)

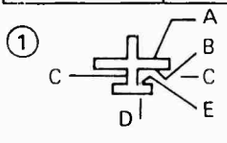


Table 24.—Results of Radiographic Inspections on Flawed Aluminum Specimens (Continued)

Flaw length interval, in.	Flaw location	Specimen number	Laboratory		Production	
			Detection ratio	Total	Detection ratio	Total
Con't	B	C-3	2/2		2/2	
	B	B-11	1/1	17/17	3/3	14/14
0.160-	C	B-1	2/2			
0.179	D	A-4	2/2		1/1	
	C	B-2	2/2		1/1	
	C	A-11	1/1	7/7		2/2
0.180-	E	A-1	6/6		4/4	
0.199	B	C-2	3/3		1/1	
	A	B-31	2/2		3/3	
	E	A-3	4/4	15/15		8/8
0.200-0.219	C	A-11	1/1	1/1		
0.220-	C	B-3	2/2		3/3	
0.239	C	B-4	4/4		1/1	
	C	A-11	1/1			
	A	B-11	1/1	8/8	3/3	7/7

Flaw length interval, in.	Flaw location	Specimen number	Laboratory		Production	
			Number of specimens	Total	Number of specimens	Total
NONFLAW		D1	5		1	
SPECIMENS		D2	4		2	
		D3	4		2	
		D4	2		2	
		D12	2		3	
		D21	2	19	4	14

Table 25.—Statistical Analysis of Radiographic Inspection Results on Flawed Aluminum Specimens

Flaw length interval, in.	Laboratory			Production			Combined		
	Detection ratio	Probability		Detection ratio	Probability		Detection ratio	Probability	
		Observed	Lower 95% conf limit		Observed	Lower 95% conf limit		Observed	Lower 95% conf limit
0.020-0.039	1/7	0.143	0.007	3/8	0.375	0.111	4/15	0.267	0.097
0.040-0.059	30/34	0.882	0.751	21/26	0.809	0.637	51/60	0.850	0.717
0.060-0.079	11/11	1.000	0.930 ①	10/11	0.909	0.636	21/22	0.955	0.802
0.080-0.099	14/14			6/6	1.000	0.916 ①	20/20	1.000	0.933 ①
0.100-0.119	16/16			7/7			23/23		
0.120-0.139	6/6	1.000	0.607	7/7			13/13	1.000	0.794
0.140-0.159	17/17	1.000	0.838	14/14			31/31	1.000	0.908
0.160-0.179	7/7	1.000	0.652	2/2	1.000	0.224	9/9	1.000	0.717
0.180-0.199	15/15	1.000	0.819	8/8	1.000	0.688	23/23	1.000	0.878
0.200-0.219	1/1	1.000					1/1	1.000	
0.220-0.239	8/8	1.000	0.688	7/7	1.000	0.652	15/15	1.000	0.819

① Program objective demonstrated

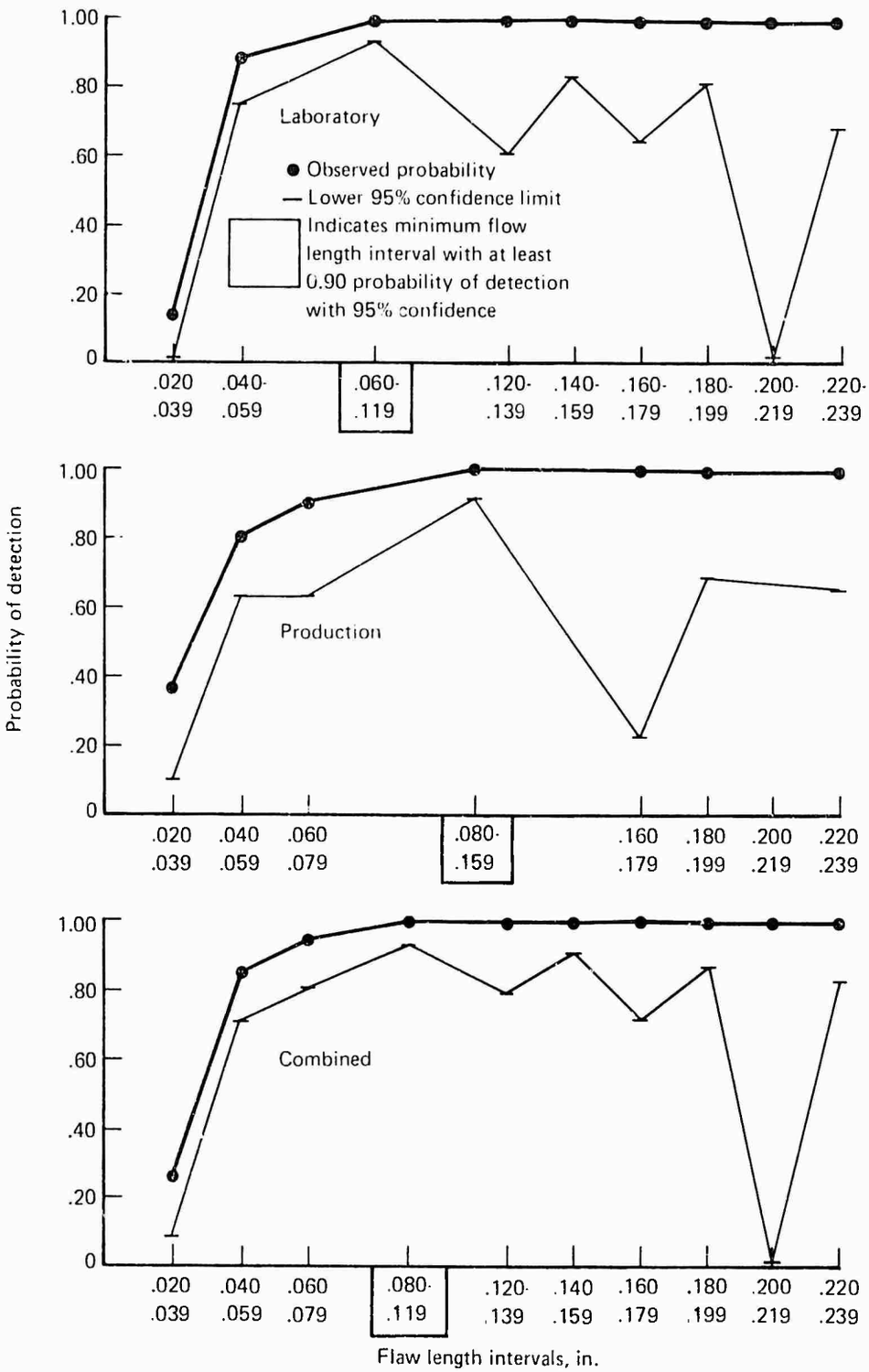


Figure 47.—Radiographic Results on Flawed Aluminum Specimens

Table 26. – Results of Magnetic Particle Inspections on Internally Flawed Hollow Steel Specimens

Flaw length interval, in.	Specimen configuration ①	Specimen number	Laboratory		Production	
			Detection ratio	Total	Detection ratio	Total
0.060-0.079	H	H-11	9/9		0/1	
	H	H-15	9/9		0/1	
	HF-H	T1-1	9/9	27/27		0/2
0.080-0.099	HF	H6	11/11		0/3	
	HF	H8	11/11		0/3	
	HF	H-12	6/6		0/1	
	HF	H14	2/2		2/3	
	H	H13	1/1	31/31		2/10
0.100-0.119	H	H1	4/4		1/4	
	H	H4	3/3		2/4	
	H	H9	2/2		2/4	
	H	H11	9/9		0/1	
	HF	H7	6/8	24/26	0/4	5/13
0.120-0.139	HF	H16	1/1		2/3	
	H	H3	4/4		1/4	
	HF	H6	11/11		0/3	
	H	H15	9/9	25/25	0/1	3/11
0.140-0.159	HF	H7	8/8		0/4	
	HF	H10	8/8		1/4	
	H	H1	4/4		2/4	
	H	H13	1/1			
	H	H17	3/3	24/24	1/2	4/14
0.160-0.179	HF	H18	2/2		0/2	
	H	H5	1/1		1/3	
	H	H19	1/1	4/4		1/5
0.180-0.199	HF-H	T1-1	9/9			
	H	H3	4/4	13/13	2/4	2/4
0.200-0.239	H	H17	3/3	3/3	1/2	1/2
0.240-0.279	HF	H27	1/1		1/2	
	HF	H22	2/2	3/3	2/5	3/7
0.280-0.319	HF	H24	1/1		1/2	
	HF-H	T1-1	9/9			

① H –

HF –

Table 26.—Results of Magnetic Particle Inspections on Internally Flawed Hollow Steel Specimens (Continued)

Flaw length interval, in.	Specimen configuration	Specimen number	Laboratory		Production	
			Detection ratio	Total	Detection ratio	Total
Con't	HF	H14	2/2		2/3	
	HF	H16	1/1		2/3	
	H	H21	1/1	14/14	3/4	8/12
0.320-0.359	H	H19	1/1			
	H	H29	2/2		4/4	
	H	H23	1/1	4/4	3/4	7/8
0.360-0.570	HF	H26	1/1			
	H	H21	1/1		4/4	
	HF	H28	1/1		3/4	
	HF	H18	2/2		0/2	
	HF	H24	1/1		1/2	
	H	H19	1/1			
	H	H23	1/1	8/8	4/4	12/16

Flaw length interval, in.	Specimen configuration	Specimen number	Laboratory		Production	
			Number of inspections	Total	Number of inspections	Total
NONFLAW SPECIMENS	H	H2	2		4	
	H	H20			3	
	H	H25	1		2	
	H	H62	3		1	
	H	H63	1		4	
	H	H64			4	
	HF	HF6	6		2	
	HF	HF29	8		3	
	HF	HF30	9		1	
	HF	HF24	2		5	
	HF	HF25	3			
	HF	HF26	3	38	1	30

Table 27.--Statistical Analysis of Magnetic Particle Inspection Results on Internally Flawed Hollow Steel Specimens

Flaw length interval, in.	Laboratory			Production			Combined		
	Detection ratio	Probability		Detection ratio	Probability		Detection ratio	Probability	
		Observed	Lower 95% conf limit		Observed	Lower 95% conf limit			
0.060-0.079	27/27	1.000	0.895	0/2	0.000	–			
0.080-0.099	31/31	1.000	0.908	2/10	0.200	0.037			
0.100-0.119	24/26	0.923	0.777	5/13	0.385	0.166			
0.120-0.139	25/25	1.000	0.887	3/11	0.273	0.079	DATA CANNOT		
0.140-0.159	24/24	1.000	0.883	4/14	0.286	0.061	BE COMBINED		
0.160-0.179	4/4	1.000	0.473	1/5	0.200	0.010			
0.180-0.199	13/13	1.000	0.794	2/4	0.500	0.098			
0.200-0.239	3/3	1.000	0.368	1/2	0.500	0.025			
0.240-0.279	3/3	1.000	0.368	3/7	0.429	0.129			
0.280-0.319	14/14	1.000	0.807	8/12	0.667	0.391			
0.320-0.359	4/4	1.000	0.473	7/8	0.875	0.529			
0.360-0.570	8/8	1.000	0.688	12/16	0.750	0.516			

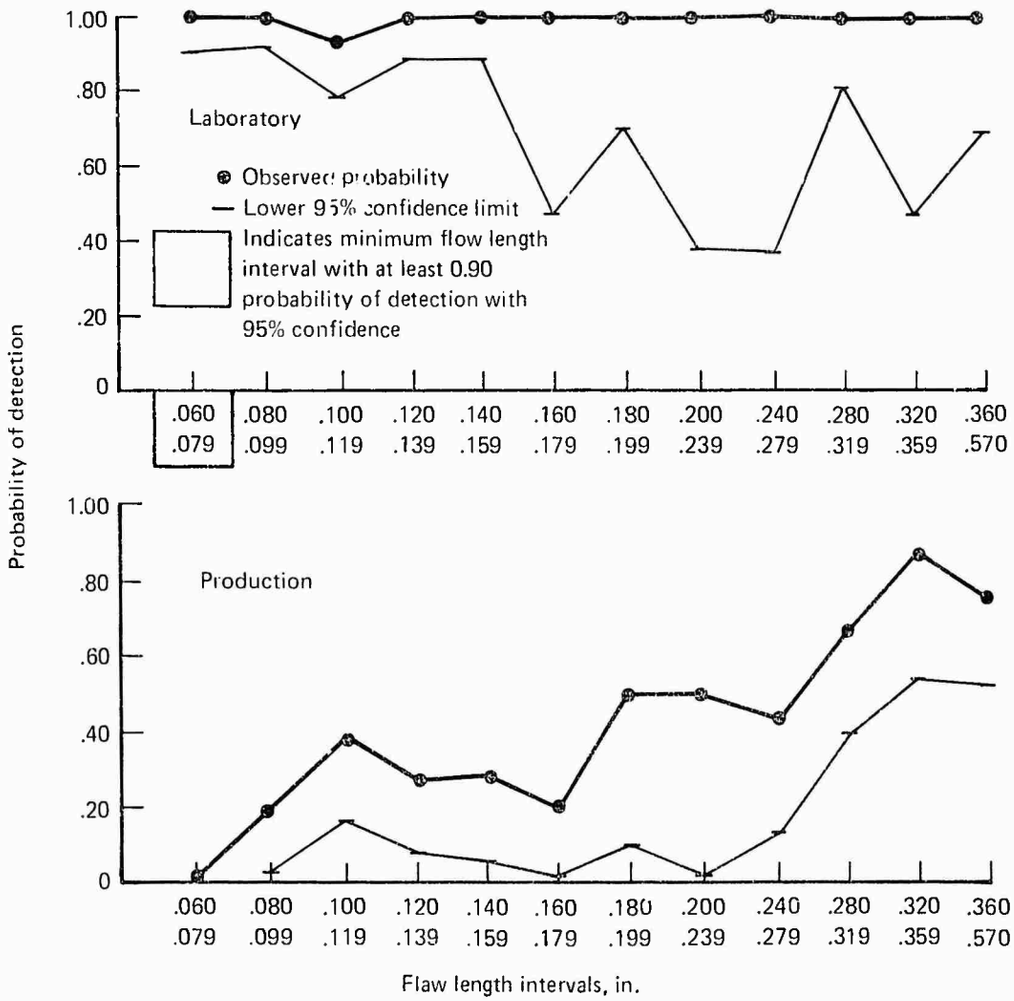


Figure 48.—Magnetic Particle Results on Internally Flawed Hollow Steel Specimens

Table 28.—Results of Penetrant Inspections on Internally Flawed Hollow Steel Specimens

Flaw length interval, in.	Specimen configuration (1)	Specimen number	Laboratory (2)		Production (2)	
			Detection ratio	Total	Detection ratio	Total
0.060-0.079	H	H-11	2/5		0/1	
	H	H-15	0/5		0/1	
	HF-H	T1-1	3/3	5/13		0/2
0.080-0.099	HF	H6	1/10		0/2	
	HF	H8	6/10		0/2	
	HF	H-12	7/9		0/1	
	HF	H14	4/4		2/3	
	H	H13		18/33		2/8
0.100-0.119	H	H1	2/2		0/4	
	H	H4	2/2		1/4	
	H	H9			0/4	
	H	H11	3/5		0/1	
	HF	H7	2/8	9/17	0/3	1/16
0.120-0.139	HF	H16	4/4		1/3	
	H	H3	0/2		0/4	
	HF	H6	5/10		0/2	
	H	H15	2/5	11/21	0/1	1/10
0.140-0.159	HF	H7	5/8		0/3	
	HF	H10	8/8		3/3	
	H	H1	2/2		1/4	
	H	H13				
	H	H17	1/1	16/19	1/2	5/12
0.160-0.179	HF	H18	3/3		1/3	
	H	H5			1/2	
	H	H19		3/3		2/5
0.180-0.199	HF-H	T1-1	3/3			
	H	H3	0/2	3/5	0/4	0/4
0.200-0.239	H	H17	1/1	1/1	1/2	1/2
0.240-0.279	HF	H27	2/2		1/2	
	HF	H22	1/1	3/3	3/5	4/7
0.280-0.319	HF	H24	2/2		1/2	
	HF-H	T1-1	3/3			

(1) H– 

HF– 

(2) Includes inspections on contaminated and/or smeared flaws

Table 28.—Results of Penetrant Inspections on Internally Flawed Hollow Steel Specimens (Continued)

Flaw length interval, in.	Specimen configuration	Specimen number	Laboratory		Production	
			Detection ratio	Total	Detection ratio	Total
Con't	HF	H14	4/4		2/3	
	HF	H16	4/4		2/3	
	H	H21		13/13	3/4	8/12
0.320-0.359	H	H19				
	H	H29	1/1		3/4	
	H	H23		1/1	3/5	6/9
0.360-0.399	HF	H26	4/4			
	H	H21		4/4	4/4	4/4
0.440-0.479	HF	H28			2/4	
	HF	H18	3/3		2/3	
	HF	H24	2/2	5/5	1/2	5/9
0.480-0.599	H	H19				
	H	H23			5/5	5/5

Flaw length interval, in.	Specimen configuration	Specimen number	Laboratory		Production	
			Number of inspections	Total	Number of inspections	Total
NONFLAW SPECIMENS	H	H2	2		4	
	H	H20	4		3	
	H	H25	3		2	
	H	H62	2		1	
	H	H63			4	
	H	H64			4	
	HF	HF6	6		2	
	HF	HF29	8		3	
	HF	HF30	4		1	
	HF	HF24	3		5	
	HF	HF25	5			
	HF	HF26	7	44	1	30

Table 29.—Statistical Analysis of Penetrant Inspection Results on Internally Flawed Hollow Steel Specimens

Flaw length interval, in.	Laboratory ①			Production ①			Combined		
	Detection ratio	Probability		Detection ratio	Probability		Detection ratio	Probability	
		Observed	Lower 95% conf limit		Observed	Lower 95% conf limit			
0.060-0.079	5/13	0.385	0.166	0/2	0.000				
0.080-0.099	18/33	0.545	0.403	2/8	0.250	0.046			
0.100-0.119	9/17	0.529	0.311	1/16	0.063	0.003			
0.120-0.139	11/21	0.524	0.328	1/10	0.100	0.005	DATA CANNOT BE		
0.140-0.159	16/19	0.842	0.641	5/12	0.417	0.181	COMBINED		
0.160-0.179	3/3	1.000	0.368	2/5	0.400	0.076			
0.180-0.199	3/5	0.600	0.189	0/4	0.000	–			
0.200-0.239	1/1	1.000	0.895 ②	1/2	0.500	0.025			
0.240-0.279	3/3			4/7	0.571	0.225			
0.280-0.319	13/13			8/12	0.667	0.391			
0.320-0.359	1/1			6/9	0.667	0.345			
0.360-0.399	4/4			4/4	1.000	0.473			
0.400-0.439	–			–	–	–			
0.440-0.479	5/5			5/9	0.556	0.251			
0.480-0.599				5/5	1.000	0.549			

① Includes inspections on contaminated and/or smeared flaws

② Minimum flaw length interval with at least 0.90 probability of detection with 95% confidence

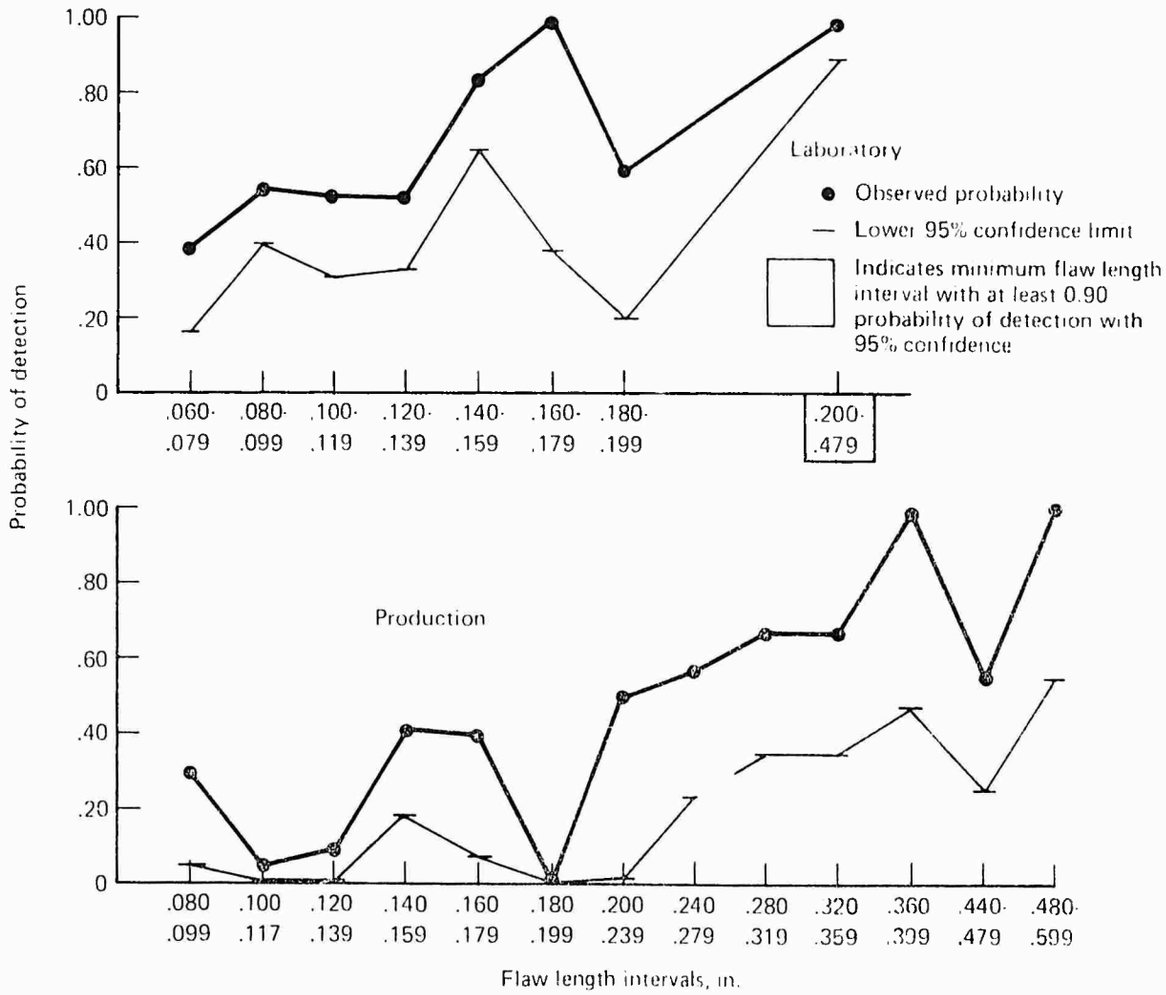


Figure 49.–Penetrant Results on Internally Flawed Hollow Steel Specimens

Table 30.—Results of Eddy Current Inspections on Internally Flawed Hollow Steel Specimens

Flaw length interval, in.	Specimen configuration ①	Specimen number	Laboratory		Production	
			Detection ratio	Total	Detection ratio	Total
0.060-0.079	H	H-11	0/1		2/2	
	H	H-15	0/3		2/2	
	HF-H	T1-1	3/3	3/7	1/1	5/5
0.080-0.099	HF	H6	4/6		3/3	
	HF	H8	6/6		3/3	
	HF	H-12	3/3		2/2	
	HF	H14	4/4		3/3	
	H	H13		17/19		11/11
0.100-0.119	H	H1	4/8		2/2	
	H	H4	3/4		2/2	
	H	H9	3/3		2/2	
	H	H11	0/1		2/2	
	HF	H7	10/10	20/26	4/4	12/12
0.120-0.139	HF	H16	1/5		1/1	
	H	H3	1/4		2/2	
	HF	H6	6/6		3/3	
	H	H15	2/3	13/18	2/2	8/8
0.140-0.159	HF	H7	10/10		4/4	
	HF	H10	14/14		3/3	
	H	H1	7/8		2/2	
	H	H13				
	H	H17	5/5	36/37		9/9
0.160-0.179	HF	H18	5/5			
	H	H5	2/2		2/3	
	H	H19		7/7		2/3
0.180-0.199	HF H	T1-1	3/3		1/1	
	H	H3	3/4	6/7	2/2	3/3
0.220-0.239	H	H17	5/5	5/5		
0.240-0.319	HF	H27				
	HF	H22	2/2			
	HF	H24				
	HF-H	T1-1	3/3		1/1	

① H 

HF 

Table 30.—Results of Eddy Current Inspections on Internally Flawed Hollow Steel Specimens (Continued)

Flaw length interval, in.	Specimen configuration	Specimen number	Laboratory		Production	
			Detection ratio	Total	Detection ratio	Total
Con't	HF	H14	4/4		3/3	
	HF	H16	5/5		1/1	
	H	H21		14/14		5/5
0.320	H	H19				
0.570	H	H29				
	H	H23				
	HF	H26				
	H	H21				
	HF	H28				
	HF	H18	5/5			
	HF	H24				
	H	H19				
	H	H23		5/5		

Flaw length interval, in.	Specimen configuration	Specimen number	Laboratory		Production	
			Number of inspections	Total	Number of inspections	Total
NONFLAW	H	H2	5		2	
SPECIMENS	H	H20	3		2	
	H	H25	6		1	
	H	H62			1	
	H	H63				
	H	H64				
	HF	HF6	7		2	
	HF	HF29	4		3	
	HF	HF30	7		3	
	HF	HF24	2			
	HF	HF25	2			
	HF	HF26	3	39		14

Table 31.—Statistical Analysis of Eddy Current Inspection Results on Internally Flawed Hollow Steel Specimens

Flaw length interval, in.	Laboratory			Production			Combined		
	Detection ratio	Probability		Detection ratio	Probability		Detection ratio	Probability	
		Observed	Lower 95% conf limit		Observed	Lower 95% conf limit			
0.060-0.079	3/7	0.429	0.129	5/5	1.000	0.899①			
0.080-0.099	17/19	0.895	0.704	11/11					
0.100-0.119	20/26	0.769	0.595	12/12			DATA CANNOT BE COMBINED		
0.120-0.139	13/18	0.722	0.502	8/8	1.000	0.688			
0.140-0.159	36/37	0.977	0.897①	9/9	1.000	0.717			
0.160-0.179	7/7			2/3	0.667	0.135			
0.180-0.199	6/7	0.857	0.479	3/3	1.000	0.368			
0.200-0.219									
0.220-0.239	5/5	1.000	0.549						
0.240-0.319	14/14	1.000	0.779	5/5	1.000	0.549			
0.320-0.570	5/5	1.000	0.549						

① Minimum flaw length interval with at least 0.90 probability of detection with 95% confidence

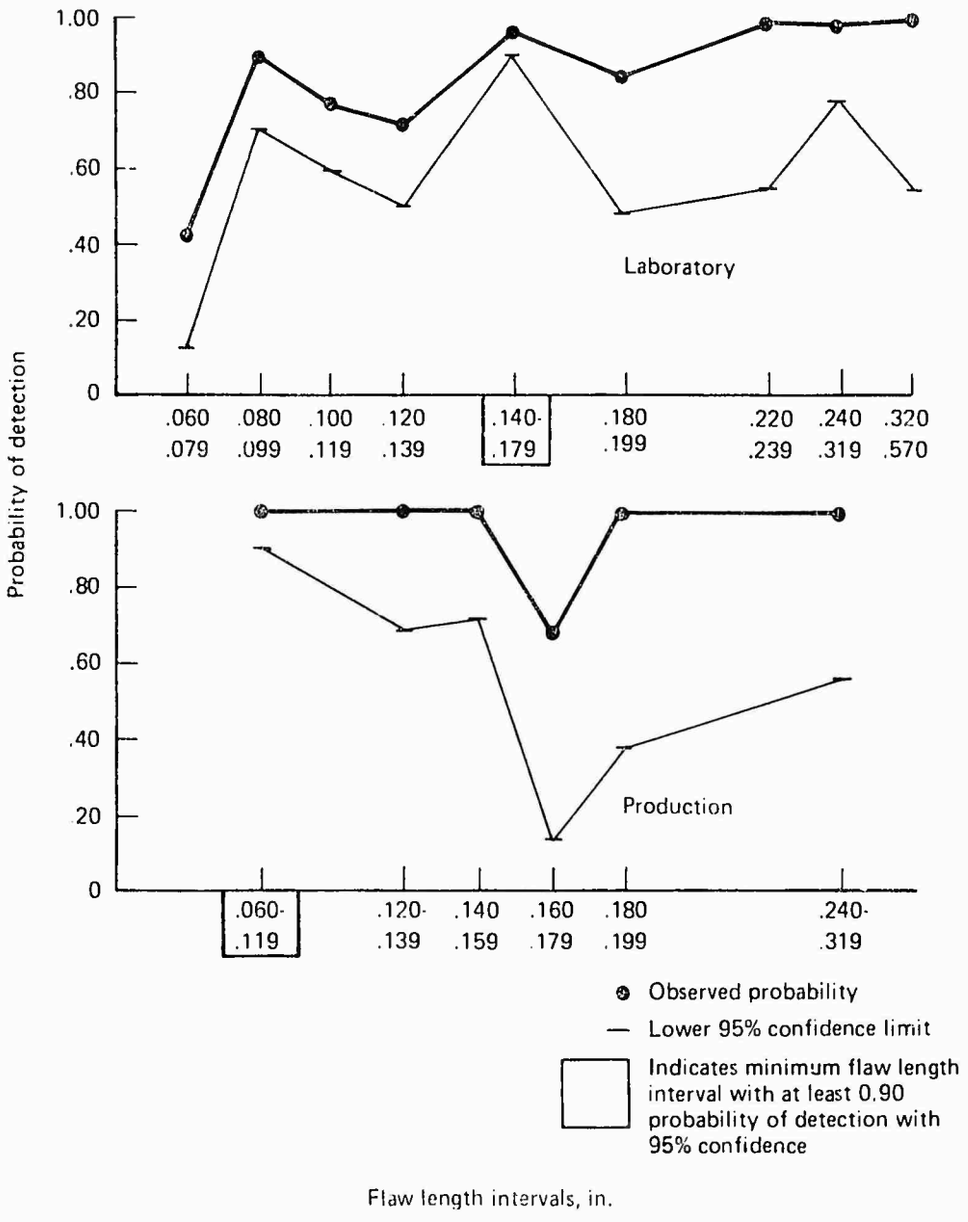
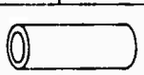


Figure 50.—Eddy Current Results on Internally Flawed Hollow Steel Specimens

Table 32.—Results of Ultrasonic Inspections on Internally Flawed Hollow Steel Specimens

Flaw length interval, in.	Specimen configuration (1)	Specimen number	Laboratory		Production	
			Detection ratio	Total	Detection ratio	Total
0.060-	H	H 11	11/11		5/7	
0.079	H	H-15	6/6		5/5	
	HF-H	T1-1	5/5	22/22	1/1	11/13
0.080	HF	H6	7/7		8/8	
0.099	HF	H8	8/8		7/7	
	HF	H-12	4/4		4/4	
	HF	H14	1/1		1/1	
	H	H13		20/20		12/12
0.100-	H	H1			3/3	
0.119	H	H4	6/6		7/7	
	H	H9	5/5		5/5	
	H	H11	11/11		7/7	
	HF	H7	4/4	26/26	3/3	25/25
0.120-	HF	H16	4/4		5/5	
0.139	H	H3			6/6	
	HF	H6	7/7		8/8	
	H	H15	6/6	17/17	5/5	24/24
0.140-	HF	H7	4/4		3/3	
0.159	HF	H10	5/5		1/1	
	H	H1			4/4	
	H	H13				
	H	H17	1/1	10/10	1/1	9/9
0.160-	HF	H18			1/1	
0.179	H	H5			2/3	
	H	H19				3/4
0.180-	HF-H	T1-1	5/5		1/1	
0.199	H	H3		5/5	6/6	7/7
0.220-0.239	H	H17	1/1	1/1	1/1	1/1
0.240-	HF	H27				
0.279	HF	H22				
0.280-	HF	H24				
0.319	HF-H	T1-1	5/5		1/1	

(1) H– 

HF– 

Table 32. Results of Ultrasonic Inspections on Internally Flawed Hollow Steel Specimens (Continued)

Flaw length interval, in.	Specimen configuration	Specimen number	Laboratory		Production	
			Detection ratio	Total	Detection ratio	Total
Con't	HF	H14	1/1		1/1	
	HF	H16	4/4		5/5	
	H	H21		10/10	1/1	8/8
0.320-	H	H19				
0.570	H	H29			1/1	
	H	H23			1/1	
	HF	H26				
	H	H21			1/1	
	HF	H28				
	HF	H18			1/1	
	HF	H24				
	H	H19				
	H	H23			1/1	5/5

Flaw length interval, in.	Specimen configuration	Specimen number	Laboratory		Production	
			Number of inspections	Total	Number of inspections	Total
NONFLAW	H	H2	1		3	
SPECIMENS	H	H20	1		4	
	H	H25	5		4	
	H	H62			5	
	H	H63				
	H	H64	4			
	HF	HF6	5		6	
	HF	HF29	1		2	
	HF	HF30	6		1	
	HF	HF24				
	HF	HF25				
	HF	HF26		23	2	27

Table 33.—Statistical Analysis of Ultrasonic Inspection Results on Internally Flawed Hollow Steel Specimens

Flaw length interval, in.	Laboratory			Production			Combined		
	Detection ratio	Probability		Detection ratio	Probability		Detection ratio	Probability	
		Observed	Lower 95% conf limit		Observed	Lower 95% conf limit		Observed	Lower 95% conf limit
0.060-0.079	22/22	1.000	0.931①	11/13	0.846	0.590	33/35	0.970	0.909①
0.080-0.099	20/20			12/12	1.000	0.922①	32/32		
0.100-0.119	26/26	1.000	0.891	25/25			51/51	1.000	0.943
0.120-0.139	17/17	1.000	0.838	24/24	1.000	0.883	41/41	1.000	0.930
0.140-0.159	10/10	1.000	0.741	9/9	1.000	0.717	19/19	1.000	0.854
0.160-0.179				3/4	0.750	0.249	3/4	0.750	0.249
0.180-0.199	5/5	1.000	0.549	7/7	1.000	0.652	12/12	1.000	0.778
0.200-0.219	--			--			--		
0.220-0.239	1/1	1.000		1/1	1.000		2/2	1.000	0.224
0.240-0.279	--						--		
0.280-0.319	10/10	1.000	0.741	8/8	1.000	0.688	18/18	1.000	0.847
0.320-0.570	--			5/5	1.000	0.549	5/5	1.000	0.549

① Minimum flaw length interval with at least 0.90 probability of detection with 95% confidence

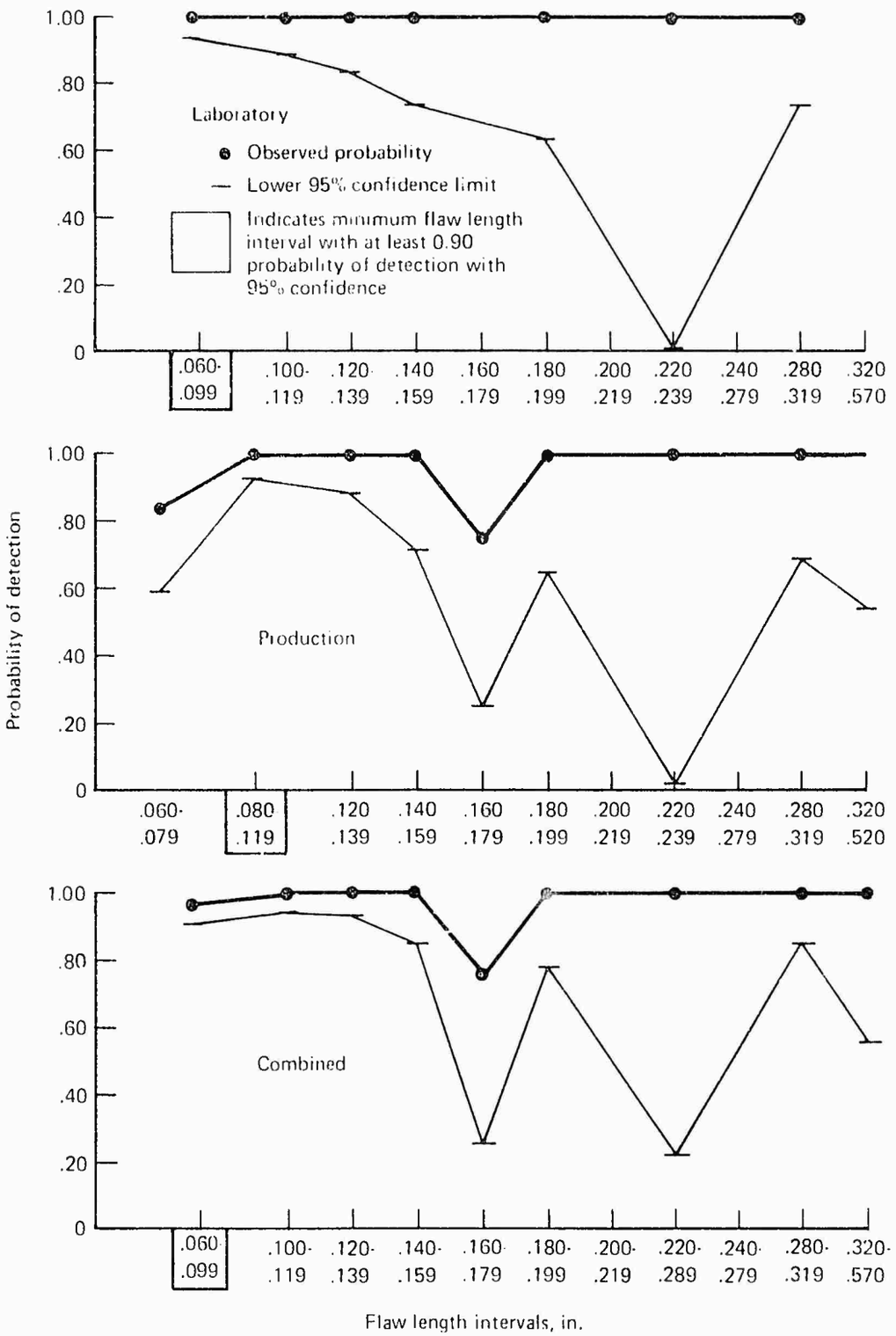
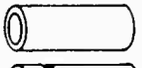


Figure 51.—Ultrasonic Results on Internally Flawed Hollow Steel Specimens

Table 34. Results of Radiographic Inspections of Internally Flawed Hollow Steel Specimens

Flaw length interval, in.	Specimen configuration	Specimen number	Laboratory		Production	
			Detection ratio	Total	Detection ratio	Total
0.060	[illegible]	H-11				
0.079	[illegible]	H-15				
	HF-H	T1-1	1/1	1/1	1/1	1/1
0.080	HF	H6			0/2	
0.099	HF	H8			0/2	
	HF	H-12				
	HF	H14			2/3	
	H	H13				2/7
0.100	H	H1	0/1		0/4	
0.119	H	H4	0/2		0/2	
	H	H9	0/1		0/2	
	H	H11				
	HF	H7		0/4	0/2	0/10
0.120	HF	H16				
0.139	H	H3	0/1		0/4	
	HF	H6			1/2	
	H	H15		0/1		1/6
0.140-	HF	H7			1/1	
0.159	HF	H10	1/1		0/1	
	H	H1	0/1		1/4	
	H	H13				
	H	H17	1/1	2/3	2/2	4/9
0.160-	HF	H18	1/1		0/1	
0.179	H	H5	0/1		0/3	
	H	H19		1/2		0/4
0.180-	HF-H	T1-1	1/1		1/1	
0.199	H	H3	0/1	1/2	0/4	1/5
0.220-0.239	H	H17	1/1	1/1	2/2	2/2
0.240-0.259	HF	H27	1/1	1/1	3/4	3/4
0.260-0.279	HF	H22	1/1	1/1	0/1	0/1
0.280-0.299	HF	H24	2/2	2/2	3/3	3/3
0.300-	HF-H	T1-1	1/1		1/1	

① H–



HF–



Table 34.—Results of Radiographic Inspections on Internally Flawed Hollow Steel Specimens (Continued)

Flaw length interval, in.	Specimen configuration	Specimen number	Laboratory		Production	
			Detection ratio	Total	Detection ratio	Total
0.319	HF	H14			3/3	
	HF	H16				
	H	H21	1/1	2/2	3/3	7/7
0.320-	H	H19				
0.359	H	H29	1/1		2/2	
	H	H23	1/1	2/2	3/3	5/5
0.360-	HF	H26	2/2			
0.399	H	H21	1/1	3/3	3/3	3/3
0.440-	HF	H28	2/2			
0.570	HF	H18	2/2		0/1	
	HF	H24	2/2		3/3	
	H	H19				
	H	H23	1/1	7/7	3/3	6/7

Flaw length interval, in.	Specimen configuration	Specimen number	Laboratory		Production	
			Number of inspections	Total	Number of inspections	Total
NONFLAW	H	H2	1		3	
SPECIMENS	H	H20	1		1	
	H	H25	1		2	
	H	H62				
	H	H63			1	
	H	H64			1	
	HF	HF6	1		1	
	HF	HF29			2	
	HF	HF30	1		1	
	HF	HF24				
	HF	HF25				
	HF	HF26		5		12

Table 35 —Statistical Analysis of Radiographic Inspection Results on Internally Flawed Hollow Steel Specimens

Flaw length interval, in.	Laboratory			Production			Combined		
	Detection ratio	Probability		Detection ratio	Probability		Detection ratio	Probability	
		Observed	Lower 95% conf limit		Observed	Lower 95% conf limit		Observed	Lower 95% conf limit
0.060-0.079	1/1	1.000	–	1/1	1.000	–	2/2	1.000	0.224
0.080-0.099	–			2/7	0.286	0.053	2/7	0.286	0.053
0.100-0.119	0/4	0.000	–	0/10	0.000	–	0/14	0.000	–
0.120-0.139	0/1	0.000	–	1/6	0.167	0.009	1/7	0.143	0.007
0.140-0.159	2/3	0.667	0.135	4/9	0.444	0.169	6/12	0.500	0.245
0.160-0.179	1/2	0.500	0.025	0/4	0.000	–	1/6	0.167	0.009
0.180-0.199	1/2	0.500	0.025	1/5	0.200	0.009	2/7	0.286	0.053
0.200-0.219									
0.220-0.239	1/1	1.000	0.854	2/2	1.000	0.224	3/3	1.000	0.368
0.240-0.259	1/1			3/4	0.750	0.249	4/5	0.800	0.343
0.260-0.279	1/1			0/1	0.000	–	1/2	0.500	0.025
0.280-0.299	2/2			3/3	1.000	0.847	5/5	0.976	0.889
0.300-0.319	2/2			7/7			9/9		
0.320-0.359	2/2			5/5			7/7		
0.360-0.399	3/3			3/3			6/6		
0.040-0.439									
0.440-0.570	7/7			6/7	0.857	0.479	13/14		

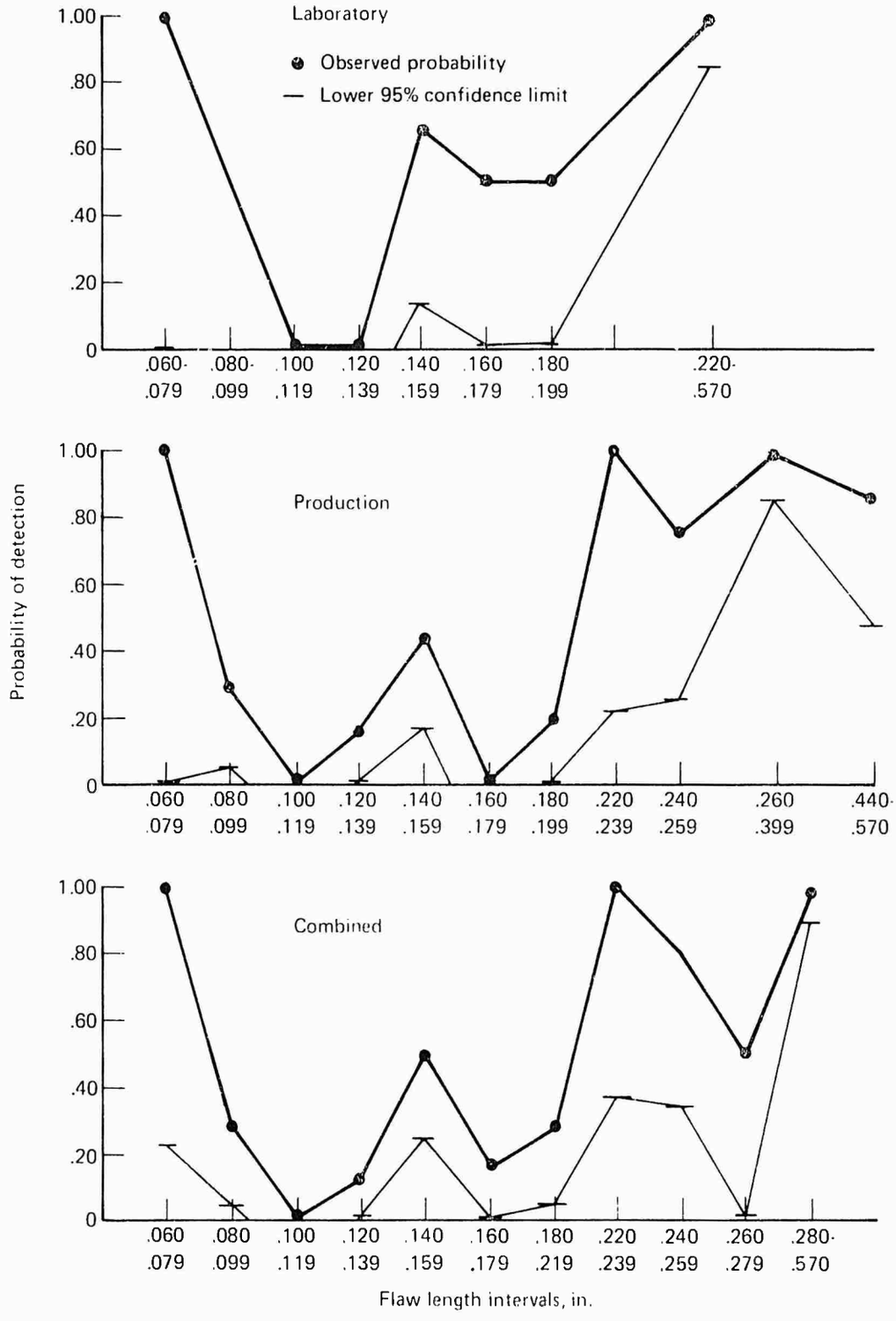


Figure 52.—Radiographic Results on Internally Flawed Hollow Steel Specimens

The major differences between results demonstrated for the externally flawed steel specimens presented earlier and the hollow steel, internal surface flawed specimens were revealed in magnetic particle and radiographic inspections. The magnetic particle results showed extremely low detection capabilities in production for internal surface flaws. Laboratory results, on the other hand, were essentially the same for both internal or external flaws. Human factors apparently played an important role in production where flaw indications in the less accessible areas were completely missed until inspector experience increased and flaws were expected in these areas.

Human factors are also believed to have contributed to the marked difference between production and laboratory results for penetrant methods. However, later production inspections were adversely affected because the internal surfaces of the hollow specimens experienced more corrosion and the flaws were more subject to contamination.

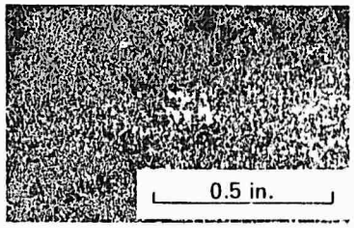
Ultrasonic and eddy-current inspectors and method capabilities were apparently less affected by the internal placement of flaws.

Radiography showed improved effectiveness to the internal flaws primarily because of reduced specimen thickness; i.e., 0.30-in. wall thickness compared to over 1.7 in. on the externally flawed, solid steel specimens.

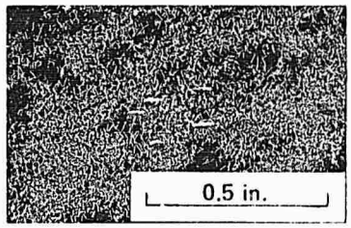
GRINDING AND EMBRITTLEMENT CRACK SPECIMENS

The test results obtained on the flat ground bar specimens were combined for both hydrogen embrittlement cracks and grinding cracks. Because of the lesser numbers of specimens of these types and because of the irregular distribution of flaw sizes attained for each type, lots submitted for inspection were composed of both kinds of specimens. This permitted a wider distribution of flaw sizes, more varied flaw locations, and larger lot sizes than was possible had the two types been inspected separately.

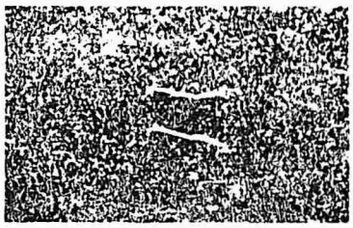
The hydrogen embrittlement cracks were, for the most part, discrete singular cracks oriented transversely to the long axis of the part. The grinding cracks occurred mostly as groups of multiple cracks with a predominant longitudinal orientation. Fluorescent magnetic particle indications of the grinding cracks are shown in figure 53. The two types of cracks were similar in that they were very tight, very shallow surface cracks. By contrast, the depths and the areas of the more open compressed notch flaws varied directly with changes in length. For purposes of combining the inspection results, an arbitrary decision was made to use the major dimensions of the rectangular area, which would enclose the grinding cracks, as equivalent to the length of a single crack. This was not wholly satisfactory as can be seen in the tabulated results. The areas of extremely fine cracks shown in figure 53 as appearing in specimens SN2 and 19 were not detected as readily as larger cracks in similar areas, as in specimen SN8. This was true for each inspection method and was related to the very shallow depths and narrow widths of the minute cracks making up those groups. The unique nature of these very small cracks became evident upon examining the tabulated inspection results obtained on the smaller flaw areas of specimens SN2 and 19. That these groupings of minute flaws were distinctly different from the population of hydrogen embrittlement cracks and the grosser grinding cracks is very apparent in the graphical presentations where abrupt dips occur at the 0.120- to 0.139- and 0.220- to 0.259-in. flaw intervals.



SN2 0.13 x 0.08



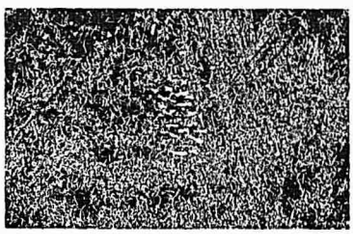
SN2 0.25 x 0.16



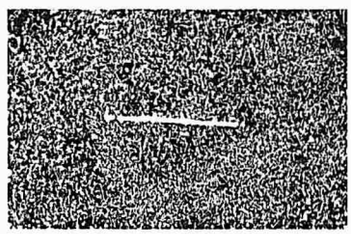
SN8 0.18 x 0.14



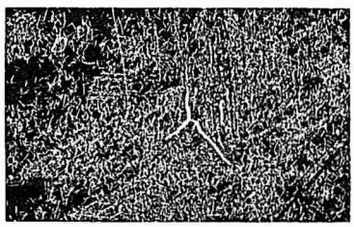
19 0.21 x 0.26



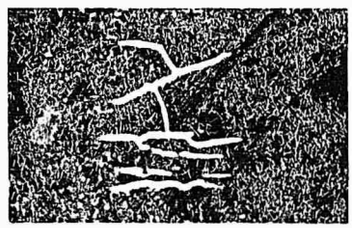
19 0.15 x 0.20



SN10 0.36 x 0.04



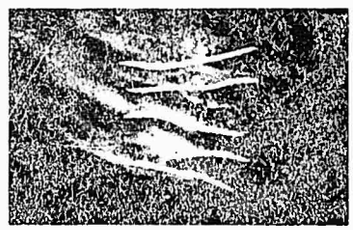
16 0.21 x 0.21



SN7 0.38 x 0.38



19 0.22 x 0.16



SN5 0.35 x 0.40

Figure 53.—Fluorescent Indications of Multiple Grinding Cracks; Specimen Number and Dimensions of Cracked Area are Given (2X)

The detection capabilities of magnetic particle inspection generally were quite different for embrittlement and grinding cracks. In tables 36 and 37 and figure 54, a disproportionate number of missed detections are shown for the grinding crack specimens. This was less true for ultrasonic inspection except for the smaller cracks of SN2 and the detection capabilities seem relatively independent of flaw type as can be seen in tables 38 and 39, and figure 55.

Eddy-current results in tables 40 and 41 and figure 56 show differing results between laboratory and production inspections that are related to the instruments used. The Magnatest ED-520 was used predominantly for production inspections, and the detection ratios exhibit an apparent superiority over laboratory results for the smaller ($\leq$ 0.119 in.) flaws, obtained mostly with the ED-400. However, production inspections were largely ineffectual on the larger areas of grinding cracks because of reported excessive noise. An investigation into the source of noise was conducted, and it was found that ED-520 instrument responses equal to full-scale flaw signals were being caused by local changes in metallurgical structure developed during the abrasive grinding employed to generate the flaws. Figure 57 illustrates an area of magnetic particle indications of grinding cracks under black light illumination together with a white light photograph of the same surface following etching to reveal a pattern of grinding burn. This nonuniform structure represents a pattern of similar nonuniform magnetic and electrical properties, which is readily detected by the ED-520 instrumentation. Strip chart recordings were obtained and are shown which compare the eddy-current responses obtained through the burned half of the specimen and in the unburned region.

Penetrant inspection results and calculated probabilities, tables 42 and 43, were influenced by changes developing in the specimens during the course of the program. A degradation of detection capabilities became apparent with increasing numbers of inspections and the passage of time. That such changes were real was confirmed by special inspections performed in the laboratory on a number of flaws which were unexpectedly missed in production inspections. These flaws had been successfully detected by much earlier laboratory inspections and could no longer be detected by these special attempts, following the same earlier inspection techniques. Buildup of corrosion products within the cracks from repeated exposure to water during immersion ultrasonic inspections and accumulation of residues from successive penetrant inspections and possible incomplete cleanings are likely factors accounting for the decreasing sensitivity of the later penetrant inspections. Therefore, the detection ratios and calculated probabilities are not to be considered as constant values and the data have not been plotted graphically. If each inspection could have been performed on a new specimen, the observed probability of detection by this method on these very narrow cracks would have been much higher than the values shown.

The flaws in these specimens were the least suited for detection by radiographic methods and the probability of detection in tables 44 and 45 is extremely low for even the largest cracks. Radiography cannot be considered a competitive method of detecting such shallow and tight surface cracks.

THREADED STEEL SPECIMENS

The threaded specimens presented unique characteristics which caused uncertainties in evaluating the recorded inspection results. When this became apparent, inspection of these

Table 36. Results of Magnetic Particle Inspections on Grinding and Embrittlement Cracked Steel Specimens

Flaw length (1) interval, in.	Flaw Type (2)	Specimen number	Laboratory		Production	
			Detection ratio	Total	Detection ratio	Total
0.040 0.059	H	6	15/15	15/15	11/11	11/11
0.080 0.099	H	6	15/15	15/15	11/11	11/11
0.100	H	7	18/18		7/13	
0.119	H	8	23/23	41/41	14/14	21/27
0.120 0.139	G (0.13×0.08)	SN2	2/5	2/5	2/3	2/3
0.180	H	3	7/7		7/8	
0.219	H	5	7/7		9/9	
	H	5	7/7		9/9	
	G (0.18×0.14)	SN8	5/5		5/5	
	H	2	7/7		9/9	
	G (0.15×0.20)	19	2/5		4/5	
	G (0.21×0.21)	16	5/5	40/43	5/5	48/50
0.220	G (0.22×0.16)	19	5/5		5/5	
0.259	G (0.25×0.16)	SN2	3/5	8/10	2/3	7/8
0.260	H	7	18/18		13/13	
0.299	G (0.21×0.26)	19	5/5	23/23	5/5	18/18
0.340 0.379	G (0.36×0.04)	SN10	4/4	4/4	5/5	5/5
0.380	G (0.38×0.38)	SN7	5/5		5/5	
0.419	G (0.35×0.40)	SN5	5/5	10/10	5/5	10/10
0.420 0.459	H	4	6/6	6/6	6/6	6/6
0.500	H	4	6/6		5/6	
0.549	H	4	6/6	12/12	6/6	11/12

(1) Grinding crack lengths represent longest dimension of cracked area

2) H = hydrogen embrittlement crack

G = grinding cracks

Table 36.– Results of Magnetic Particle Inspections on Grinding and Embrittlement Cracked Steel Specimens (Continued)

Flaw length interval, in.	Flaw Type	Specimen number	Laboratory		Production	
			Number of inspections	Total	Number of inspections	Total
NONFLAW		888132-1	21		9	
SPECIMENS		888132-3	8		2	
		888132-4	19		6	
		888132-6	16		12	
		888132-7	14		10	
		888132-8	15		8	
		SN-4	5		3	
		SN-6	2		4	
		SN-9	1		4	
		20			2	
		27	2	103	2	62

Table 37 – Statistical Analysis of Magnetic Particle Inspection Results on Grinding and Embrittlement Cracked Specimens

Flaw length interval, in.	Laboratory			Production			Combined		
	Detection ratio	Probability		Detection ratio	Probability		Detection ratio	Probability	
		Observed	Lower 95% conf limit		Observed	Lower 95% conf limit		Observed	Lower 95% conf limit
0.040-0.059	15/15	1.000	0.905 ①	11/11	1.000	0.873	26/26	1.000	0.944 ①
0.060-0.079	–			–			–		
0.080-0.099	15/15			11/11			26/26		
0.100-0.119	41/41	1.000	0.930	21/27	0.778	0.608	62/68	0.912	0.856
0.120-0.139	2/5	0.400	0.076	2/3	0.667	0.135	4/8	0.500	0.193
0.140-0.179	–			–			–		
0.180-0.219	40/43	0.930	0.829	48/50	0.960	0.879	88/93	0.946	0.905
0.220-0.259	8/10	0.800	0.493	7/8	0.875	0.529	15/18	0.833	0.623
0.260-0.299	23/23	1.000	0.878	18/18	1.000	0.837	41/41	1.000	0.930
0.300-0.339	–			–			–		
0.340-0.379	4/4	1.000	0.473	5/5	1.000	0.549	9/9	1.000	0.717
0.380-0.419	10/10	1.000	0.741	10/10	1.000	0.741	20/20	1.000	0.861
0.420-0.459	6/6	1.000	0.607	6/6	1.000	0.607	12/12	1.000	0.779
0.460-0.499	–			–			–		
0.500-0.549	12/12	1.000	0.779	11/12	0.917	0.661	23/24	0.958	0.817

① Minimum flaw length interval with at least 0.90 probability of detection with 95% confidence

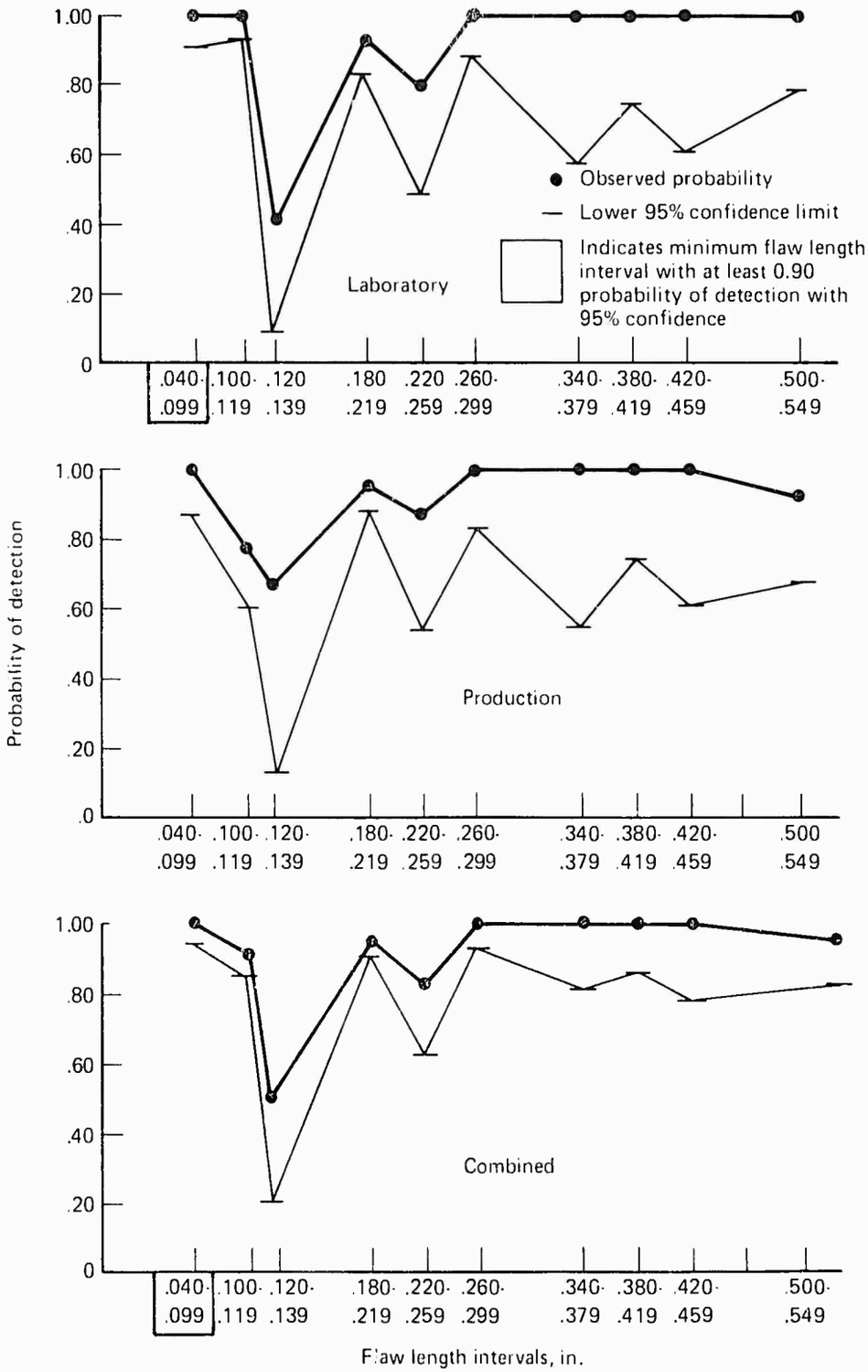


Figure 54.–Magnetic Particle Results on Grinding and Embrittlement Cracked Steel Specimens

Table 38.—Results of Ultrasonic Inspections on Grinding and Embrittlement Cracked Steel Specimens

Flaw length (1) interval, in.	Flaw Type (2)	Specimen number	Laboratory		Production	
			Detection ratio	Total	Detection ratio	Total
0.040-0.079	H	6	14/15	14/15	3/5	3/5
0.080-						
0.119	H	6	15/15		7/7	
	H	7	15/16		6/10	
	H	8	20/20	50/51	9/9	22/26
0.120-0.159	G (0.13x0.08)	SN2	0/3	0/3	3/4	3/4
0.160-						
0.199	H	3	4/4		8/8	
	H	5	4/4		8/9	
	H	5	4/4		8/9	
	G (0.18x0.14)	SN8	3/3	15/15	5/5	29/31
0.200	H	2	4/4		9/9	
0.239	G (0.15x0.20)	19	3/3		4/5	
	G (0.21x0.21)	16	3/3		5/5	
	G (0.22x0.16)	19	3/3	13/13	5/5	23/24
0.240	G (0.25x0.16)	SN2	3/3		4/4	
0.279	H	7	16/16		9/10	
	G (0.21x0.26)	19	3/3	22/22	5/5	18/19
0.280-0.359						
0.360	G (0.36x0.04)	SN10	3/3		5/5	
0.399	G (0.38x0.38)	SN7	3/3	6/6	5/5	10/10
0.400-	G (0.35x0.40)	SN5	3/3		5/5	
0.439	H	4	4/4	7/7	3/3	8/8
0.140-0.479						
0.480	H	4	4/4		3/3	
0.559	H	4	4/4	8/8	3/3	6/6

1 Grinding crack lengths represent longest dimension of cracked area

2 H hydrogen embrittlement crack

G grinding cracks

Table 38.—Results of Ultrasonic Inspections on Grinding and Embrittlement Cracked Steel Specimens (Continued)

Flaw length interval, in.	Flaw Type	Specimen number	Laboratory		Production	
			Number of inspections	Total	Number of inspections	Total
NONFLAW		888132-1	3		8	
SPECIMENS		888132-3			2	
		888132-4	3		3	
		888132-6	15		8	
		888132-7	15		5	
		888132-8	3		5	
		SN-4	3		4	
		SN-6	1		2	
		SN-9	1		2	
		20			1	
		27		44	1	41

Table 39.–Statistical Analysis of Ultrasonic Inspection Results on Grinding and Embrittlement Cracked Steel Specimens

Flaw length interval, in.	Laboratory			Production			Combined		
	Detection ratio	Probability		Detection ratio	Probability		Detection ratio	Probability	
		Observed	Lower 95% conf limit		Observed	Lower 95% conf limit		Observed	Lower 95% conf limit
0.040-0.079	14/15	0.970	0.908①	3/5	0.600	0.189	17/20	0.850	0.656
0.080-0.199	50/51			22/26	0.846	0.682	72/77	0.935	0.890
0.120-0.159	0/3	0.000	–	3/4	0.750	0.249	3/7	0.429	0.129
0.160-0.199	15/15	1.000	0.819	29/31	0.935	0.810	44/46	0.964	0.909①
0.200-0.239	13/13	1.000	0.794	23/24	0.958	0.817	36/37		
0.240-0.279	22/22	1.000	0.873	18/19	0.947	0.774	40/41	0.976	0.889
0.280-0.319	–			–			–		
0.320-0.359	–			–			–		
0.360-0.399	6/6	1.000	0.607	10/10	1.000	0.741	16/16	1.000	0.829
0.400-0.439	7/7	1.000	0.652	8/8	1.000	0.688	15/15	1.000	0.819
0.440-0.479	–			–			–		
0.480-0.559	8/8	1.000	0.688	6/6	1.000	0.607	14/14	1.000	0.807

① Minimum flaw length interval with at least 0.90 probability of detection with 95% confidence

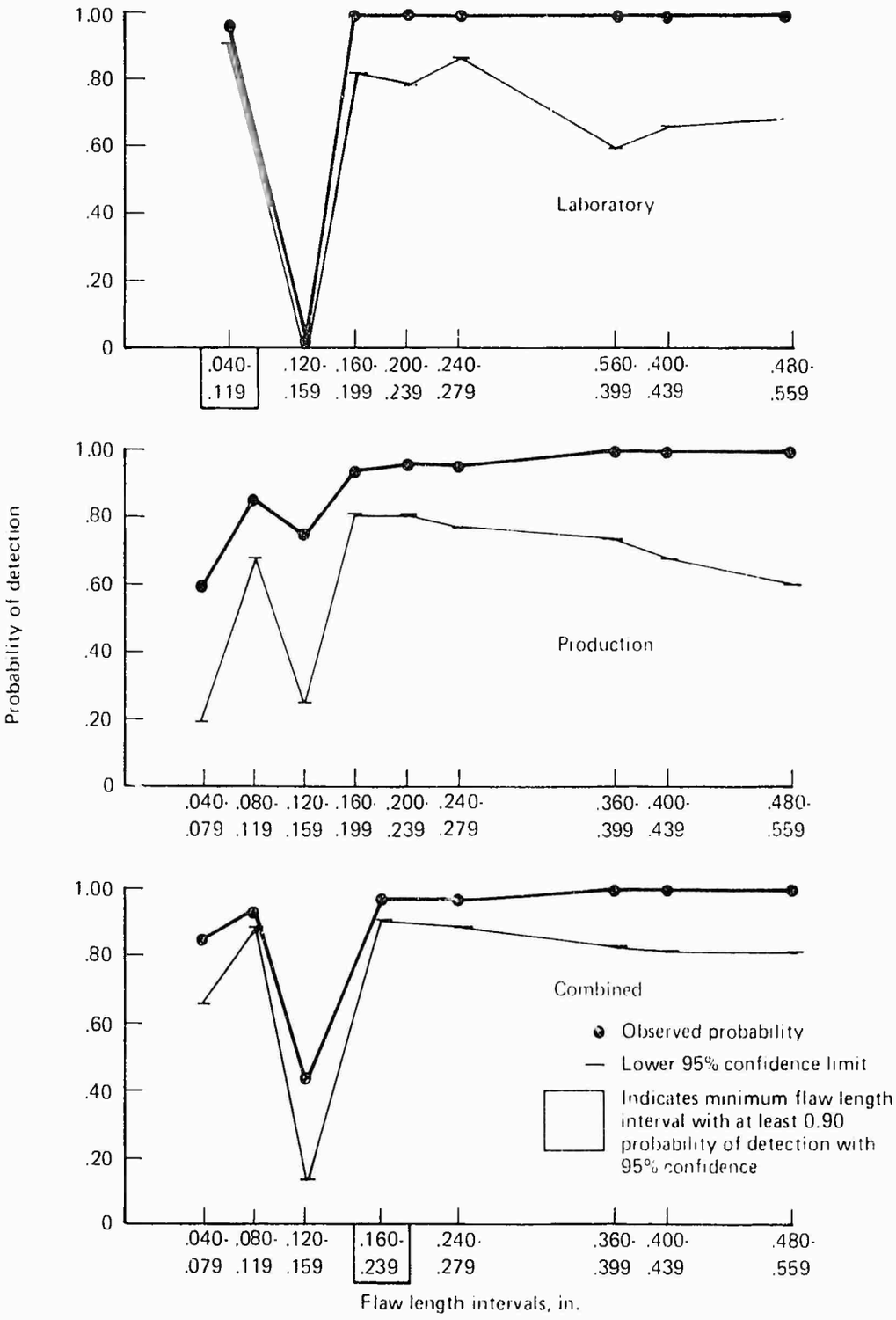


Figure 55.—Ultrasonic Results on Grinding and Embrittlement Cracked Steel Specimens

Table 40.–Eddy Current Inspections on Grinding and Embrittlement Cracked Steel Specimens

Flaw length (1) interval, in.	Flaw type (2)	Specimen number	Laboratory		Production	
			Detection ratio	Total	Detection ratio	Total
0.040-0.079	H	6	0/5	0/5	1/5	1/5
0.080-						
0.119	H	6	1/5		5/5	
	H	7	1/7		4/8	
	H	8	4/5	6/17	7/7	16/20
0.120-0.159	G-(0.13x0.08)	SN2	2/3	2/3	0/2	0/2
0.160-						
0.199	H	3	9/9		6/6	
	H	5	6/7		4/7	
	H	5	6/7		6/7	
	G-(0.18x0.14)	SN8	3/3	24/26	0/2(1)	16/22
0.200-	H	2	10/10		7/8	
0.239	G-(0.15x0.20)	19	0/3		0/2(1)	
	G-(0.21x0.21)	16	2/3		0/2(1)	
	G-(0.22x0.16)	19	2/3	14/19	0/2(1)	7/14
0.240-	G-(0.25x0.16)	SN2	2/3		0/2(1)	
0.279	H	7	7/7		8/8	
	G-(0.21x0.26)	19	3/3	12/13	0/2(1)	8/12
0.280-0.359						
0.360-	G-(0.36x0.04)	SN10	3/3		2/2	
0.399	G-(0.38x0.38)	SN7	3/3	6/6	1/2	3/4
0.400-	G-(0.35x0.40)	SN5	3/3		0/2(1)	
0.439	H	4	6/6	9/9	4/4	4/6
0.440-0.479						
0.480-	H	4	6/6		4/4	
0.559	H	4	6/6	12/12	4/4	8/8

(1) Grinding crack lengths represent longest dimension of cracked area

(2) H - hydrogen embrittlement crack

G - grinding cracks

(1) High background noise due to grinding burn

Table 40. Eddy Current Inspections on Grinding and Embrittlement Cracked Steel Specimens (Continued)

Flaw length interval, in.	Flaw type	Specimen number	Laboratory		Production	
			Number of inspections	Total	Number of inspections	Total
NONFLAW		888132 1	5		6	
SPECIMENS		888132 3	2		2	
		888132-4	7		4	
		888132-6	5		6	
		888132-7	4		6	
		888132-8	8		6	
		SN-4	3		2	
		SN-6	1		2	
		SN-9	1		2	
		20				
		27		36		36

Table 41.—Statistical Analysis of Eddy Current Inspection Results on Grinding and Embrittlement Cracked Steel Specimens

Flaw length interval, in.	Laboratory			Production			Combined		
	Detection ratio	Probability		Detection ratio	Probability		Detection ratio	Probability	
		Observed	Lower 95% conf limit		Observed	Lower 95% conf limit		Observed	Lower 95% conf limit
0.040-0.079	0/5	0.000	–	1/5	0.200	0.010	1/10	0.100	0.005
0.080-0.119	6/17	0.353	0.166	16/20	0.800	0.599	22/37	0.595	0.463
0.120-0.159	2/3	0.667	0.135	0/2	0.000	–	2/5	0.400	0.076
0.160-0.199	24/26	0.923	0.777	16/22	0.727	0.532	40/48	0.833	0.743
0.200-0.239	14/19	0.737	0.524	7/14	0.500	0.264	21/33	0.636	0.500
0.240-0.279	12/13	0.923	0.684	8/12	0.667	0.391	20/25	0.800	0.625
0.280-0.319	–			–			–		
0.320-0.359	–			–			–		
0.360-0.399	6/6	1.000	0.895①	3/4	0.750	0.249	9/10	0.900	0.606
0.400-0.439	9/9			4/6	0.667	0.271	13/15	0.867	0.637
0.440-0.479	–			–			–		
0.480-0.559	12/12			8/8	1.000	0.688	20/20	1.000	0.861

① Minimum flaw length interval with at least 0.90 probability of detection with 95% confidence

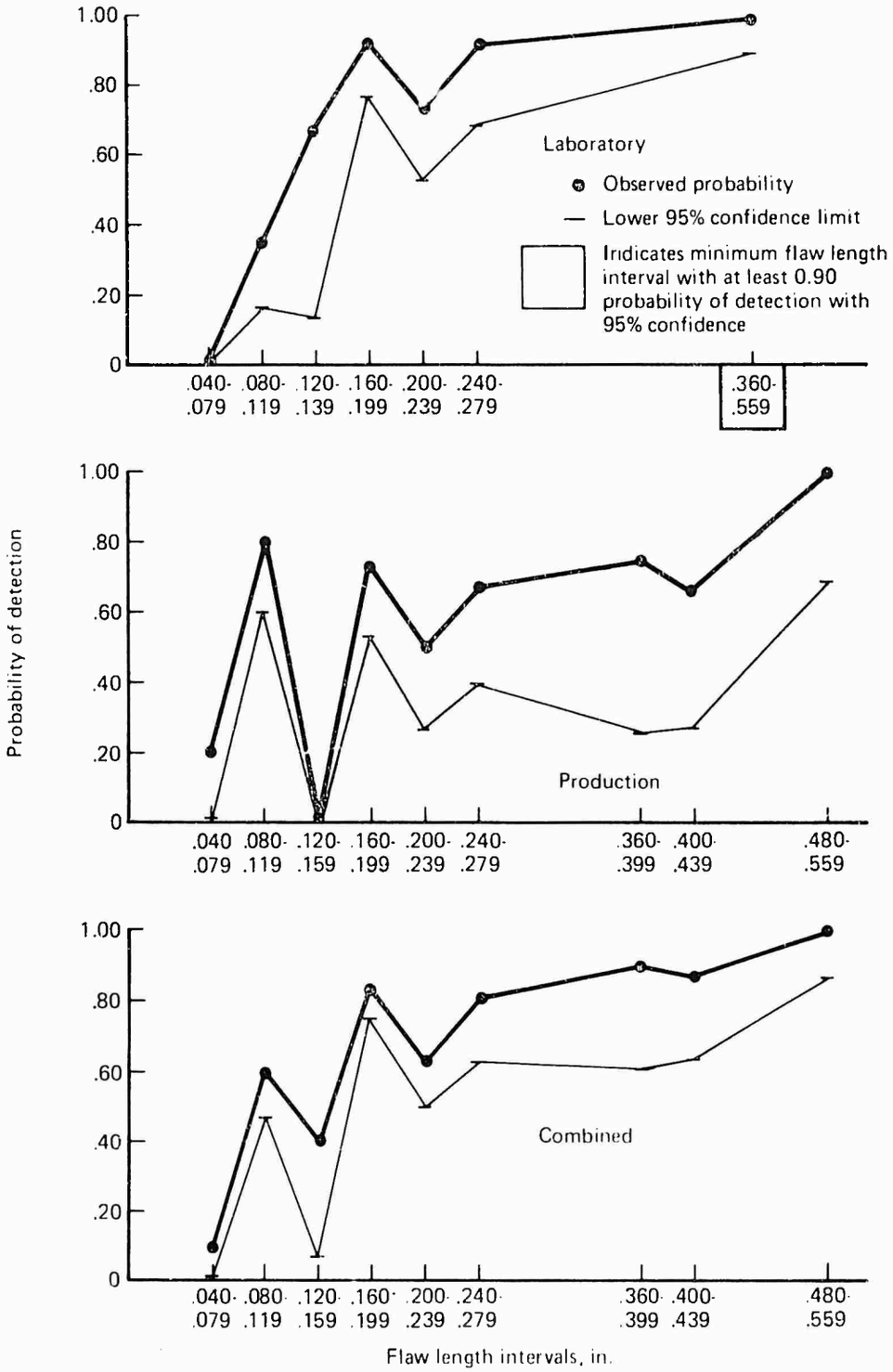
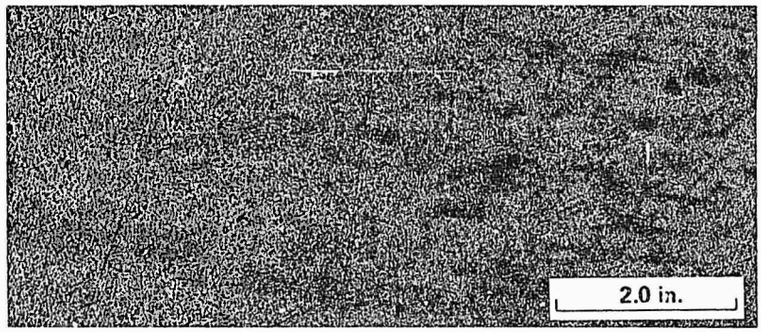
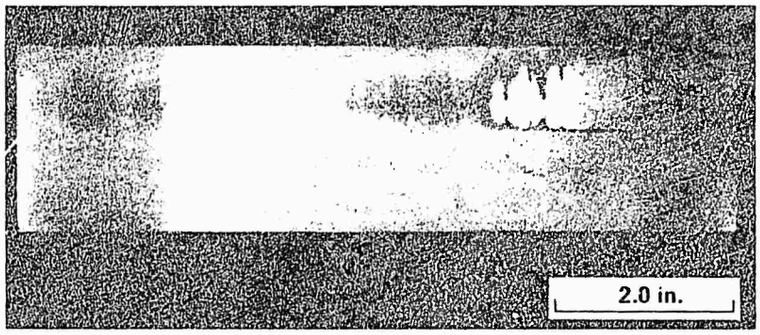


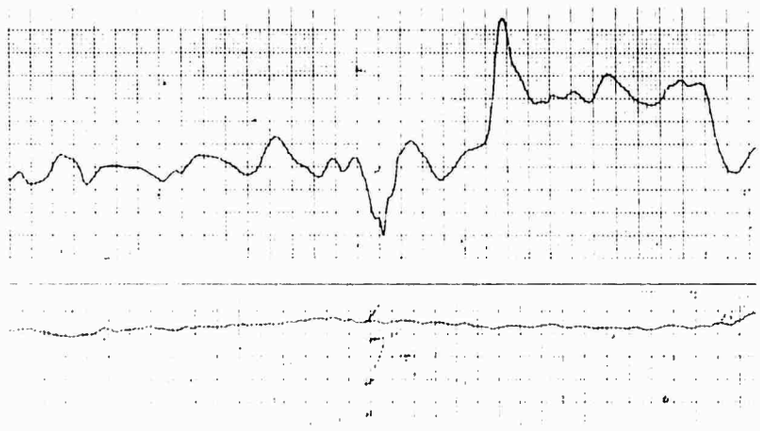
Figure 56.—Eddy Current Results on Grinding and Embrittlement Cracked Steel Specimens



a. Fluorescent Magnetic Particle Indications of Grinding Cracks in Specimen SN-5 (0.5X)



b. Surface Shown in a After Etching to Reveal Nonuniform Metallurgical Structure (0.5X)



c. Recordings of Eddy Current Response Obtained from Scans Above and Below Centerline of Specimen

Figure 57.—Abusive Grinding to Develop Cracks Interferes with Eddy Current Inspection

Table 42. – Results of Penetrant Inspections on Grinding and Embrittlement Cracked Steel Specimens

Flaw length (1) interval, in.	Flaw type (2)	Specimen number	Laboratory (3)		Production (3)	
			Detection ratio	Total	Detection ratio	Total
0.040-0.059	H	6	0/2	0/2	4/8	4/8
0.060-0.079						
0.080-0.099	H	6	2/2	2/2	7/8	7/8
0.100-	H	7	4/9		1/10	
0.119	H	8	9/10	13/19	1/9	2/19
0.120-0.139	G-(0.13x0.08)	SN2	0/2	0/2	1/3	1/3
0.140-0.179						
0.180-	H	3	7/8		1/9	
0.219	H	5	2/8		0/7	
	H	5	6/8		1/7	
	G-(0.18x0.14)	SN8	3/3		4/5	
	H	2	2/8		2/9	
	G-(0.15x0.20)	19	0/4		2/5	
	G-(0.21x0.21)	16	3/3	23/42	5/5	15/47
0.220-	G-(0.22x0.16)	19	1/4		3/5	
0.259	G-(0.25x0.16)	SN2	2/2	3/6	1/3	4/8
0.260-	H	7	9/9		5/10	
0.299	G-(0.21x0.26)	19	1/4	10/13	3/5	8/15
0.300-0.339						
0.340-0.379	G-(0.36x0.04)	SN10	2/2	2/2	5/5	5/5
0.380-	G-(0.38x0.38)	SN7	4/4		5/5	
0.419	G-(0.35x0.40)	SN5	4/4	8/8	3/5	8/10
0.420-0.459	H	4	3/3	3/3	5/8	5/8
0.460-0.479						
0.500-	H	4	3/3		1/8	
0.559	H	4	3/3	6/6	7/8	8/16

(1) Grinding crack lengths represent lc gest dimension of cracked area

(2) H = hydrogen embrittlement crack

G = grinding cracks

(3) Includes inspections on contaminated and/or smeared flaws

Table 42. Results of Penetrant Inspections on Grinding and Embrittlement Cracked Steel Specimens (Continued)

Flaw length interval, in.	Flaw type	Specimen number	Laboratory		Production	
			Number of inspections	Total	Number of inspections	Total
NONFLAW		888132-1	9		9	
SPECIMENS		888132-3	8		2	
		888132-4	6		5	
		888132-6	9		7	
		888132-7	6		5	
		888132-8	6		7	
		SN-4	2		3	
		SN-6			4	
		SN-9			3	
		20			2	
		27		46	2	49

Table 43.–Statistical Analysis of Penetrant Inspection Results on Grinding and Embrittlement Cracked Steel Specimens

Flaw length interval, in.	Laboratory ①			Production ①			Combined		
	Detection ratio	Probability		Detection ratio	Probability		Detection ratio	Probability	
		Observed	Lower 95% conf limit		Observed	Lower 95% conf limit		Observed	
0.040-0.059	0/2	0.000	–	4/8	0.500	0.193			
0.060-0.079	–	–	–	–	–	–			
0.080-0.099	2/2	1.000	0.224	7/8	0.875	0.529			
0.100-0.119	13/19	0.684	0.470	2/19	0.105	0.019	DATA CANNOT		
0.120-0.139	0/2	0.000	–	1/3	0.333	0.017	BE COMBINED		
0.140-0.179	–	–	–	–	–	–			
0.180-0.219	23/42	0.548	0.423	15/47	0.319	0.204			
0.220-0.259	3/6	0.500	0.153	4/8	0.500	0.193			
0.260-0.299	10/13	0.769	0.505	8/15	0.533	0.300			
0.300-0.339	–	–	–	–	–	–			
0.340-0.379	2/2	1.000	0.854	5/5	1.000	0.543			
0.380-0.419	8/8	1.000		8/10	0.800				
0.420-0.459	3/3	1.000		5/8	0.625				
0.460-0.479									
0.500-0.559	6/6	1.000		8/16	0.500				

① Includes data on contaminated and/or smeared flaws

Table 44. Results of Radiographic Inspections on Grinding and Embrittlement Cracked Steel Specimens

Flaw length [1] interval, in.	Flaw type [2]	Specimen number	Laboratory		Production	
			Detection ratio	Total	Detection ratio	Total
0.040 0.079	H	6	0/2	0/2	0/1	0/1
0.080						
0.119	H	6	0/2		0/1	
	H	7	0/2		0/5	
	H	8	0/3	0/7	0/5	0/11
0.120 0.159	G (0.13×0.08)	SN2			0/2	0/2
0.160						
0.199	H	3	0/4		0/3	
	H	5	0/3		0/2	
	H	5	0/3		0/2	
	G (0.18×0.14)	SN8		0/10	0/4	0/11
0.200	H	2	1/3		0/3	
0.239	G (0.15×0.20)	19	0/1		0/4	
	G (0.21×0.21)	16			1/4	
	G (0.22×0.16)	19	0/1	1/5	1/4	2/15
0.240	G (0.25×0.16)	SN2			0/2	
0.279	H	7	1/2		0/5	
	G (0.21×0.26)	19	0/1	1/3	1/4	1/11
0.280 0.359						
0.360	G (0.36×0.04)	SN10			2/4	
0.399	G (0.38×0.38)	SN7	0/1	0/1	1/4	3/8
0.400	G (0.35×0.40)	SN5	0/1		1/4	
0.439	H	4	0/3	0/4	0/2	1/6
0.440 0.479						
0.480	H	4	0/3		0/2	
0.559	H	4	2/3	2/6	1/2	1/4

1 Grinding crack lengths represent longest dimension of cracked area

2 H hydrogen embrittlement crack

G grinding cracks

Table 44.—Results of Radiographic Inspections on Grinding and Embrittlement Cracked Steel Specimens (Continued)

Flaw length interval, in.	Flaw type	Specimen number	Laboratory		Production	
			Number of inspections	Total	Number of inspections	Total
NONFLAW		888132-1	2		5	
SPECIMENS		888132-3	1		3	
		888132-4	1		2	
		888132-6	1		5	
		888132-7	1		1	
		888132-8	2		2	
		SN-4			2	
		SN-6				
		SN-9				
		20			2	
		27		8	2	24

Table 45.—Statistical Analysis of Radiographic Inspection Results on Grinding and Embrittlement Cracked Steel Specimens

Flaw length interval, in.	Laboratory			Production			Combined		
	Detection ratio	Probability		Detection ratio	Probability		Detection ratio	Probability	
		Observed	Lower 95% conf limit		Observed	Lower 95% conf limit		Observed	Lower 95% conf limit
0.040-0.079	0/2	0.000		0/1	0.000		0/3	0.000	
0.080-0.119	0/7	0.000		0/11	0.000		0/18	0.000	
0.120-0.159	–			0/2	0.000		0/2	0.000	
0.160-0.199	0/10	0.000		0/11	0.000		0/21	0.000	
0.200-0.239	1/5	0.200		2/15	0.133		3/20	0.150	
0.240-0.279	1/3	0.333		1/11	0.091		2/14	0.143	
0.280-0.359	–			–			–		
0.360-0.399	0/1	0.000		3/8	0.375		3/9	0.333	
0.400-0.439	0/4	0.000		1/6	0.167		1/10	0.100	
0.440-0.479	–			–			–		
0.480-0.559	2/6	0.333		1/4	0.250		3/10	0.300	

specimens was curtailed. Also, the eddy-current inspections were not applied to this design as the pronounced surface irregularities in the form of the threads interfered with this method of inspection.

In the design and fabrication of these specimens one-half of the number were to contain flaws in two separate thread root locations and most were to have adjacent flaws at each thread root location. Distortion during compression to close the EDM notches was such that in the finished specimens half of the flaws were developed at the crests of the threads rather than being confined to the roots. Also, it became apparent that the adjacent flaws were close enough together as to cause uncertainty in interpreting the inspection reports. For example, which of two flaws was detected if only one was reported? If penetrant indications of adjacent flaws merge and are reported as one, are both detected? Because of such questions, the results were interpreted and recorded conservatively in that only the largest flaw in a group was recorded as detected if only one was reported. All others were excluded from the data. Because this resulted in most of the methods being penalized for peculiarities of the arrangement and distribution of flaws within this specimen design, extensive inspections were not performed and more emphasis was placed on the other externally flawed steel designs. The limited results obtained are presented in tables 46 through 53 for information, but they should not be directly compared with the capabilities demonstrated on other designs.

EFFECTS OF SPECIMEN CONFIGURATION AND FLAW TYPES ON DETECTABILITY

Although the effects of differences of flaw types and of configurations on inspection results cannot be isolated completely, some general comparisons have been made for several of the inspection methods.

Comparisons between flaw types as in figure 38 cannot be made wholly independent of configuration effects. For example, embrittlement cracks were in flat bars, whereas compressed notches were in solid or hollow steel rounds and in the aluminum cruciform shapes. Comparison of results obtained on the different configurations with the same flaw types are more valid, as in the case of solid versus hollow steel specimens. See figures 59 and 60. However, in addition to the simple differences in geometry, the handling ease and relative areas to be inspected differ in these designs and must be assumed to exert some influence on the results. Some comparisons between configurations would have very limited value as in the case of penetrant inspection of compressed notch flaws in aluminum cruciform specimens and any of the steel specimens. The initial widths of flaw openings in the two alloys were considerably different, and both materials were exposed to conditions during the program which changed the initial flaws and affected their inspectability to differing and unknown degrees. The aluminum alloy specimens suffered smearing effects under the repeated application of eddy-current probes, while the steel specimens suffered some corrosive attack within the flaws from the repeated water immersion ultrasonic inspections. Both experiences strongly influenced penetrant inspection results for both types of specimens.

The very important role of human factors becomes apparent in some comparisons. For example, the magnetic particle inspection capabilities demonstrated in production on the hollow steel specimens were markedly inferior to results obtained on the external surface

Table 46. Results of Magnetic Particle Inspections on Flawed Threaded Steel Specimens

Flaw length interval, in.	Flaw location R-root C-crest (1)	Specimen number	Laboratory		Production	
			Detection ratio	Total	Detection ratio	Total
0.040 0.069	R	T5	1 1	1 1	2 3	2 3
0.070 0.099	C	T9				
0.100	R	T6	1 1		1 2	
0.129	C	T8				
	R	T1	1 1		2 2	
	R	T2	1 1		2 3	
	R	T5	1 1		3 3	
	R	T9	1 1		3 3	
	R	T13	1 1	6 6	2 3	13 16
0.130	R	T7	1 1		3 3	
0.159	C	T12				
	C	T13				
	R	T13	1 1	2 2	3 3	6 6
0.160 0.189						
0.190	C	T1				
0.219	C	T9				
0.220	R	T6	1 1		2 2	
0.279	R	T4	1 1		3 3	
	R	T9	1 1		3 3	
	C	T7		3 3		8 8
0.280	R	T12	1 1		3 3	
0.359	R	T5	1 1		3 3	
	C	T13				
	R	T3	1 1	3 3	2 2	8 8
0.360	R	T4	1 1		3 3	
0.459	R	T7	1 1		3 3	
	R	T6	1 1	3 3	2 2	8 8
0.460	R	T1	1 1		2 2	
0.659	R	T11	1 1		2 2	
	R	T8	1 1	3 3	2 2	6 6

(1) Results on thread root flaws only

Table 46.—Results of Magnetic Particle Inspections on Flawed Threaded Steel Specimens (Continued)

Flaw length interval, in.	Flaw location R-root C-crest	Specimen number	Laboratory		Production	
			Number of inspections	Total	Number of inspections	Total
NONFLAW		T10	1		3	
SPECIMENS		T14	1		2	
		T15	1		2	
		T16	1	4	3	10

Table 47.—Statistical Analysis of Magnetic Particle Inspection Results ① on Flawed Threaded Steel Specimens

Flaw length interval, in.	Laboratory			Production			Combined		
	Detection ratio	Probability		Detection ratio	Probability		Detection ratio	Probability	
		Observed	Lower 95% conf limit		Observed	Lower 95% conf limit			
0.040-0.069	1/1	1.000		2/3	0.667				
0.070-0.099	–	–		–	–				
0.100-0.129	6/6	1.000		13/16	0.813				
0.130-0.159	2/2	1.000		6/6	1.000				
0.160-0.189	–	–		–	–				
0.190-0.219	–	–		–	–				
0.220-0.279	3/3	1.000		8/8	1.000				
0.280-0.359	3/3	1.000		8/8	1.000				
0.360-0.459	3/3	1.000		8/8	1.000				
0.560-0.659	3/3	1.000		6/6	1.000				

① Includes data on thread root flaws only

Table 48. Results of Penetrant Inspections on Flawed Threaded Steel Specimens

Flaw length interval, in.	Flaw location R-root C-crest	Specimen number	Laboratory		Production	
			Detection ratio	Total	Detection ratio	Total
0.040-0.069	R	T5	4/4	4/4		
0.070-0.099	C	T9	4/4	4/4	1/2	1/2
0.100	R	T6	5/5		1/2	
0.129	C	T8	4/4		1/3	
	R	T1	4/4		1/1	
	R	T2	4/4		4/4	
	R	T5	4/4		4/4	
	R	T6	4/4		3/3	
	R	T10	4/4	28/29	2/2	16/19
0.130	R	T7	4/4		3/3	
0.159	C	T12	4/4		3/4	
	C	T13	4/4		2/3	
	R	T12	4/4	16/16	2/3	16/13
0.160-0.189						
0.190	C	T1	4/4		2/2	
0.219	C	T9	4/4	8/8	2/3	4/5
0.220	R	T6	5/5		2/3	
0.279	R	T4	4/4		1/1	
	R	T9	4/4		3/3	
	C	T7	4/4	17/17	2/3	8/10
0.280	R	T12	4/4		4/4	
0.359	R	T5	4/4		4/4	
	C	T13	4/4		2/3	
	R	T3	4/4	16/16	3/3	13/14
0.360	R	T4	4/4		3/3	
0.459	R	T7	4/4		3/3	
	R	T6	5/5	13/13	3/3	9/9
0.460	R	T1	4/4		2/2	
0.659	R	T11	4/4		3/3	
	R	T8	4/4	12/12	3/3	8/8

Table 48.--Results of Penetrant Inspections on Flawed Threaded Steel Specimens (Continued)

Flaw length interval, in.	Flaw location R-root C-rest	Specimen number	Laboratory		Production	
			Detection ratio	Total	Detection ratio	Total
NONFLAW		T10	4		4	
SPECIMENS		T14	4		3	
		T15	4		2	
		T16	4	16	3	12

Table 49. Statistical Analysis of Penetrant Inspection Results on Flawed Threaded Steel Specimens

Flaw length interval, in.	Laboratory			Production			Combined		
	Detection ratio	Probability		Detection ratio	Probability		Detection ratio	Probability	
		Observed	Lower 95% conf limit		Observed	Lower 95% conf limit			
0.040-0.069	4/4	1.000	0.914 ①						
0.070-0.099	4/4	1.000		1/2	0.500				
0.100-0.129	28/29	0.966		16/19	0.842				
0.130-0.159	16/16	1.000		10/13	0.769				
0.160-0.189									
0.190-0.219	8/8	1.000		4/5	0.800				
0.220-0.279	17/17	1.000		8/10	0.800				
0.280-0.359	16/16	1.000		13/14	0.968	0.856			
0.360-0.459	13/13	1.000		9/9					
0.560-0.659	12/12	1.000		8/8					

① Minimum flaw length interval with at least 0.90 probability of detection with 95% confidence

Table 50.—Results of Ultrasonic Inspections on Flawed Threaded Steel Specimens

Flaw length interval, in.	Flaw location R-root C-crest	Specimen number	Laboratory		Production	
			Detection ratio	Total	Detection ratio	Total
0.040-0.069	R	T5			0/1	0/1
0.070-0.099	C	T9			0/1	0/1
0.100-	R	T6				
0.129	C	T8			1/2	
	R	T1				
	R	T2			1/2	
	R	T5			0/1	
	R	T9				
	R	T13			0/1	2/6
0.130-	R	T7				
0.159	C	T12			1/2	
	C	T13				
	R	T13			0/1	1/3
0.160-0.189						
0.190	C	T1			1/1	
0.219	C	T9			0/1	1/2
0.220	R	T6			2/2	
0.279	R	T4			2/2	
	R	T9			1/1	
	C	T7				5/5
0.280	R	T12			2/2	
0.359	R	T5			1/1	
	C	T13			1/1	
	R	T3			2/2	6/6
0.360-	R	T4			2/2	
0.459	R	T7				
	R	T6			2/2	4/4
0.460-	R	T1			1/1	
0.659	R	T11			2/2	
	R	T8			2/2	5/5

Table 50. Results of Ultrasonic Inspections on Flawed Threaded Steel Specimens (Continued)

Flaw length interval, in.	Flaw location R-root C crest	Specimen number	Laboratory		Production	
			Detection ratio	Total	Detection ratio	Total
NONFLAW SPECIMENS		T10			2	
		T14			2	
		T15				
		T16				4

Table 51. Statistical Analysis of Ultrasonic Inspection Results on Flawed Threaded Steel Specimens

Flaw length interval, in.	Laboratory			Production			Combined		
	Detection ratio	Probability		Detection ratio	Probability		Detection ratio	Probability	
		Observed	Lower 95% conf limit		Observed	Lower 95% conf limit			
0.040-0.069				0/1	0.000				
0.070-0.099				0/1	1.000				
0.100-0.129				2/6	0.333				
0.130-0.159				1/3	0.333				
0.160-0.189									
0.190-0.219				1/2	0.500				
0.220-0.279				5/5	1.000				
0.280-0.359				6/6	1.000				
0.360-0.459				4/5	0.800				
0.560-0.659				5/5	1.000				

Table 52. – Results of Radiographic Inspections on Flawed Threaded Steel Specimens

Flaw length interval, in.	Flaw location R-root C-crest	Specimen number	Laboratory		Production	
			Detection ratio	Total	Detection ratio	Total
0.040-0.069	R	T5				
0.070-0.099	C	T9				
0.100-	R	T6			0/1	
0.129	C	T8			0/1	
	R	T1			0/1	
	R	T2				
	R	T5				
	R	T9				
	R	T13				0/3
0.130-	R	T7				
0.159	C	T12				
	C	T13				
	R	T13				
0.160-0.189						
0.190-	C	T1			0/1	
0.219	C	T9				0/1
0.220-	R	T6			0/1	
0.279	R	T4				
	R	T9				
	C	T7				0/1
0.280-	R	T12				
0.359	R	T5				
	C	T13				
	R	T3			0/1	0/1
0.360-	R	T4			1/1	
0.459	R	T7				
	R	T6			0/1	1/2
0.460-	R	T1			0/1	
0.659	R	T11			1/1	
	R	T8			1/1	2/3

Table 52. Results of Radiographic Inspections on Flawed Threaded Steel Specimens (Continued)

Flaw length interval, in.	Flaw location R-root C-crest	Specimen number	Laboratory		Production	
			Number of inspections	Total	Number of inspections	Total
NONFLAW		T10				
SPECIMENS		T14			1	
		T15			1	
		T16				2

Table 53.--Statistical Analysis of Radiographic Inspection Results on Flawed Threaded Steel Specimens

Flaw length interval, in.	Laboratory			Production			Combined		
	Detection ratio	Probability		Detection ratio	Probability		Detection ratio	Probability	
		Observed	Lower 95% conf limit		Observed	Lower 95% conf limit			
0.040-0.069									
0.070-0.099									
0.100-0.129				0/3	0.000				
0.130-0.159				--	--				
0.160-0.189				--	--				
0.190-0.219				0/1	0.000				
0.220-0.279				0/1	0.000				
0.280-0.359				0/1	0.000				
0.360-0.459				1/2	0.500				
0.560-0.659				2/3	0.667				

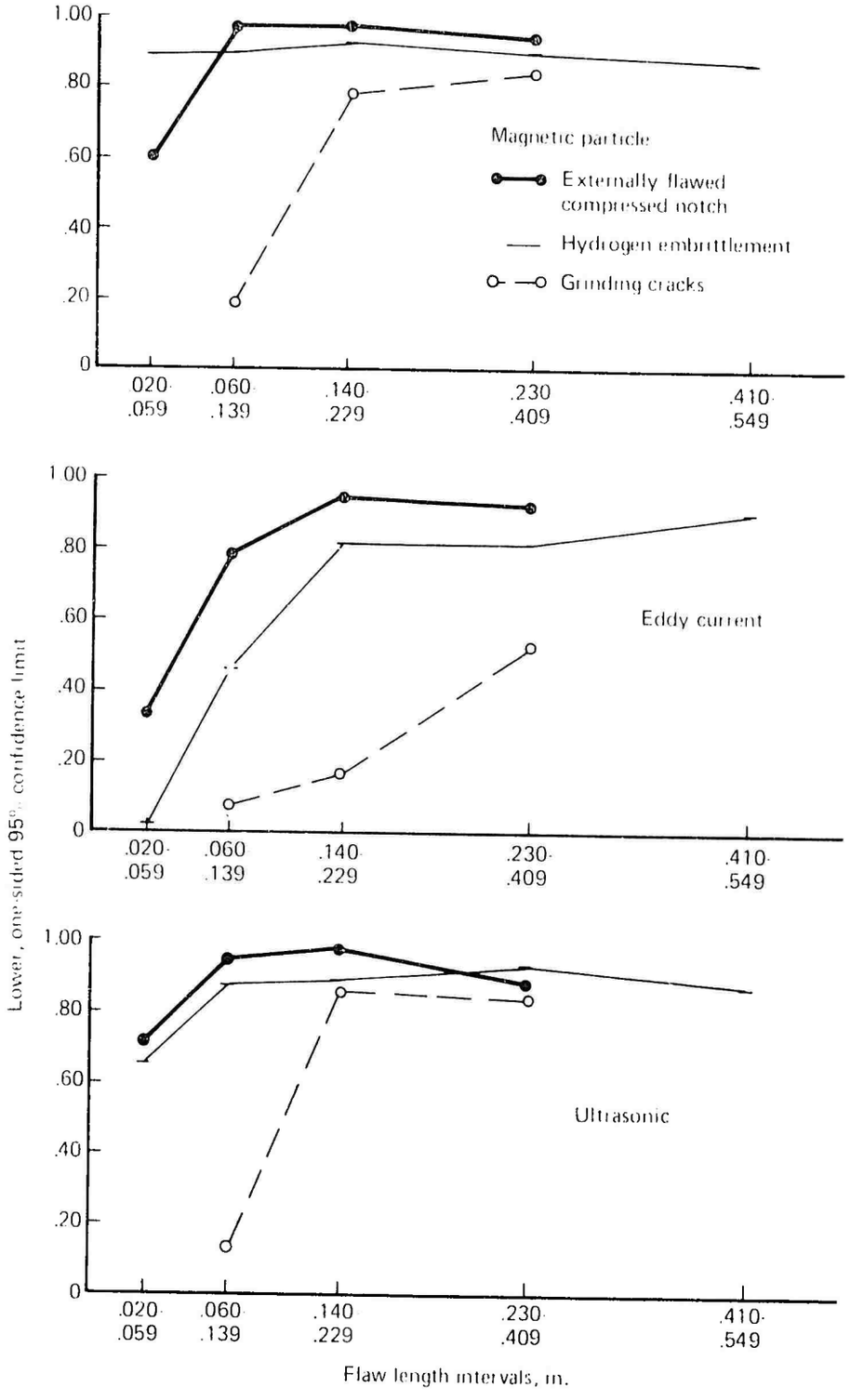


Figure 58. Effects of Flaw Type on Detectability (Combined Laboratory and Production Data)

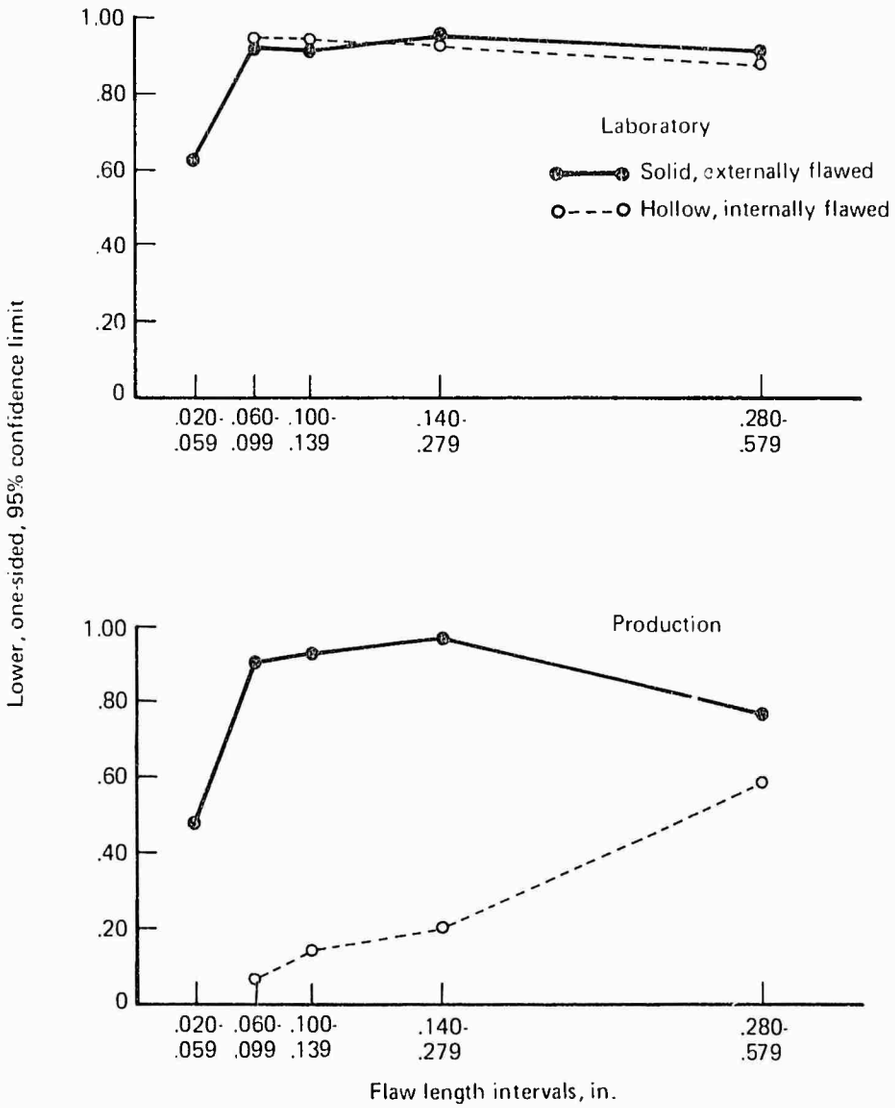


Figure 59.—Effects of Specimen Configuration on Detectability by Magnetic Particle Inspection

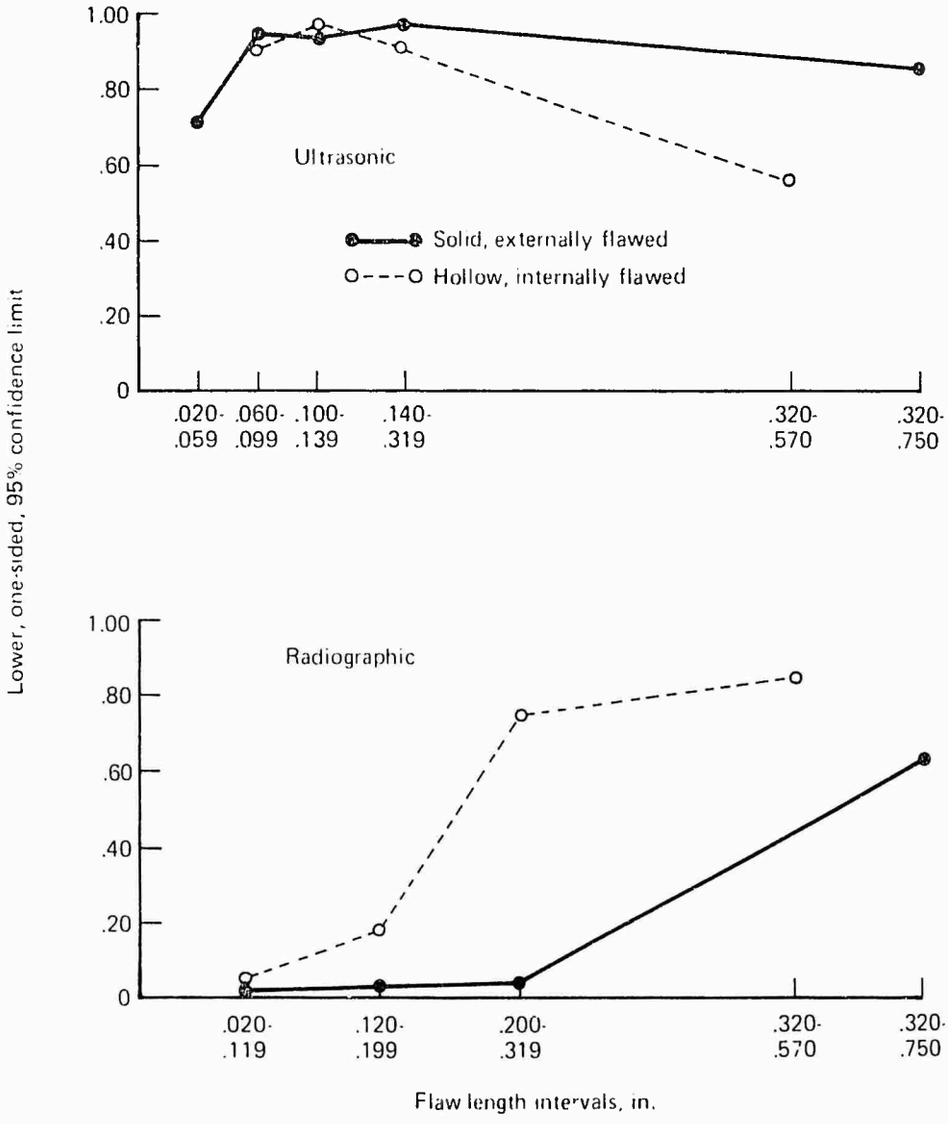


Figure 60.—Effects of Specimen Configuration on Detectability by Ultrasonics and Radiography (Combined Laboratory and Production Data)

flaws in the solid steel specimens. The most likely accountable factor is the difference in visual accessibility between the internal and external surfaces since the method should indicate flaws in either location equally well. This was confirmed by the results of the more carefully performed laboratory inspections.

INTENTIONALLY OXIDIZED FLAWS

Inspection results obtained on the selected steel and aluminum specimens following high temperature oxidation are shown in tables 54 and 55. The specimens were selected to represent small and medium sized flaws. The inspection results are tabulated and shown in comparison to previous results obtained on nonoxidized flaws within the same size intervals. While the objective was to reveal any adverse effects of oxidation contamination on the various inspection capabilities, it became apparent that a number of concurrent changes took place so that any effects due to the contaminations could not be isolated.

In addition to oxidation of the flaws, the prolonged furnace exposure of the steel specimens resulted in considerable decarburization of the outer surfaces. Upon reheat treatment to restore the specimens to the previous strength level, the surfaces remained considerably softer. The lower carbon content of the surface would result in a surface of different magnetic and electrical properties than previously obtained, which might influence magnetic particle and eddy-current testing. Also, grinding performed so this soft surface to remove the heat treat scale could obscure the surface openings and interfere with penetrant inspection. The grinding did result in a rougher surface which created increased noise in both eddy-current and ultrasonic inspections.

The thermal treatments caused fewer recognized changes in the structure or properties of the aluminum. However, it was necessary to restore the surface to its original, brighter appearance with the use of abrasive pads. This could adversely affect subsequent penetrant inspections.

The appearances of the steel and aluminum specimens, when reintroduced to the then current inspection lots were somewhat distinguishable. Whether this resulted in particular notice or identification on the part of the inspectors could not be evaluated.

Despite the interactions of the above influences, few significant differences between results on unoxidized or oxidized flaws of equivalent sizes were determined.

SPECIMEN DEGRADATION

It became apparent during the program that penetrant inspection results were degrading for most specimen configurations, both in the laboratory and production environments. Larger flaws were passing undetected following earlier successful inspections. Initial inspections in the laboratory were able to reveal many compressed notch flaws without developer, and it was apparent during later inspections that most flaws were not indicated until developer was applied.

As inspections were accumulated, visual evidence of progressive factors adversely affecting penetrant capabilities became evident. Superficial rusting of the steel specimens occasionally

Table 54. – Intentionally Oxidized Flaws–Comparative Results on External Flaw Steel Specimens

Inspection method	Flaw size interval	Detection ratio		Significant ② or apparent difference
		Before ①	Oxidized	
Magnetic particle	0.020-0.039	29/48	3/8	NO ②
	0.100-0.119	40/40	8/8	NO
	0.120-0.139	66/67	8/8	NO
	0.200-0.750	73/73	8/8	NO
Penetrant	0.020-0.039	22/42	4/7	NO ②
	0.100-0.119	21/24	4/6	NO
	0.120-0.139	29/33	8/8	NO
	0.200-0.750	32/32	8/8	NO
Eddy current	0.020-0.039	5/21	2/5	NO
	0.100-0.119	28/28	4/5 ③	NO
	0.120-0.139	38/41	4/5 ③	NO
	0.200-0.750	101/101	4/5 ③	YES ②
Ultrasonic	0.020-0.039	20/31	0/10	YES ② ④
	0.110-0.139	38/38	16/18 ③	NO
	0.200-0.750	29/29	9/10 ③	NO

① Data from tables 8 to 17

② Comparison made using CHI square test at the 95% level with one degree of freedom

③ High background noise interfered with the inspection and was reported

④ Probability of detection in this flaw length interval is relatively low and changing rapidly. There is no know reason for the inability of ultrasonics to detect this flaw

Table 55 –Intentionally Oxidized Flaws–Comparative Results on Aluminum Specimens

Inspection method	Flaw size interval	Detection ratio		Significant (2) or apparent difference
		Before (1)	Oxidized	
Penetrant	0.040-0.059	54/62	4/7	NO (2)
	0.080-0.099	29/29	13/13	NO
	0.100-0.119	46/53	6/6	NO
	0.160-0.239	85/89	1/6 (3)	YES (2)
Eddy current	0.040-0.059	22/31	3/5	NO (2)
	0.080-0.099	30/43	8/9	NO (2)
	0.100-0.119	53/63	5/5	NO
	0.160-0.179	29/29	8/9	NO
Ultrasonic	0.040-0.059	28/46	3/4	NO (2)
	0.080-0.099	29/34	9/10	NO
	0.100-0.119	52/57	5/6	NO
	0.160-0.179	24/25	6/6	NO
Radiography	0.040-0.059	51/60	5/5	NO
	0.080-0.099	20/20	8/8	NO
	0.100-0.119	23/23	4/4	NO
	0.160-0.179	9/9	4/4	NO

(1) Data from tables 18 to 25

(2) Comparison made using CHI square test at the 95% level with one degree of freedom

(3) This flaw was found to be essentially closed after oxidation

was noted following production inspections which suggested that possibly more advanced corrosion was developing within the flaws. This was relatable to ultrasonic immersion inspections. Aluminum specimens began to exhibit signs of wear and handling damage. More significant to the program was evidence of scrubbing action of eddy-current probes where inspectors evaluated flaw responses. This localized wear contributed to partial closure of the flaws by smearing of the metal surface.

These factors prevented reliable assessment of results, and penetrant inspections were therefore terminated in many instances. The experience suggests that penetrant inspection evaluation programs should only be conducted with specimens that have not been subjected to other procedures.

Table 56 has been prepared to illustrate the changes encountered with repeated penetrant inspections of selected aluminum cruciform specimens and hollow steel specimens.

NONRELEVANT CALLOUTS

A normal occurrence during the performance of nondestructive examinations for flaws is the occasional incorrect interpretation of an NDI signal or indication. This may result from the method responding to a real but nonflaw condition such as a scratch or may be a completely false indication with no identified cause. While these occurences do not affect the reliability of the inspections, they are relatable and constitute an economic penalty which increases as the reliability increases. A high percentage of nonrelevant callouts is probably indicative of cautious, conservative inspections.

The number of nonrelevant inspection callouts recorded during this program has been compiled in table 57 according to specimen material and inspection method. The callouts are given in two columns. When it could be reasonably determined that the reported indication or signal was from a real but nonflaw discontinuity or imperfection such as scratches, deep grinding marks, etc., they were listed in the nonflaw callout column. Where no flaw or other significant feature could account for the callout, it was listed as a false callout.

A few general observations concerning relative frequency of nonrelevant callouts can be made. The insensitivity of radiography to minor imperfections is apparent in the relatively low number of false and nonflaw callouts. The susceptibility of eddy-current instrumentation to noise in ferromagnetic materials is evident in comparing the number of callouts for steel and aluminum specimens. The vacuum-arc remelted steel was "cleaner" than the aluminum alloy extrusion, and stringers of intermetallic compounds inherent in the microstructure of the aluminum accounted for a higher percentage of nonflaw callouts by ultrasonic and penetrant procedures.

Table 56. Effects of Repeated Inspections on Penetrant Results (1)

Aluminum specimens												
Flaw interval	Specimen number	Inspection order and results (2)										
		1	2	3	4	5	6	7	8	9	10	11	12
0.100 - 0.119	C4	L	P	(P)	P	(P)	(P)	(P)					
	C3	L	L	P	L	L	(P)	P	(P)				
0.120 - 0.139	B2	L	(L)	(P)	L	(L)	(L)	(P)	(P)				
	A21	L	L	P	P	L	(P)	(P)	(P)				
0.160 - 0.239	B2	L	L	P	L	L	L	P	(P)				
	A11	L	L	P	L	(P)							
	B3	L	L	P	(P)	(P)							

Hollow steel specimens													
Flaw interval	Specimen number	Inspection order and results											
		1	2	3	4	5	6	7	8	9	10	11	12
0.060 - 0.079	H11	(P)	L	L	(L)	(L)	(L)						
0.080 - 0.099	H8	L	L	L	L	L	(P)	(L)	(L)	L	(L)	(L)	
0.100 - 0.119	H11	(P)	L	L	L	(L)	(L)						
	H7	(L)	L	(L)	L	(L)	(P)	(P)	(P)	(L)	(L)	(L)	
0.120 - 0.139	H6	L	L	L	L	L	(P)	(P)	(L)	(L)	(L)	(L)	(L)
	H15	(P)	L	L	(L)	(L)	(L)						
0.140 - 0.159	H7	L	L	L	L	L	(P)	(P)	(P)	(L)	(L)	(L)	

(1) For those flaws noted or suspected of being contaminated and or smeared

(2) L Successful laboratory inspection
P Successful production inspection
} (O) indicates an unsuccessful inspection

Table 57. Summary of Nonrelevant Callouts

Material	Inspection method	Number of inspections	False callouts [1]	Nonflaw callouts [1]
Steel	Magnetic	812	14	102
	Penetrant	844	38	69
	Eddy current	512	23	51
	Ultrasonic	639	15	34
	Radiography	217	2	3
Aluminum	Penetrant	195	12	54
	Eddy current	206	- -	8
	Ultrasonic	201	18	58
	Radiography	128	2	3

[1] *False callouts* were determined to be inspector-recorded flaws where no flaws existed, and discontinuities were not the cause of irrelevant responses. *Nonflaw callouts* were inspector-recorded flaws where no flaws existed but where surface irregularities such as scratches, hardness impressions, and coarse grinding marks could be presumed to cause the nonflaw response.

SECTION VII
CONCLUSIONS

The sensitivity capabilities achieved and expressed in this report with statistical probability and confidence terms represent average capabilities of a large number of personnel, equipment, and facilities normally associated with inspection of aircraft structures. The results do not indicate the final, outgoing quality level of actual production parts nor do they reflect the extreme capabilities commonly exhibited in critical inspections of items such as turbine engine blading and hydraulic tubing. The results do show that the minimum sizes of detected flaws are considerably less than those detected with 0.90 probability and 95% confidence. It is apparent from this that the minimum size flaw that can be detected with 0.90 probability and 95% confidence will depend on what are acceptable inspection costs and the amount of available inspection time.

During this program, three new methods of creating controlled, artificial flaws in varied specimen configurations were proven. These included a compressed notch flaw, hydrogen embrittlement cracks, and hydrogen induced grinding cracks.

The program inspection results revealed the varied capabilities of the five inspection methods with respect to the types of flaws, the different flaw locations and the two alloys. However, comparison of the results should be made with caution. For example, when comparing capabilities as demonstrated on the different types of flaws, such as compressed notch versus grinding crack, the difference in specimen designs must also be considered. Similarly, comparisons between results on aluminum and steel alloys involving different specimen designs have been shown to influence the results. Even comparisons between laboratory and production inspections do not show a consistent laboratory superiority as might be expected.

In general, the magnetic particle and penetrant methods were significantly influenced by visual accessibility. The results from external flaws were in most cases superior to those obtained on the internal surface flaws of the hollow steel specimens. By contrast, the ultrasonic and eddy-current methods were not similarly affected and the results from the external flaws in steel were similar to the hollow steel specimen results. Inspections were affected by geometric factors which interferes with proper introduction of the ultrasonic energy into the part. This was apparent in the results obtained in the central web regions (flaw location C in table 22) which accounted for a high percentage of the misses in both the laboratory and production inspections.

The types of flaws in the steel specimens had little influence on the capabilities determined for magnetic particle, ultrasonic, or eddy-current methods, with the exception of the very small and shallow grinding cracks. These presented some difficulty for all three methods. The eddy-current method with one kind of instrument was so strongly affected by nonuniform metallurgical properties of the abusively ground surfaces that it practically lost all capability.

Preceding page blank

Penetrant methods generally exhibited an initial high sensitivity to very small flaws, but results for all specimens in both alloys demonstrated a gradually decreasing probability of detection. It was confirmed that the specimens were being adversely affected by the repeated inspection processings, surface wear, and possible corrosion within the flaws. Therefore, the "true" capability of the penetrant method is undoubtedly superior to what was demonstrated.

Radiography was not practically competitive on the heavy, solid steel specimens nor on the extremely tight embrittlement and grinding cracks. It exhibited somewhat better capability on the thinner hollow steel specimens and performed quite well on the aluminum extruded specimens.

Tests on the oxidation contaminated specimens showed neither significant nor apparent differences in detectability. Additional inspections to more critically reveal differences were not developed because it was found that other specimen characteristics that could not be separated had changed during the oxidation.

SECTION VIII
RECOMMENDATIONS

During the performance of this program a number of observations were made which are offered here as recommendations for consideration in planning or accomplishing further related investigations.

1. Continue to develop methods of creating low cost, reproducible, and standardized flawed specimens. Some study should be directed to creating small cracks by embrittlement procedures in local areas of large and complex shaped parts.

2. Strive to attain acceptance of standard kinds of flaws among concerned investigators so that data may be commingled.

3. Perform fewer tests on more specimens to avoid development of a shop-worn appearance and local wear patterns that signal flaw locations.

4. Introduce new flaws in new locations during the course of the inspections to avoid inspection familiarization with the likely flaw locations. The presence of the new specimen should be unknown to the inspectors.

5. Give considerable attention to identifying and evaluating human factors influencing inspection capabilities. Comparative results should be obtained to reveal the degrees of improvement possible by minimizing human factors. For example, compare the reliability of automated versus manual scanning and chart recordings versus meter watching.

   Also, include the contribution of detailed technique instructions for individual parts in improving probability.

6. Develop improvements in the basic approaches to quantitative evaluation of penetrant inspection. Perhaps specimens should not be used for simultaneous evaluations of other methods. Consideration should be given to using a special corrosion resistant material for the penetrant evaluation specimens. An alternative might be the development of an inexpensive specimen that can be discarded after a few tests.

7. Direct efforts toward evaluating the value of repeated inspections or supplemental inspection methods in achieving improved flaw detection capabilities. Where the desired probability of detection (such as 0.90 with 95% confidence) is not limited by the sensitivity of the method, improved reliability might be better attained by a supplemental inspection than by an effort to improve the basic method capability.

SECTION IX
REFERENCES

1. Gwendolyn B. Wood, "A Study of Embrittlement of High Strength Steels by Hydrogen Isotopes," *Journal of Electrochemical Society*, 867-885, August 1963.

2. F.F. Fletcher and A.R. Elsea, *Hydrogen Movement in Steel - Entry Diffusion and Elimination*, DMIC Report 219, 22-30, June 1965.

3. C.A. Bennett and N.L. Franklin, *Statistical Analysis in Chemistry and the Chemical Industry*, John Wiley, New York, 1954.

4. B. Ostle, *Statistics in Research*, Iowa State University Press, 1963.

5. W.G. Ireson, et al., *Reliability Handbook*, McGraw-Hill Book Company, New York, 1966.

Preceding page blank